catalysts

MDPI

Review

Non-Covalent Interactions in Enantioselective Organocatalysis: Theoretical and Mechanistic Studies of Reactions Mediated by Dual H-Bond Donors, Bifunctional Squaramides, Thioureas and Related Catalysts

Ana Maria Faisca Phillips [1,*], Martin H. G. Prechtl [1] and Armando J. L. Pombeiro [1,2]

[1] Centro de Química Estrutural, Instituto Superior Técnico, Universidade de Lisboa, Av. Rovisco Pais, 1049-001 Lisboa, Portugal; martin.prechtl@tecnico.ulisboa.pt (M.H.G.P.); pombeiro@tecnico.ulisboa.pt (A.J.L.P.)
[2] Research Institute of Chemistry, Peoples' Friendship University of Russia (RUDN University), 6 Miklukho-Maklaya Street, 117198 Moscow, Russia
* Correspondence: anafaiscaphillips@tecnico.ulisboa.pt; Tel.: +351-21-841-9225

Abstract: Chiral bifunctional dual H-bond donor catalysts have become one of the pillars of organocatalysis. They include squaramide, thiosquaramide, thiourea, urea, and even selenourea-based catalysts combined with chiral amines, cinchona alkaloids, sulfides, phosphines and more. They can promote several types of reactions affording products in very high yields and excellent stereoselectivities in many cases: conjugate additions, cycloadditions, the aldol and Henry reactions, the Morita–Baylis–Hilman reaction, even cascade reactions, among others. The desire to understand mechanisms and the quest for the origins of stereoselectivity, in attempts to find guidelines for developing more efficient catalysts for new transformations, has promoted many mechanistic and theoretical studies. In this review, we survey the literature published in this area since 2015.

Keywords: asymmetric synthesis; H-bonding; nonbonding interactions; density functional theory calculations; Michael addition; cycloadditions; anion-binding catalysis; cascade reactions; transition states; organocatalysis

Citation: Phillips, A.M.F.; Prechtl, M.H.G.; Pombeiro, A.J.L. Non-Covalent Interactions in Enantioselective Organocatalysis: Theoretical and Mechanistic Studies of Reactions Mediated by Dual H-Bond Donors, Bifunctional Squaramides, Thioureas and Related Catalysts. *Catalysts* **2021**, *11*, 569. https://doi.org/10.3390/catal11050569

Academic Editor: Cristina Trujillo

Received: 14 April 2021
Accepted: 26 April 2021
Published: 29 April 2021

1. Introduction

The activation of reactants by hydrogen bonding and other noncovalent interactions has enabled the development of an enormous variety of reactions in recent years, and consequently, the production of chiral substances for several applications. This was possible due to the discovery of an array of very efficient chiral bifunctional catalysts, mostly thiourea- or squaramide-based, usually combined with chiral amines or cinchona alkaloids, and more recently also amides, phosphines or sulfides [1–4]. Urea, thiosquaramide and even selenosquaramide chiral bifunctional catalysts are also starting to appear. They are usually assembled on a modular basis, which allows for easy structural modifications and optimization of the results.

The hydrogen bond-donors differ in duality, rigidity, H-bond spacing, H-bond angle, and pK_a, which influence their catalytic behavior [1,5]. The average distance between the N–H groups in these substances is shown in Figure 1a. Squaramides are distinct from the ureas in their hydrogen bond donor and acceptor character since, upon hydrogen bond formation, aromaticity is enhanced in the latter. The cyclobutadienone ring contains two coplanar carbonyls and two NHs that are almost coplanar and essentially sp^2 hybridized so that the lone pairs are available for conjugation into the π-system orthogonal plane [6].

Similarly, the ability of thioureas to recognize cations is also more limited [6]. As a result of their ambivalent hydrogen bonding characteristics, squaramides also form dimeric species.

The distance between the N–H groups is larger in squaramides than in thioureas. Due to the geometry of the cyclobutenedione ring, the N–H groups are also oriented towards each other by ~6°, a characteristic, which is absent in the amido/thioamido groups of ureas/thioureas [7]. This property may result in increased linearity in hydrogen bonding with some substrates and provide different binding properties in the transition state.

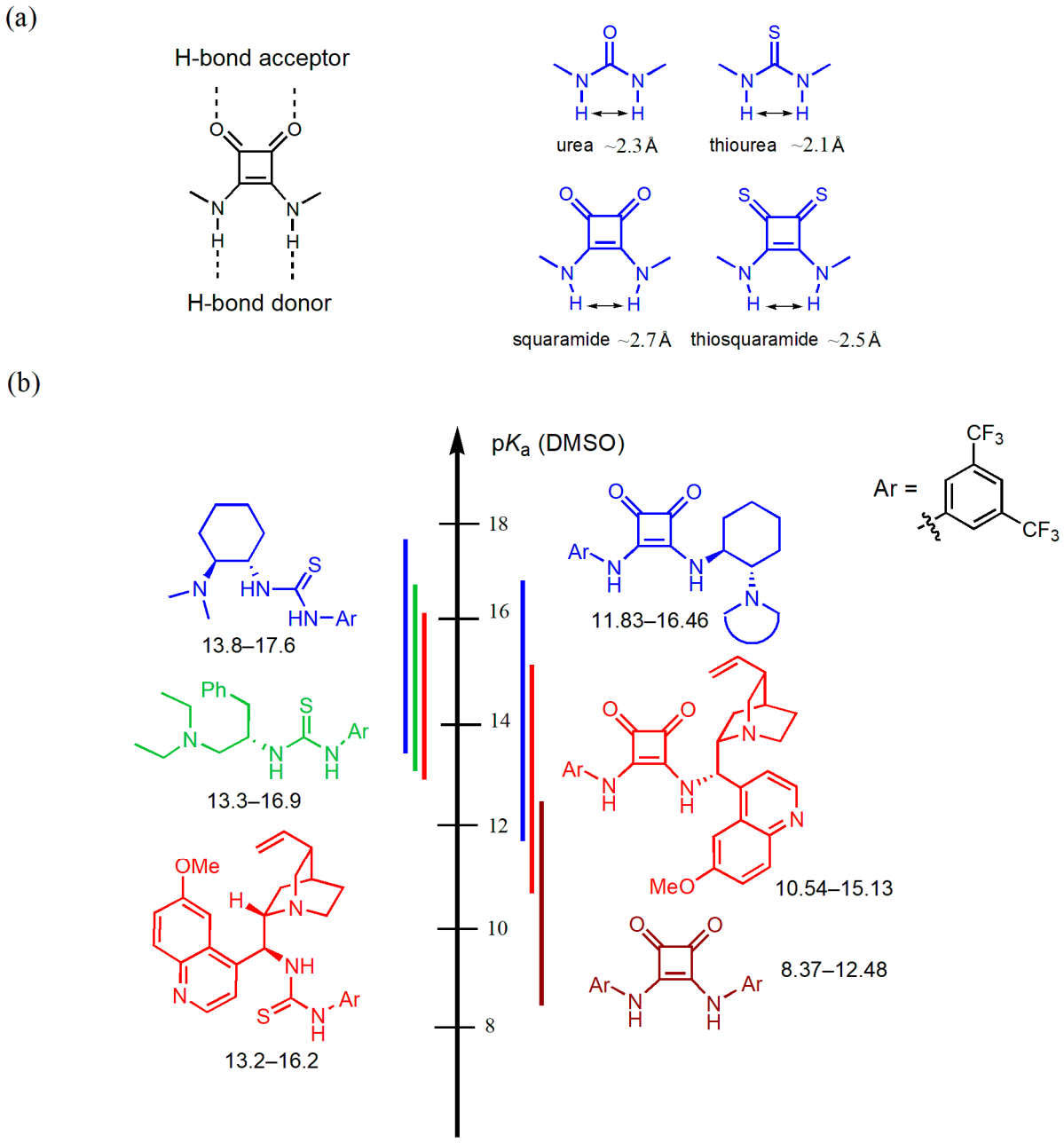

Figure 1. (**a**) Duality in hydrogen bonding in squaramides and H-bond spacing distances in H-bond donor catalysts and (**b**) the pK_a value acidity scales of typical thiourea and squaramide-based catalysts [7,8].

The determination of the pK_a values has been the subject of some studies. Since, according to the proton affinity–pK_a equalization principle, the strength of hydrogen bonds can be approximated by the pK_a values of the donor and the acceptor species, these values can be used to characterize the catalytic activity and allow predictions to be made that are useful for developing novel catalysts [8]. The higher the acidity of a hydrogen-bonding donor, the stronger is the resulting hydrogen bond, and therefore, introducing stronger hydrogen-bonding donor groups in a catalyst should result in higher catalytic activity. In

addition, the formation of a strong hydrogen bond should also help with stereocontrol and enantioselectivity. Figure 1b shows the pK_a values of some well-known thiourea- and squaramide-based catalysts, determined by applying the classical overlapping indicator method in DMSO through UV spectrophotometric titrations [5,8–10]. Comparing the pK_a values of related catalysts, it was found that the pK_a values of squaramides are lower than those of their thiourea analogs, with a gap of 0.13–1.97 pK_a units [8]. The actual value itself depends on the nature of other groups attached to the thiourea/squaramide group. However, since squaramides are more acidic than thioureas, they form stronger hydrogen bonds, which may explain why squaramides can often be used at lower catalytic loadings and display higher activity in a range of reactions.

Li, Cheng and coworkers found, from a plot of pK_a values of thioureas versus the pK_a values of the analog squaramides, that there is a good correlation, two good straight lines with R values of 0.995 and 0.932 were obtained, which implies that if desired, the pK_a values of squaramides might be roughly estimated from those of the corresponding thioureas, which have been more studied [8]. In addition, the linear free energy relationship (LEFR) between the acidity and activity of thiourea catalysts was determined with the Michael addition of diethyl malonate to nitrostyrene as a model reaction. Excellent LEFRs were observed for the stereoselectivity correlated with the p*K*a values of the corresponding thioureas. Although there were significant differences between the catalysts, the slopes of the LFERs between p*K*a values and enantioselectivities were almost identical, which suggests a similar process for forming the transition states of these reactions, and hence that the catalysts react by similar mechanisms.

Lu and Wheeler demonstrated that thiosquaramides provide even stronger hydrogen-bonding interactions, and since the introduction of chiral bifunctional catalysts containing this motif by Rawal, they are gaining more interest [11,12].

The literature on mechanistic and density functional theory (DFT) studies concerning hydrogen-bonding organocatalysts has been reviewed occasionally [13]. In many cases, the B3LYP method was used since it has become a favorite in organocatalysis, as it yields accurate geometries and energies. Although we are still far from predicting exactly what will be the stereochemical outcome of a reaction, these studies aim to clarify the mode of action of the catalysts, and to reveal the nature of asymmetric induction, the factors responsible for it, so that better and more efficient catalysts can be designed for future applications. In this review, we survey the information published since 2015, when the last general overview of the field was reported [13].

The review is divided into the following sections:

1. Introduction;
2. Michael and other conjugate addition reactions;
3. Cycloaddition reactions;
4. Aldol and Henry reactions;
5. Miscellaneous reactions involving anion-binding catalysis;
6. Miscellaneous;
7. Conclusions.

2. Michael and Other Conjugate Addition Reactions

2.1. Additions to Nitroalkenes

The largest number of papers encountered covering studies falling within the scope of this review were developments on the Michael addition reaction and its variants [14,15]. The first report on utilizing a bifunctional thiourea-based organocatalyst in synthesis was by Takemoto and coworkers in 2003 [16]. It involved a Michael addition of malonates (**1**) to nitroolefins (**2**) that were achieved with high yields and *ee*s with catalyst **C1** in toluene at room temperature (rt) (Figure 2a). Catalytic asymmetric versions of this reaction were known at the time but required either metal catalysis or strict reaction conditions. This reaction opened the way to intensive research, and soon after, this and other thiourea-based bifunctional catalysts were applied in several reactions, e.g., the aza–Henry reaction,

dynamic kinetic resolution of aza-lactones, Michael addition to α,β-unsaturated imides, the aldol reaction, sp^2-alkylations, spiro-ketal formation and many others [1–4]. The authors showed through experiments using only either the amine or the thiourea as catalysts that for any significant amount of product **3** to be obtained and for high enantiomeric excesses to be achieved, the simultaneous presence of both units in the catalyst molecule was essential. Kinetic studies to elucidate the reaction mechanism suggested that the active catalyst is a monomeric species, and a bifunctional mode of activation of both reactants was proposed [17]. The catalytic cycle (Figure 2b) begins with the deprotonation of the diester by the tertiary amine moiety of the catalyst and the formation of complex **4**. Enolate addition takes place preferentially on the *Si* face of the nitronate via TS2, affording complex **5**. Proton transfer to the nitronate yields the product (**3a**) and regenerates the catalyst.

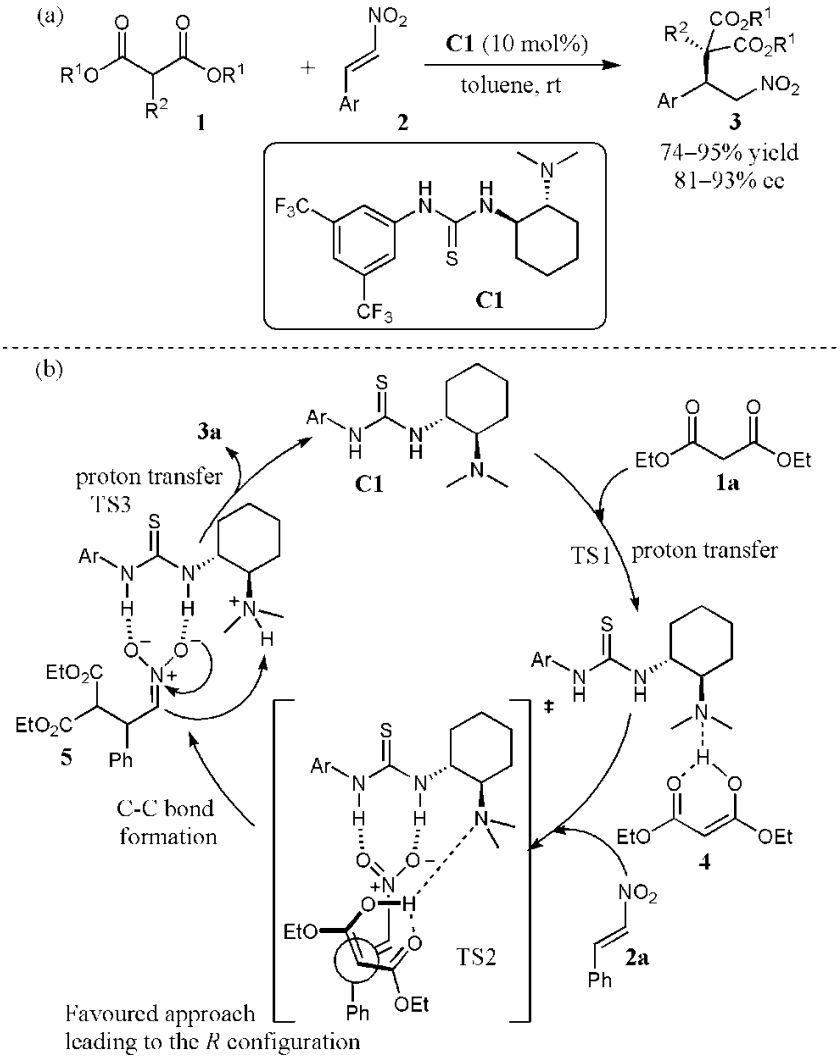

Figure 2. The first bifunctional thiourea-catalyzed reaction (**a**) and its mechanism (**b**) [16,17].

Soon after, two theoretical studies were reported with conflicting results. Liu and coworkers identified, through DFT calculations, proton transfer to the nitronate carbon of complex **5** as the rate-determining step in the catalytic cycle [18]. Papái and coworkers identified two possible binding modes, A and B, for TS2, in which either the nitronate bonds to the thiourea moiety and the diester to the tertiary amine (binding mode A) or vice versa (binding mode B) (Figure 3) [19]. It was calculated that binding mode B is energetically favored by 2.7 kcal mol^{-1} and that carbon–carbon bond formation is the rate-determining step. Other studies have been performed on this reaction and other bifunctional thiourea-based organocatalyzed Michael additions since then, but only the

more recent literature is reviewed here. NMR, crystallographic, and computational studies on related systems have revealed that in the lowest energy-binding conformation, the catalyst displays a "*syn, anti*" configuration of the thiourea functional group and not the traditional thiourea "*anti, anti*" configuration shown in Figure 4a [20–23]. Generally, there are three main activation modes possible to explain thiourea-tertiary amine organocatalysis, namely mode A, attributed to Takemoto et al. [17], mode B, attributed to Pápai et al. [19] and mode C, attributed to Wang et al. [24] (Figure 4b). These three possible modes of activation are usually taken into consideration in this field in theoretical studies when a search is done for the transition state, which better describes a certain reaction and the origins of stereoinduction.

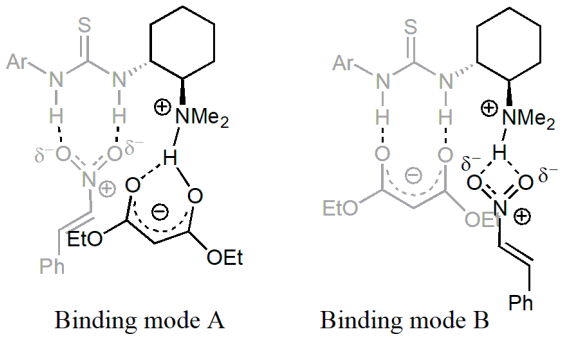

Figure 3. Possible binding modes initially selected by Pápai [19].

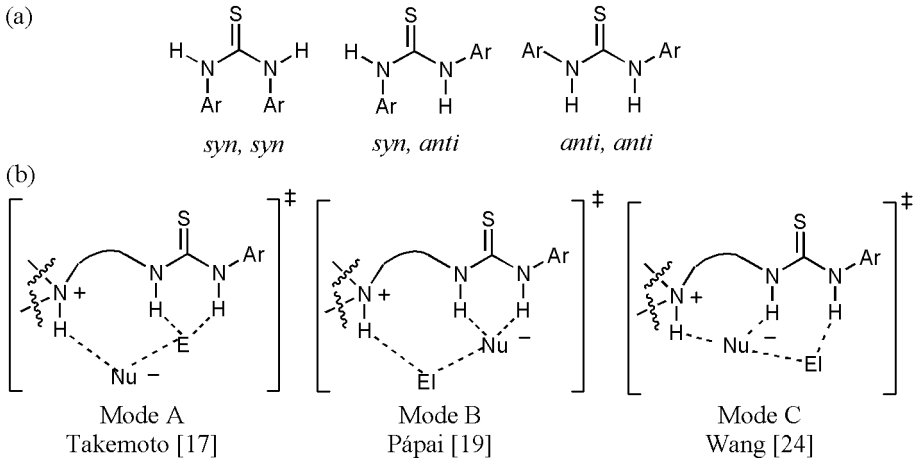

Figure 4. (**a**) Possible binding conformations of thiourea and (**b**) modes of activation proposed for thiourea-tertiary amine organocatalysis [17,19,24].

A recent study by Hirschi, Vetticatt and coworkers on the Michael addition of malonates to nitro olefins aimed to clarify the mechanism of catalysis by tertiary amine thiourea organocatalysts [25]. The addition of diethyl malonate to *trans*-β-nitrostyrene catalyzed by Takemoto's catalyst (**C1**) was selected as a model system. Kinetic isotope effects (KIEs) were determined for both the malonate and the nitrostyrene using NMR at natural abundance from starting material analysis [26]. At ~80% conversion of the nitrostyrene (−65% in the malonate), the unreacted substances were isolated, and their ^{13}C isotopic composition was compared to samples of both substances that had not been subjected to any reaction. KIEs were calculated in the usual manner (Figure 5).

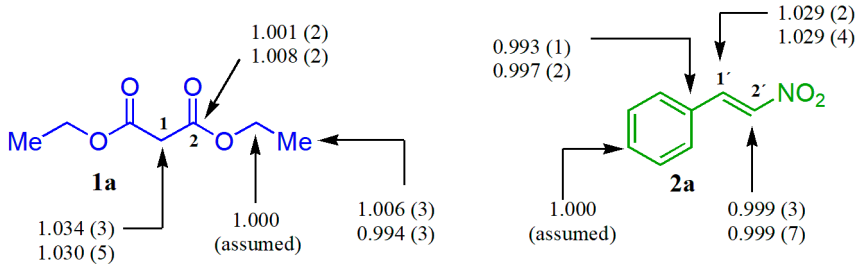

Figure 5. Experimentally measured KIEs for the enantioselective Michael addition of diethyl malonate to trans-β-nitrostyrene catalyzed by **C1** [25].

The results revealed a significant primary ^{13}C KIE on C1 of **1a** (~3%) and C1′ of **2a**, suggesting that both atoms were involved in the rate-determining TS, i.e., that carbon–carbon bond formation is the first irreversible step of the catalytic cycle, as proposed initially by Takemoto and Pápai. DFT calculations were also performed for the transition structures in each step in the catalytic cycle, using the B3LYP method and a 6-31+G** basis set [27]. A polarizable continuum model (PCM) for toluene, as implemented in Gaussian 09, was used to consider solvent effects. The procedure took into account the full system (89 atoms), and it has been shown previously to accurately describe the energetics of other bifunctional thiourea-catalyzed reactions. It was the first time that it was applied to Takemoto's full system [28]. Values of ^{13}C KIEs were also obtained from scaled vibrational frequencies of the respective transition structures using the program ISOEFF98. A Wigner tunneling correction was used. The resulting theoretical predictions at the key carbon atoms of **1a** and **2a** were found to be in good agreement with the experimentally obtained values, supporting the above conclusions.

The relative energies of the transition state structures leading to the two isomers were calculated. Single point energies were obtained using B3LYLP-D3(BJ)/6-311++G** PCM (toluene). The energies of the lowest energy structures for C–C bond formation, the enantioselectivity determining step, were determined using DFT calculations based upon existing models in the literature and a conformational search using quantum mechanical simulations as implemented in DFTB$^+$. The lowest energy structure found, TS2-BMB-S, giving rise to the major enantiomer, is 2.4 kcal mol^{-1} lower in energy than TS2-BMB-R, leading to the minor isomer (Figure 6) [25]. These values correspond to a predicted *ee* of 97% (*S*), consistent with the observed value (93% *ee* (*S*)). The origin of enantioselectivity for this reaction may be inferred from an analysis of the interactions between the different components involved. TS2-BMB-S and TS2-BMB-R possess very similar H-bonding networks. The geometry around the forming C–C bond explains the difference in energy between the two transition states. To accommodate the H-bonding stabilizing interactions with the catalyst, the substituents adopt a staggered conformation (dihedral angle of ~60° between the alkene of **2a** and the ester groups of **1a**) in TS2-BMB-S during C–C bond formation. On the contrary, transition structure TS2-BMB-R has a more eclipsed configuration for these groups (dihedral angle of ~30°) when the C–C bond is forming. The result is increased steric interactions between substrates in TS2-BMB-R compared to TS2-BMB-S, and this is very likely the origin of enantioselectivity in this reaction.

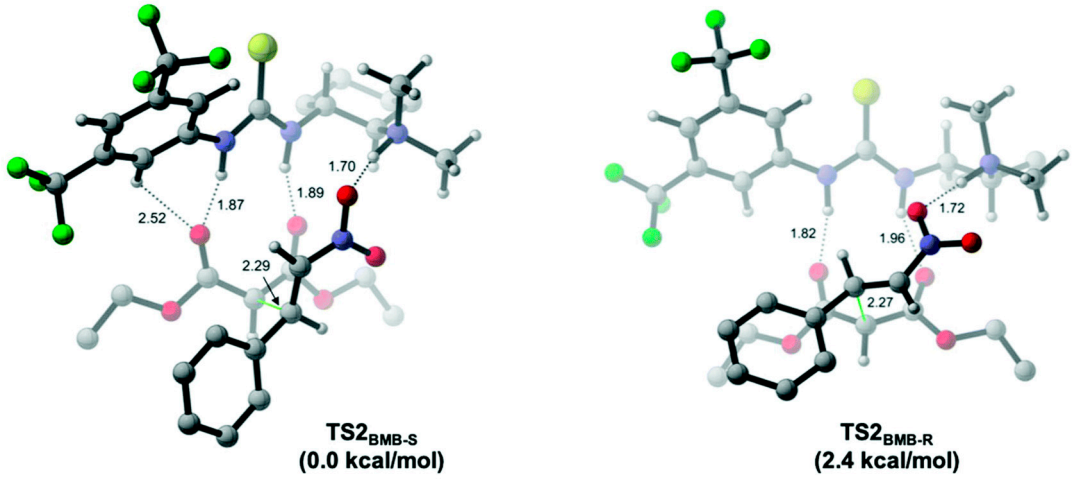

Figure 6. Lowest energy transition structures for the Michael addition of **1a** to **2a** catalyzed by **C1**. Reprinted and adapted from *Organic and Biomolecular Chemistry* with permission from Royal Society of Chemistry [25].

A recent study performed by Pliego Jr on the addition of acetylacetone to β-nitrostyrene catalyzed by Takemoto's catalyst in toluene used the PBE functional for geometry optimization and the DLPNO–CCSD(T) benchmark method for single-point energy [29]. The complete free energy profile calculated for the reaction supported the theory that carbon–carbon bond formation is the rate-determining step. The overall barrier was calculated to be 22.8 kcal mol^{-1} (experimental value ~20 kcal mol^{-1}). It was found that three transition states with S stereochemistry and one with R stereochemistry contribute to the enantioselectivity, and the *ee* was calculated as 88% (experimental value = 84–92%). Some functionals were tested for single-point energy using the DLPNO–CCSD(T) method as a reference. The M06-2X functional provided the best results, even compared to double-hybrid functionals. It was also concluded that the additivity approximation of the correlation energy worked well, and it can be used as an alternative method to obtain accurate electronic energies.

In recent years carbohydrates have been used more frequently as chiral modular units for bifunctional organocatalysts [30]. In 2016 Khan, Narula and coworkers developed thiourea-based catalysts incorporating D-glucose as a core unit and tested them on the addition of ketones to nitroalkenes. One of them, **C2**, provided high *ee*s and excellent stereoselectivities on the addition of cyclohexanone (**6**) to nitroolefins (**7**) (Figure 7) [31]. DFT studies, with the Gaussian 09 program package and the B3LYP/6-311G(d,p)//B3LYP/6-31G(d) basic set, were utilized to explain the stereochemical outcome of the reaction leading to products **8**. The QM/MM calculations suggested that cyclohexanone plays two roles, that of solvent as well as of reactant, in the rate-determining step, imparting 31.91 kcal mol^{-1} of energy towards product formation.

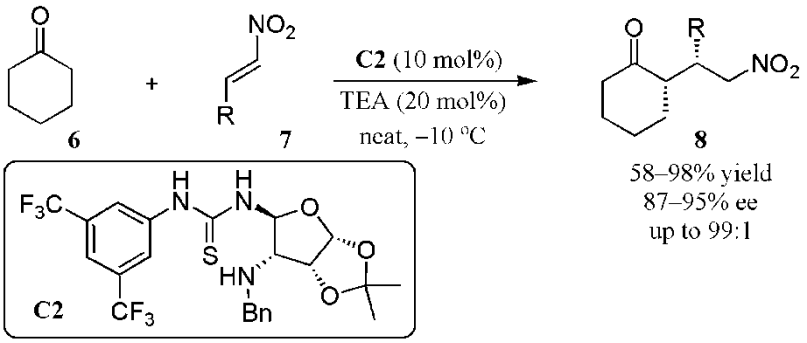

Figure 7. Michael addition reaction catalyzed by **C2** [31].

A Michael addition of isobutyraldehyde (**9**) to nitroalkenes (**2**) was achieved in a highly enantioselective manner by Chinchilla, Nájera and coworkers with primary amine-

guanidine **C3**, derived from *trans*-cyclohexane-1,2-diamine, as catalyst (Figure 8) [32]. Besides other optimizations, with DMF proving to be the best solvent, the addition of water was found to increase both the reaction rate and the *ee*s leading to **10a** (**10**, Ar = Ph) (at 25 °C, with DMF/imidazole, 99% yield, 48% *ee*, with DMF/imidazole/water, 99% yield, 70% *ee*). At lower temperatures, the *ee* improved (to 80%) with a 10% decrease in yield. DFT theoretical calculations helped to explain the origin of the stereoselectivity observed, as well as the role of water in the reaction [32].

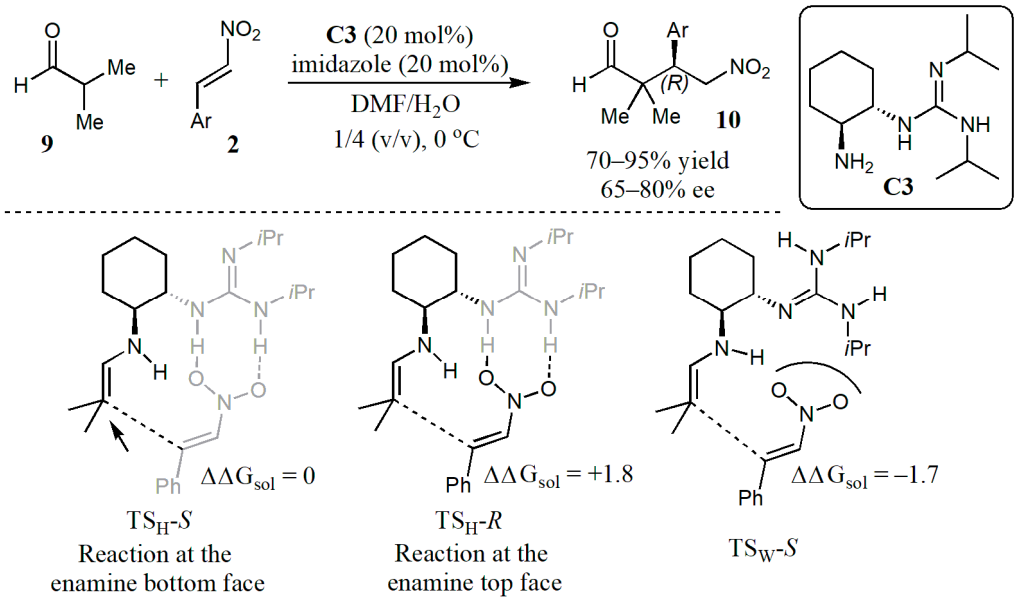

Figure 8. Enantioselective Michael addition of isobutyraldehyde to nitroalkenes catalyzed by **C3** (top) and comparison of the guanidine activated transition states (TS_H-S and TS_H-R) with the water-activated TS (TS_W-S). Free Gibbs energies computed at B3LYP/6-311+G(d,p) (CPCM, water) level [32].

Taking into account intramolecular H-bonding only (TS_H-S vs. TS_H-R), the calculations revealed a preference for the transition state leading to the wrong enantiomer, the (*S*)-enantiomer, found to be 1.8 kcal/mol lower in energy than TS_H-R. This is the result of having both the nitrostyrene and the guanidine subunit both in the lower face of the enamine (from our point of view), adopting a less strained disposition. In TS_H-R, the structure needs to twist to form the internal H-bonds, adding strain to the transition state structure. In practice, the enantiomer obtained was the (*R*)-enantiomer, suggesting that intramolecular H-bonding was not present. Another transition state was found (TS_W-S), in which the nitro group was activated by the solvent (implicit water solvent model), 1.7 kcal/mol lower in activation energy than TS_H-S. In fact, water may serve two purposes, to lower the activation energy, since it can solvate better the more polar transition state (TS_W-S vs. TS_H-S), and to form intermolecular hydrogen bonds with the nitro group, disrupting the intramolecular ones.

Although the lack of intramolecular bonding implies much more molecular freedom and a higher number of possible conformations, the two most stable conformations of the reactive enamine could eventually be found (Figure 9a,b). In theory, nitrostyrene may approach each enamine following two different trajectories. In (a), the face leading to the (*S*)-enantiomer is blocked by the guanidine group and can be ruled out. The remaining three approaches are feasible, but there is not much difference in energy between them. Hence it appears that the (*R*)-enantiomer is obtained preferentially due to the predominance of the sum of TS_A-R and TS_B-R over TS_B-S, and the non-existence of TSA-S, i.e., the steric effect of the guanidine group seems to be the final reason for the preference observed.

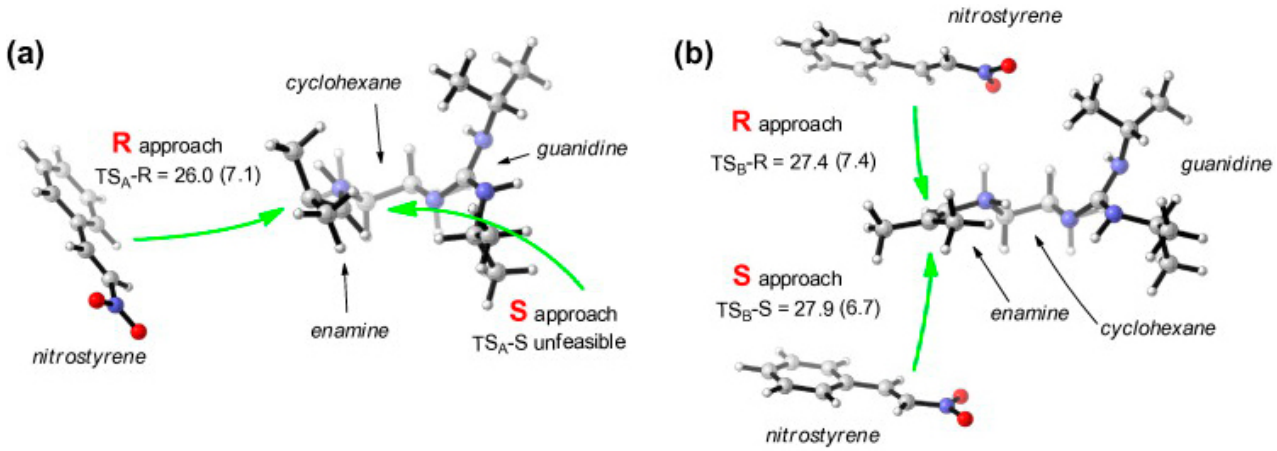

Figure 9. 3D-models for the reaction of nitrostyrene with the two most stable conformations of the enamine, as shown in (**a**) and (**b**), leading to (R)- and (S)-**10**. Free Gibbs energies computed at B3LYP/6-311+G(d,p) (CPCM, water) (M06-2X/6-311+G(d,p) (SMD, water) in parenthesis) Reprinted and adapted from Tetrahedron: Asymmetry with permission from Elsevier [32].

In 2019, Zlotin and coworkers developed a new squaramide-based organocatalyst, which promoted the conjugate addition of β-dicarbonyl compounds (**11**) and kojic acid derivatives (**13**) to nitroolefins, to yield products **12** and **14**, respectively, in nearly quantitative yields and up to 99% *ee*, with a catalytic loading of only 1 mol% (Figure 10) [33].

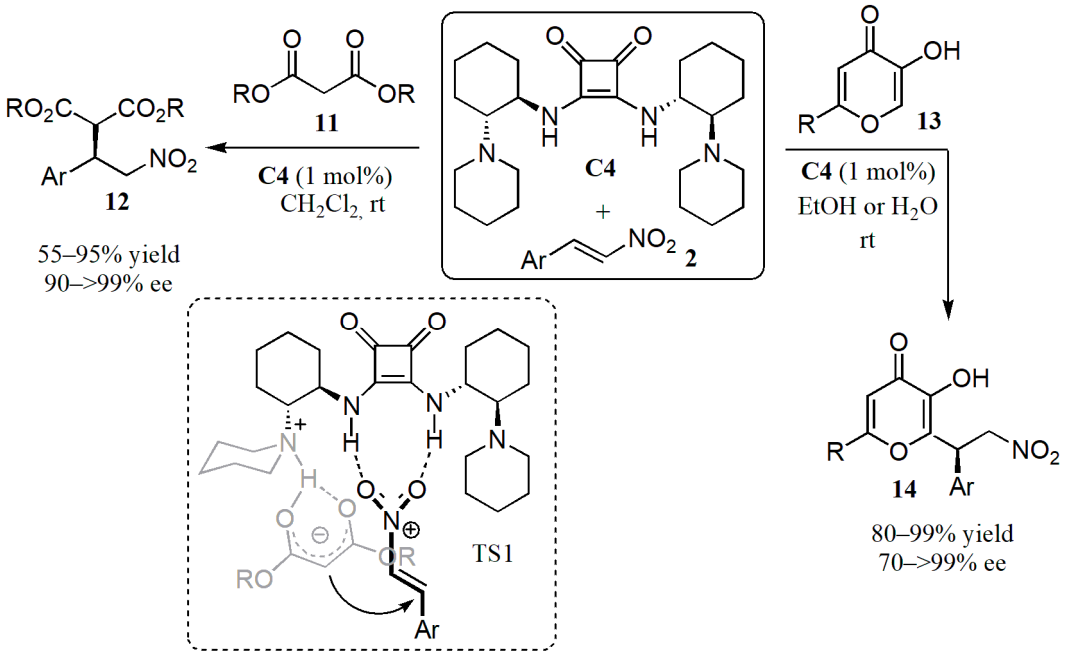

Figure 10. Asymmetric Michael reactions catalyzed by C_2-symmetric amine-squaramide catalyst **C4** and plausible transition state TS1 for the addition of the diesters to the nitroolefins [33].

The best catalyst out of a homologous series tried was **C4**, a C_2-symmetric tertiary amine-squaramide organocatalyst. The reactions with kojic acid derivatives worked well under "green" conditions (in 96% EtOH, or even in pure water). The catalyst could also be easily recovered since it has extremely low solubility in organic solvents, and it was reused up to seven times, making it attractive for applications in the industry.

To ascertain if one or both tertiary amino groups in the catalyst participate in the reaction, the relationship between the *ee* values of the catalyst and those of the corresponding products were determined in protic and aprotic solvents (96% EtOH, H_2O, and CH_2Cl_2).

Irrespective of the solvent, a linear effect was observed for both compounds, suggesting that diastereomeric associates (especially *meso* forms) between **C4** and the reaction products were absent. This can only happen if desymmetrization occurs and only one of the two tertiary amino groups in **C4** acts as deprotonating agents in the corresponding transition states TS1 and TS2. These deductions were also confirmed by experiments in which acid was added to the reaction mixture. The addition of 1 mol% of TFA did not have a negative impact on the results (on the yield or *ee* of **12**). However, if enough TFA was added to protonate both amine groups, i.e., 2 mol%, the catalyst was completely deactivated, and no reaction was observed.

In 2017 Rawal introduced bifunctional thiosquaramides as a novel type of organocatalyst [34]. A range of novel thiosquaramide-tertiary amines was tested on the enantioselective conjugate addition reaction of barbituric acid (**15**) to nitroalkenes (Figure 11). In the same way that changing an oxygen atom in urea to sulfur makes the product thioureas more catalytic active than the ureas, the new thiosquaramide catalysts based on the squaramides also proved to be highly active. The squaramides, originally introduced by Rawal and coworkers in 2008, have found many applications in organic synthesis, particularly as bifunctional organocatalysts, and have become one of the major types of organocatalysts available for developing novel reactions [12]. Despite their popularity, one of their inherent properties is low solubility in nonpolar solvents and a limited ability to modulate the pK_a of the donor hydrogens. These characteristics limit their utility in some applications. The new thiosquaramides are more acidic and significantly more soluble in nonpolar solvents than their oxo-counterparts, showing great promise for future applications. In this work, a series of barbiturates (**16**) was produced in very high yields and excellent *ee*s, with only 0.5 mol% of catalyst. However, the catalysts could be even more efficient. In a model reaction with nitrostyrene, i.e., **7a**, R^1 = Ph and **15a** (R^2 = Ph), when the catalytic loading was lowered to 0.05 mol%, the product (**16a**) was obtained with 96% *ee* and the conversion (determined by NMR spectroscopy) was >98% in a 10 h reaction. The corresponding oxosquaramide (**C6)** at 0.5 mol% afforded identical results to **C5** in terms of yield and a similar *ee* (97 versus 95%, **C5/C6**). X-ray crystallography revealed the presence of two rotameric forms. The H–H distance of the two rotamers was shown to be slightly smaller than those of the corresponding oxosquaramide by X-ray crystallography. Hartree−Fock calculations for **C7** at the 3-21G level of theory gave an H−H distance of 2.60 Å, which suggests that the smaller distance is due to the interactions with the sulfur atoms rather than packing forces or other interactions in the crystal structure. Intermolecular hydrogen bonds to give ladder structures, analogous to those found in the oxosquaramides, were not observed.

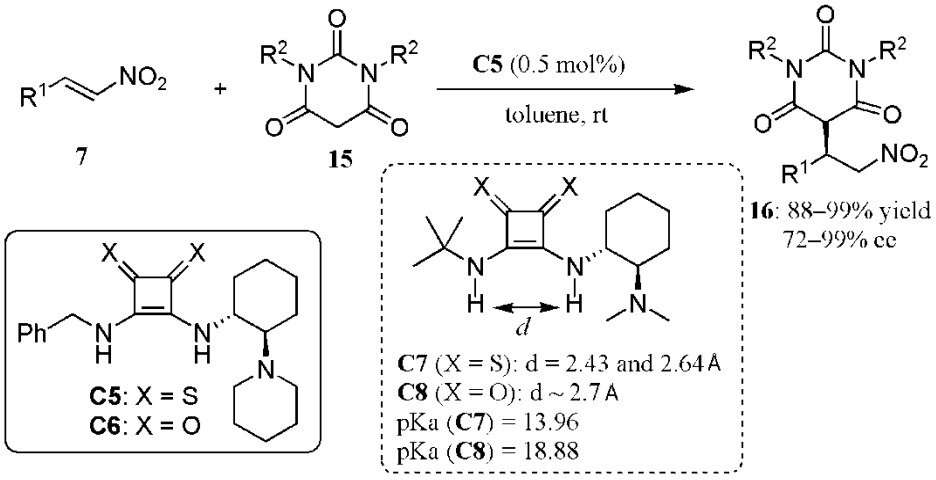

Figure 11. Enantioselective Michael additions of barbituric acids to nitroalkenes catalyzed by **C5**, a novel thiosquaramide catalyst [34].

The development of an enantio- and diastereoselective reaction provides access to the desired enantiomer of a substance whose properties may be quite distinct from those of the other enantiomer, which is of importance for several applications. For example, in pharmaceuticals, the bioactivity of one enantiomer may be different from that of its antipode, and it is not only the absolute configuration of each chiral centre that may be vital, but also the relative configuration if more than one chiral center is present. It may be desirable to access all enantiomers separately from each other, for example, to use authentic standards to test for purity in a manufacturing process, which can be a very challenging task. The development of new strategies to perform diastereodivergent asymmetric synthesis is, therefore, a subject of great interest [35,36]. The utilization of the same synthetic route for all stereoisomers wanted may be possible if a simple change in catalyst provides alternative isomers as the main product.

In 2020 Wang, Zhao and coworkers reported a catalyst-controlled stereodivergent asymmetric Michael addition of α-azido ketones **17** to nitroolefins **7** (Figure 12) [37]. A squaramide-based catalyst (**C9**) afforded selectively *anti*-adducts, while a new bifunctional tertiary amine-phosphoramide catalyst (**C10**) provided preferentially *syn*-adducts. The resulting multifunctional tertiary azides (**18**) were converted to spiro-pyrrolidines with four continuous stereocenters in a one-pot operation. Mechanistic studies were performed to elucidate the reasons for the diastereoselectivity switch, which took place simply by changing the two H-bond donor catalysts.

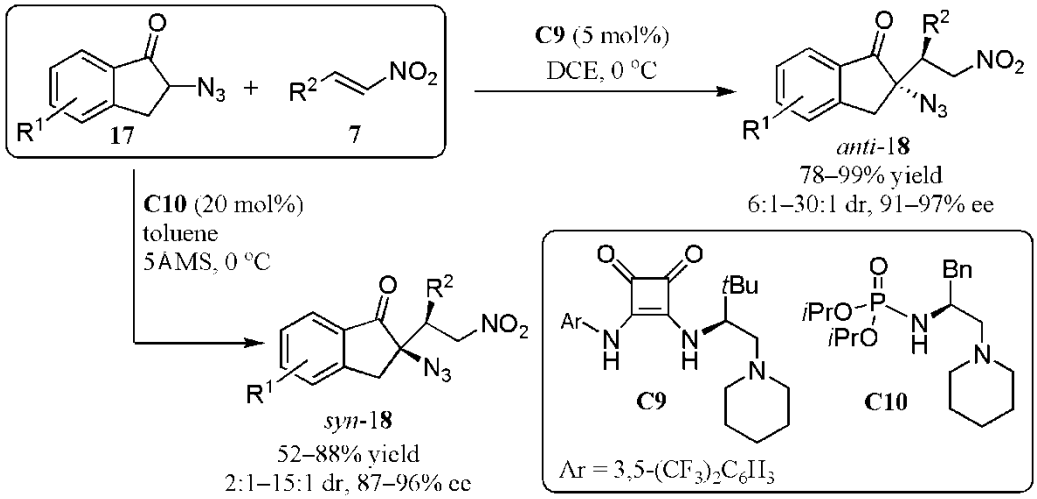

Figure 12. Stereodivergent Michael addition of α-azido ketones **17** to nitroolefins **7** [32].

To elucidate the mode of interaction of the catalysts with the substrates, control experiments were performed. In a model reaction producing **18a** (Figure 13), it was observed that in the case of **C9**, the presence of two NH groups was critical for the yield, although moderate *ee*s could be obtained. Blocking NH(3) with a methyl group caused a reversal in diastereoselectivity. Thus, both NH groups are important for a high yielding and stereoselective *anti* reaction to take place. In the reaction promoted by **C10**, both the NH group and the tertiary N are critical for high reactivity and high *ee*s to be obtained. The presence of the ring nitrogen ensures that there is *syn* selectivity.

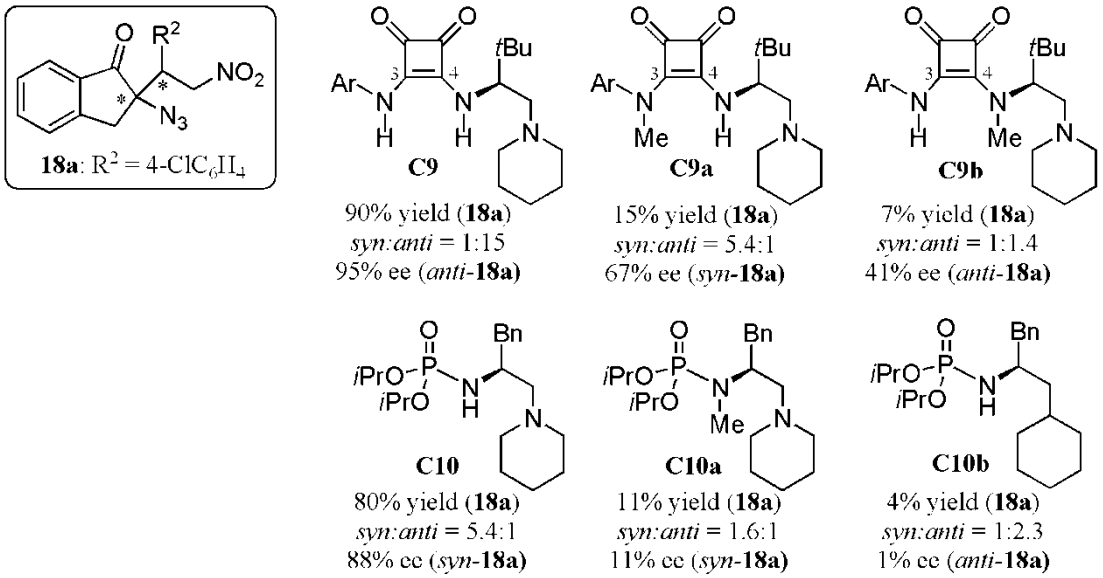

Figure 13. Stereodivergent synthesis of **18a** [37].

A search for nonlinear effects revealed that in the case of **C10,** a monomeric catalytic species was operating since there was a linear relationship between the catalyst *ee* value and that of the product *syn*-**18a**. No conclusions could be drawn for the reactions catalyzed by **C9** due to its very low solubility in CH_2Cl_2. Theoretical studies were performed, and from the lowest energy TS structures, the main interactions responsible for the reactivities observed could be identified (Figure 14). It was found that, while the squaramide-catalyzed reaction proceeded with a TS (TS1-C9) in which both squaramide N–H bonds bind to an enolate intermediate, in the phosphoramide-mediated reaction, an amide N–H bond and an alkylammonium ion formed in situ interact with the nitroolefins, while the enolate is stabilized by nonclassical C–H/O hydrogen-bonding interactions (TS1-C10). This model has no precedence in the literature.

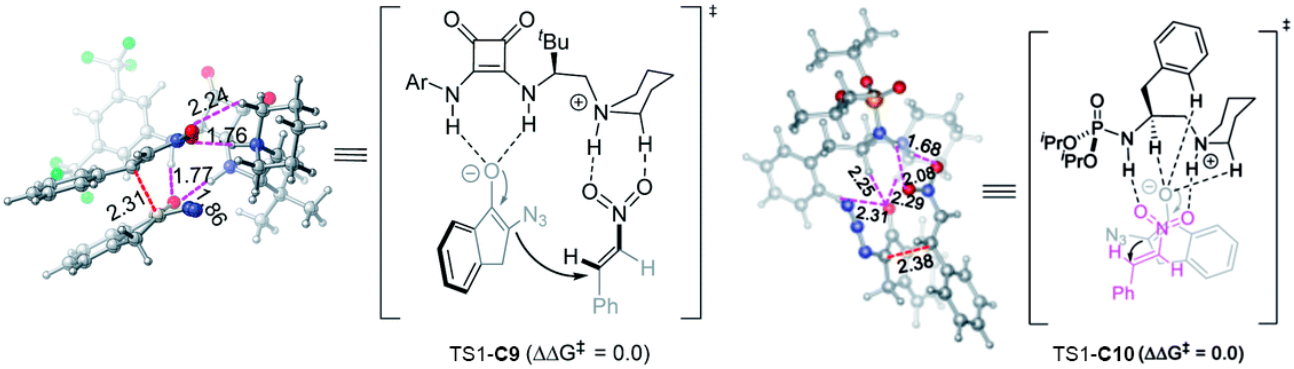

Figure 14. The optimized structures for the transition states of the squaramide and phosphoramide catalyzed reactions between **18a** (R^1 = H) and **7b** (**7**, R = Ph). Only the lowest energy structures (with $\Delta\Delta G^{\ddagger}$ = 0.0) are shown. The bond distances are given in Å. The relative Gibbs free energies are in kcal mol^{-1}, calculated at the IEFPCMM06-2X-D3/6-311++G(d,p)//IEFPCM-M06-2X/6-31G(d,p) level. Reprinted and adapted from Chemical Science with permission from Royal Society of Chemistry [37].

The thiourea-catalyzed Friedel–Crafts alkylation reaction between indoles and nitroalkenes (e.g., **19a** and **7b**) has been the subject of a few studies since its first report by Ricci and coworkers [38]. The utilization of thiourea-aminoindanol catalyst **C11a** to promote the reaction afforded the alkylated indole (**20a**) in 78% yield and 85% *ee* (Figure 15). A bifunctional mode of action was envisioned, and TS1 and TS2 were postulated as being

the TSs responsible for the results obtained. In 2014 Herrera and coworkers reported the results of theoretical studies performed on this reaction to clarify the origin of stereoselectivity [39]. Of interest were previous results that showed that if the configuration of the thiourea-aminoindanol was *R,R*, i.e., as in **C11c**, there was hardly any reaction; with **C12**, missing a hydroxyl group, the product was racemic; and with the analogous catalyst **C13**, lacking an aromatic ring in the aminoindanol skeleton, the yield was very low and the *ee* moderate only (Figure 15) [38,40]. Initially, it was envisaged that the hydroxyl group would drive the reaction to one face of the indole in preference to the other, while the configuration of product **20a** was dependent on the enantiomer of the catalyst used.

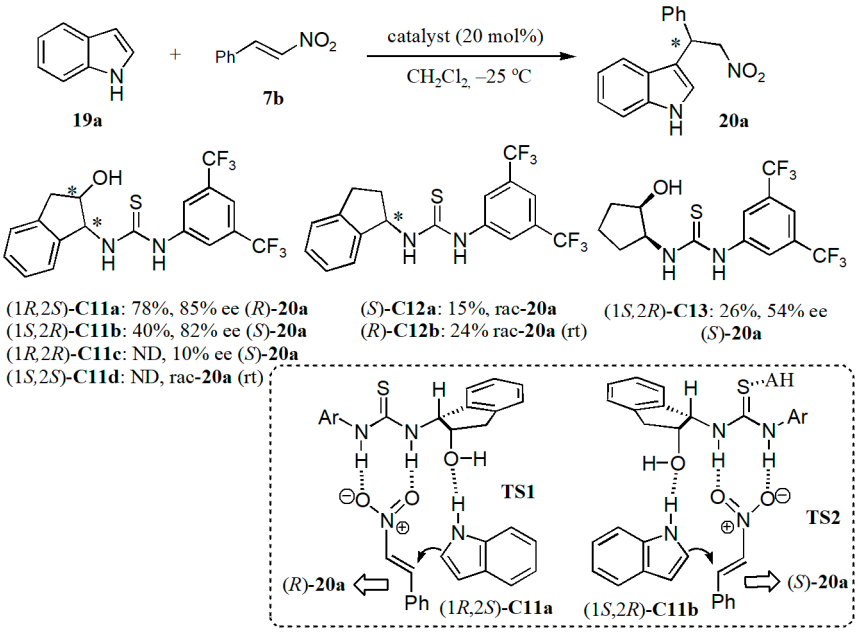

Figure 15. Thiourea-catalyzed Friedel–Crafts alkylation of indole **19a** and the results obtained with catalysts **C11–C13** [38–40]. AH = Brønsted acid additive.

The very low reactivity and selectivity of catalysts C**12** and C**13** are quite noticeable. The lack of a hydroxyl group to direct the attack of an incoming nucleophile can explain the lack of selectivity, but not the low reactivity, which suggests that the hydroxyl group may play yet another role in the reaction. In **C11c** and **C11d,** the hydroxyl group occupies a *trans* orientation, and hence the results obtained suggest the importance of a *cis* relationship in order for the hydroxyl group to play its role in directing the attack of the indole in a stereoselective manner. Theoretical calculations were performed to clarify the origin of the enantioselectivity. The calculations were carried out at the PCM(CH_2Cl_2)/M06-2X/6-311G(d,p) level. A simplified system was studied initially, but the complete system was also studied with catalyst (1*R*,2*S*)-**C11a**, indole (**19a**) and nitrostyrene (**7b**). In all the transition states obtained for the Friedel–Crafts alkylation reaction using a catalyst (1*R*,2*S*)-**C20a**, the hydroxyl group of the catalyst interacts with the NH group of the indole through H-bonding, i.e., in an H–O···H–N interaction, leading the nucleophilic attack as predicted (Figure 16). The small difference in activation energy for indole attack (TS1, 0.0 kcal mol^{-1}) for the *Si* face and (TS2, 2.1 kcal mol^{-1}) for the *Re* face explains the differences in *ee* obtained (85% *ee*). A product with (*R*)-configuration is expected, as observed. In all structures except in TS2, there is bidentate coordination of the nitroalkene, as observed previously by Etter and coworkers [41], which helps to create a more rigid transition state involving all three molecules. The higher stability of TS1 may be the result of a less hindered packaging, minimizing repulsive forces, with the relative orientation of the indole-nitroalkene playing a crucial role in the selectivity. An interesting interaction was found between the hydroxyl group and one of the oxygen atoms of the nitroalkene (O–H···O–N=O) (TS1, TS2, TS5 and

TS6), which supports the lack of reactivity observed when an OH group is not present in the catalyst, or it is not placed in the correct position (Figure 16).

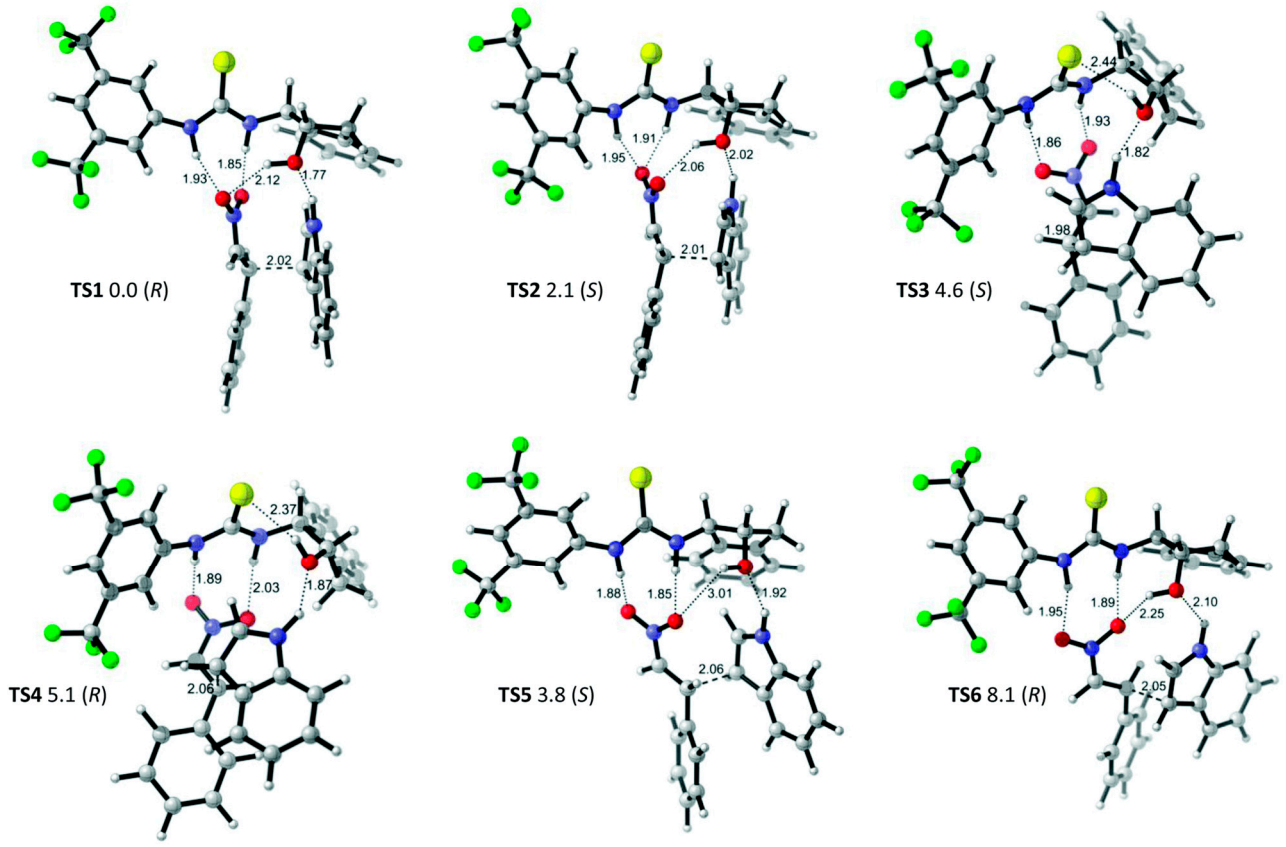

Figure 16. Transition states for the Friedel–Crafts alkylation with catalyst (1*R*,2*S*)-**C11a**. The relative free energies are given in kcal mol^{-1} and the distances in Å. Reprinted and adapted from *Organic and Biomolecular Chemistry* with permission from the Royal Society of Chemistry [39].

In 2017 Fan and Kass achieved high yielding and highly stereoselective Friedel–Crafts alkylations of indoles (**19**) with nitroalkenes using as catalysts a series of methylated and octylated pyridinium- and quinolinium-containing thiourea salts with a chiral 2-indanol substituent, e.g., **C14** (Figure 17) [42]. The new organocatalysts are positively charged analogs of the privileged bis(3,5-trifluoromethyl)phenyl-substituted thioureas. They were shown to be much more active catalysts in many cases, despite the absence of an additional hydrogen bond donor or acceptor site (i.e., the presence of a heteroatom−hydrogen bond or a heteroatom with free lone pairs). Yields in the order of 30% were observed with indoles bearing an electron-withdrawing group, i.e., 5-Cl. Otherwise, they were higher than 75% in reactions conducted at–35 °C. The temperature was kept low since the *ee* was largely influenced by temperature.

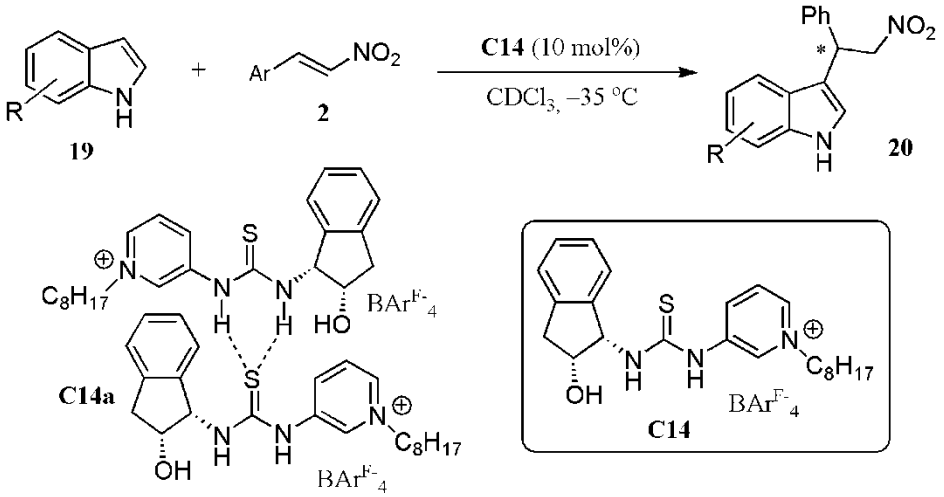

Figure 17. Enantioselective Friedel−Crafts alkylation between nitroalkenes and indoles catalyzed by charge activated thiourea organocatalyst **C14;** $BArF_4^-$ = tetrakis(3,5-bis(trifluoromethyl)phenyl)borate anion [42].

Kinetic studies showed that the reaction is first-order in both indole and *trans*-β-nitrostyrene. A plot of the second-order rate constants versus the square of the catalyst mol% is linear, which suggests that the active catalytic species of the thiourea is dimeric. It was postulated as having structure **C14a**. In the ^{1}H NMR spectra of the catalyst recorded from 5.0 to 20.0 mM, it was observed that both NH signals moved downfield linearly with increasing concentration, consistent with the occurrence of a rapidly occurring monomer/dimer equilibrium. These results suggest that the association constant is small and that the resting state for the catalyst is largely monomeric.

2.2. Additions to Enones and Unsaturated Esters

The first cinchona-thiourea catalyzed the Michael addition of nitroalkanes to enones was reported independently by four different groups in 2005 [43–46]. Given the importance of this C–C bond-forming reaction, it has been the subject of a few computational studies, but the mechanism still remains unclear, and it continues to attract attention. Three activation modes are possible, mode A, mode B and mode C, as shown in Figure 4b [17,19,24].

Since none of these studies explained the origin of selectivity, Grayson undertook a new work in 2017 (Figure 18) [47]. Quantum mechanical calculations were performed using Gaussian 09 (Revision D.01). Mode A, B and C complexes are expected to exist in rapid equilibrium, and therefore, their relative thermodynamic stabilities do not determine the course of the reaction (Curtin−Hammett conditions). In this work, the relative stabilities of the C−C bond-forming TSs (the rate-determining step) were determined to find the favored activation mode and explain the origin of stereoselectivity. Catalyst **C16** was used. DFT calculations showed that the preferred mode of activation is B, in which the electrophile is activated by the catalyst protonated amine and the nucleophile through hydrogen bonds with the thiourea moiety. The TSs that lead to the major and minor products following mode B of activation have *s-cis* and *s-trans* enone conformations, respectively, which differ from each other only by rotation of the quinoline ring by ∼180° (TS_{thio}-B*cis*-(major) and TS_{thio}-B_{trans}-(minor), Figure 19). Previous works have shown that these conformations are strongly preferred over all other possibilities [48]. The other two possible TSs may be obtained if the quinoline ring methoxy group is rotated by ∼180° so that the methyl group is oriented away from the thiourea moiety, but the new conformations were found to be disfavored by at least 2.2 kcal mol^{-1} for the *syn* and *anti*-open conformations of TS_{thio}-B_{cis}-(major) and were disregarded.

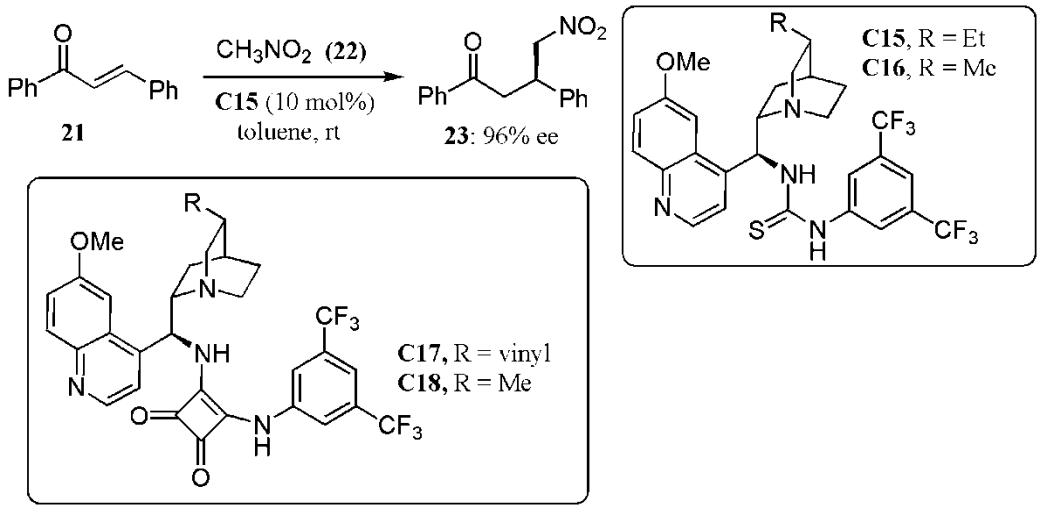

Figure 18. Cinchona-thiourea-catalyzed asymmetric Michael addition of chalcone to enones and the possible activation modes [47].

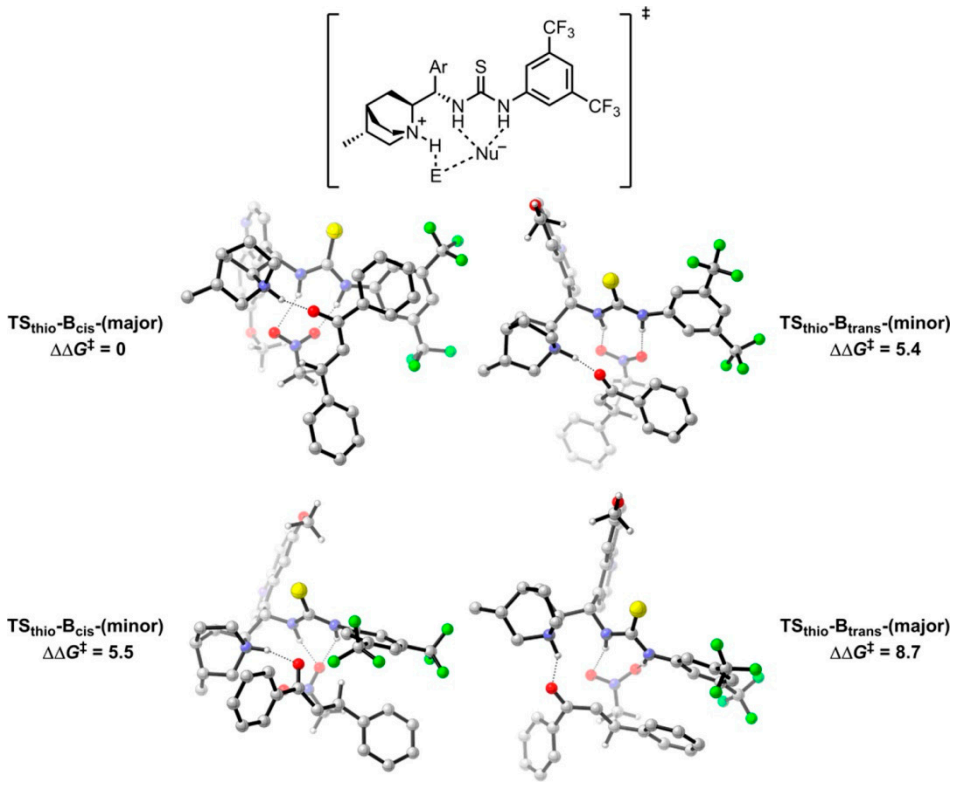

Figure 19. C−C bond-forming TSs in the cinchona thiourea-catalyzed asymmetric Michael addition of nitroalkanes to enones shown in Figure 18, according to mode B. M06-2X/def2-TZVPP-IEFPCM(toluene)//M06-2X/6-31G(d)-IEFPCM(toluene). The noncritical hydrogen atoms were omitted for clarity. All energies are in kcal mol^{-1}. Reprinted and adapted from Grayson, M.N. J. Org. Chem. 2017, 82, 4396–4401, the Journal of Organic Chemistry with permission from the American Chemical Society, Copyright 2017. Note: further permissions related to the material excerpted should be directed to the ACS [47].

The lowest energy TS, TS_{thio}-B_{cis}-(major), leads to the major product observed experimentally (Figure 19). Unfavorable interactions between the enone's phenyl substituent and the catalyst's quinuclidine ring raise the energy of TS_{thio}-B_{cis}-(minor) relative to TS_{thio}-B_{cis}-(major). TS_{thio}-B_{cis}-(major) is also stabilized by π-stacking interactions between the enone's

phenyl group and the catalyst's aromatic ring, which does not happen in TS_{thio}-B_{cis}-(minor). In the other two conformations examined, TS_{thio}-B_{trans}-(major) and TS_{thio}-B_{trans}-(minor), the enone has the less favorable s-*trans* conformation and are, therefore. They are higher in energy. They also have no favorable π-stacking interactions. The s-*cis* conformation of the enone on its own was calculated to be favored over the *s-trans* by 1.0 kcal mol^{-1}. All mode A TSs are disfavored relative to TS_{thio}-B_{cis}-(major) because in mode B TSs stabilize the enone's developing alkoxide to a greater extent than mode A TSs. In the first case, there is proton transfer from the quinuclidinium ion. In the second, there is hydrogen bonding from the thiourea. Attempts to find TSs corresponding to mode C, optimized instead to mode A.

The reaction was also studied with catalysis by cinchona squaramide **C17**. Mode B was again favored over mode A. For generality, the Michael addition of nitromethane to cyclohexenone was also studied. The calculations showed that in the case when the reaction is catalyzed by squaramide **C17** mode B is also favored, by 2.0 kcal mol^{-1}, when the two lowest energy transition states found for each mode of activation are compared, confirming the generality of the reaction.

Furthermore, in 2017 Song and coworkers reported the addition of nitromethane to α,β-unsaturated ketones **24** containing pyridine [49]. A series of cinchona-thiourea-based catalysts were evaluated for the reaction, and finally, high yields and *ee*s could be obtained with **C19** or *ent*-**C19**. The origins of enantioselectivity were probed through computational studies. DFT calculations showed that in the most stable Cat–Nu complex, there were hydrogen bonding interactions between the oxygen on the nucleophile and an N–H group on the thiourea as well as with the protonated quinine amine, in line with Wang´s mode C of activation (Figure 4b) [19]. The reaction was postulated to proceed via TS1 (Figure 20). It was also shown that the products were highly active against rice bacterial leaf blight, with the *S*-enantiomer displaying higher activity than the *R*-enantiomer (for (*S*)-**25a, b**, (a: R = 2-FC_6H_4, b: R = 4-ClC_6H_4) at 100 μM/mL, 100% inhibition).

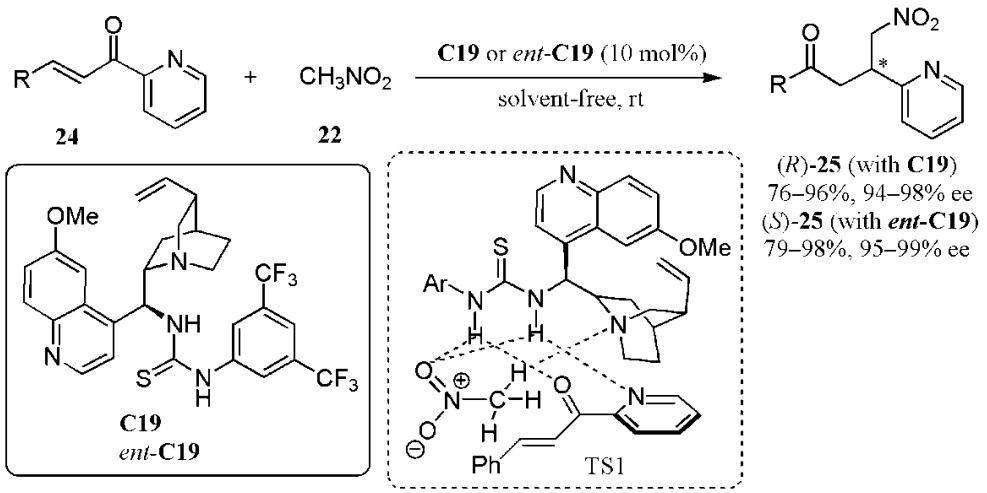

Figure 20. Solvent-free enantioselective conjugate addition of nitromethane to chalcone-containing pyridine [49].

In 2011 Rodriguez and coworkers reported the first organocatalyzed enantioselective Michael addition of β-ketoamides (**26**) to enals and enones (e.g., **27**) (Figure 21) [50]. Products **28**, containing one all-carbon quaternary stereogenic center, are useful synthetic intermediates. The reaction was subsequently the subject of further experimental, spectroscopic and theoretical studies [51]. Tertiary β-ketoamides did not react, showing that the presence of amide hydrogen is crucial for the reaction to occur. Neither did an enone containing an internal double bond, i.e., chalcone. NMR studies with **26a** (R = Ts) showed the absence of an enol form of the substrate in a reagent/catalyst mixture. The presence of hydrogen bonding was suggested by a strong downfield shift of the signals caused by

H1 (δ = 0.5 ppm) and by H7 (δ = 0.7 ppm) of the catalyst. The signals due to the aromatic protons of both the catalyst and the enone were also significantly shifted, indicating a possible interaction between the corresponding functional groups. When the ketoamide was mixed with the catalyst only, fast deprotonation was observed. From a kinetic analysis, among other results, it was found that the reaction was zero-order for the β-ketoamide. A significant primary KIE (KH/D = 1.15) was also observed in a reaction with >80% deuterated β–ketoamide, consistent with rapid deprotonation leading to the active form.

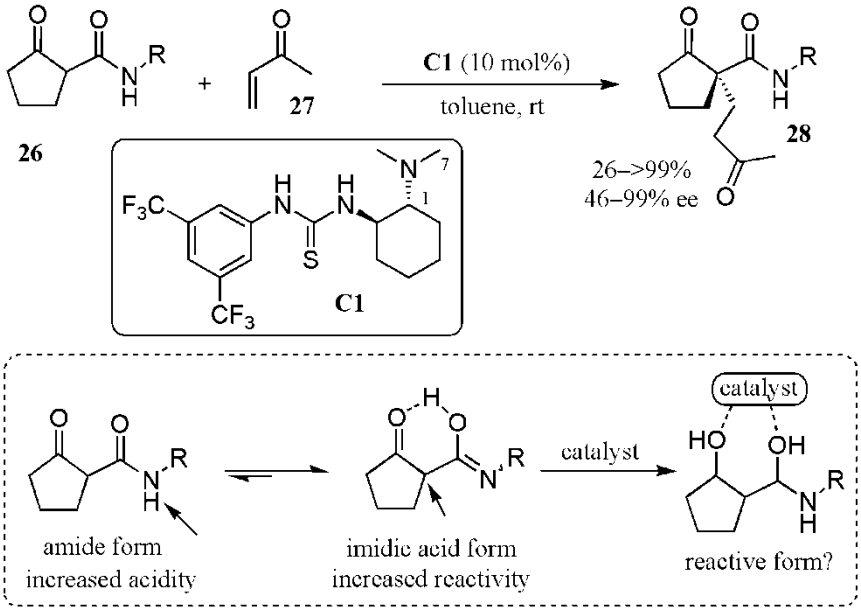

Figure 21. Michael additions of β-ketoamides to α,β-unsaturated carbonyl compounds, catalyzed by **C1** [51].

Computational studies were performed with the hybrid meta-GGA DFT functional M06-2X,34 with the 6-31G(d) basis set. Relative Gibbs free energies were determined for the TSs along the reaction coordinate. Based on the results, as well as on the experimental observations, a detailed catalytic cycle was postulated (Figure 22). It seems that amide hydrogen abstraction by the organocatalyst takes place initially, leading reversibly to an off-cycle unreactive form. An equilibrium back to the starting β-ketoamide and subsequent enolate methine hydrogen abstraction would be the preferred path. Subsequent coordination of the enone to the amide hydrogen leads to the direct formation of the most stable enolate intermediate. Nucleophilic addition takes place next, a thermodynamically unfavored process because the resulting intermediate lies higher in energy than the ternary complex deprotonated β-ketoamide-protonated catalyst-enone (ΔΔG = 3.9 kcal mol^{-1}). Enantiodifferentiation takes place in this step.

In the most favored transition states, the β-ketoamide takes up a perpendicular orientation concerning the thiourea. The TS leading to the *R* adducts was found to be lower in energy by 2.9 kcal mol^{-1} over the TS leading to the *S* adducts (e.g., **28a**), in agreement with the experimentally observed 99% *ee* value. The ease of proton transfer from the amide to the enolate, and the high stability of the resulting intermediate, are probably responsible for the equilibrium shift in this thermodynamically unfavorable C–C bond-forming step. This probably explains why the acidity of the amide proton is crucial for success. Furthermore, of interest is the fact that the deprotonated amide–ammonium complex was found to be thermodynamically more stable than the separated products (ΔΔG = 4.6 kcal mol^{-1}), in complete agreement with the experimentally observed inhibition of the catalyst by the product.

An enantioselective organocatalytic conjugate addition of α,β-unsaturated ketones **29**, promoted by a bifunctional organocatalyst, cinchona-squaramide **C17**, was described

by Fernández-Salas, Alemán and coworkers in 2019 (Figure 23) [52]. The attractiveness of this method lies in its environmentally friendly nature since employing $TMSN_3$ (**30**) as a nucleophile avoids the use or preformation of hydrazoic acid, a dangerous and highly explosive substance. No acidic additives were required either. The formation of a chiral carbon at the carbon C–N bond occurs in a highly enantioselective manner, and the product *β*-azido ketones **31** were obtained with good yields. It was found that the presence of water was important, causing a significant enantioselectivity enhancement (from 53 to 93% ee), and an initial controlled amount was used to ensure reproducibility issues. The best results were obtained in the presence of 0.5 equivalent of water.

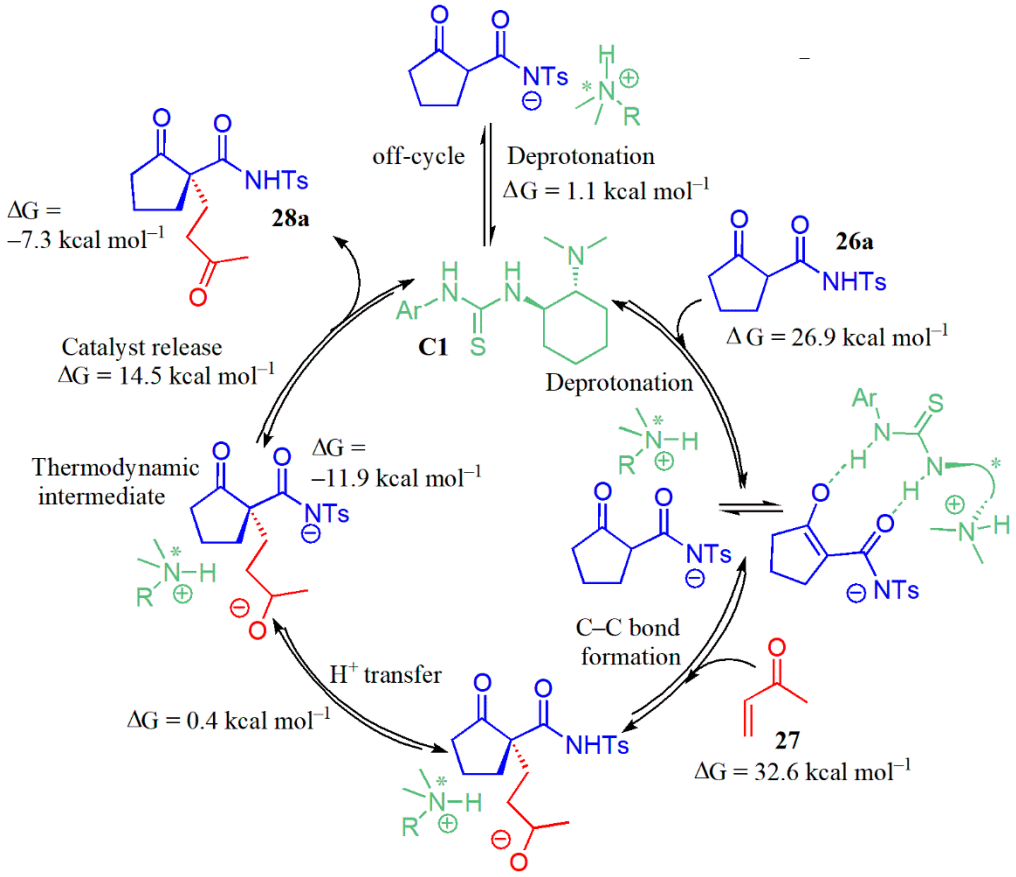

Figure 22. Mechanism postulated for the Michael addition of β-ketoamides to α,β-unsaturated carbonyl compounds, catalyzed by **C1** [51].

The reaction mechanism was studied by ^1H and ^{29}Si NMR spectroscopy and DFT calculations. The role of water was studied through analysis of the reaction side-products. It was found that after a catalytic run, even if water was not added to the system, two new silylated species had been produced, trimethyl silanol (δ 15.82 ppm (^{29}Si-NMR)) and its corresponding siloxane (δ 6.57 ppm), as observed using ^2D-HMBC{^1H,^{29}Si}. The addition of excess water accelerated the reaction but deteriorated the *ee*. These results appear to suggest that activation of $TMSN_3$ proceeds via hydrolysis, although, in the absence of catalyst, water could not activate $TMSN_3$. DFT calculations showed that proton transfer is involved in the rate-determining step (in good agreement with experimental kinetic data). In control experiments, it was observed that $TMSN_3$ hydrolyzes in hexafluorobenzene in the presence of an acid additive but not in the presence of water alone. Therefore, no NH_3 is formed in situ during the reaction, but it appears that there is proton transfer from the water molecule to the nitrogen atom of the quinuclidine unit followed by a nucleophilic attack of the resulting hydroxide to the silicon atom and N–Si bond cleavage. The theoretical results suggested that these processes take place in an asynchronous concerted manner.

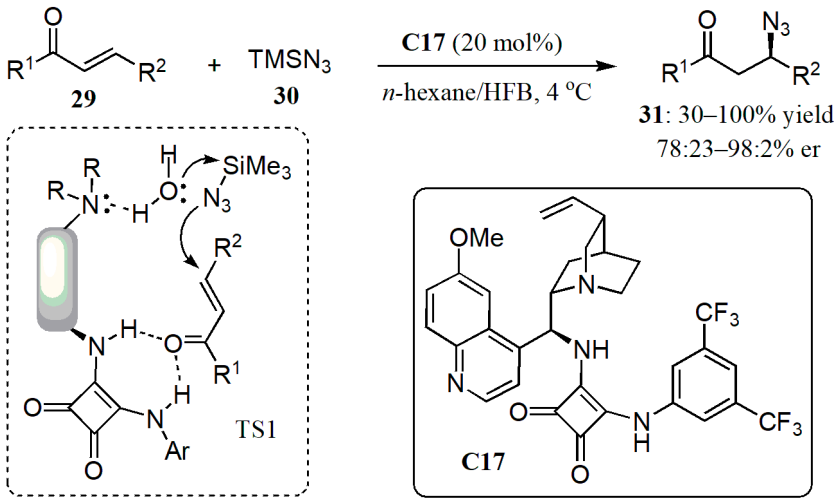

Figure 23. Enantioselective organocatalytic conjugate azidation of α,β-unsaturated ketones with $TMSN_3$; HFB = hexafluorobenzene [52].

Organocatalyzed sulfa-Michael reactions have been known since 1977, when Winberg and coworkers showed that aromatic thiols could add to cycloalkenones in an enantioselective manner in the presence of cinchona alkaloids [53]. These findings represent a milestone in organocatalysis, and since then, many cinchona alkaloid derivatives have been developed to promote a wide range of asymmetric reactions [54,55]. Wynberg proposed a dual-mode of activation in which the thiol, after deprotonation by the quinuclidine nitrogen of the organocatalyst, would remain coordinated to the tertiary amine center, while the enone hydrogen, bonded to the hydroxyl group, was placed in a good orientation for the reaction to proceed in an enantioselective manner. Catalysis by cinchona alkaloid-squaramide catalysts was introduced by Chen and coworkers in 2010 [56]. A theoretical study on this reaction was performed by Guo and Wong recently to investigate the mode of bifunctional activation and the origin of stereoselectivity [57]. The authors aimed to disclose guidelines that could be used for the rational development of more efficient bifunctional catalytic systems based on hydrogen-bonding activation. Geometry optimizations of equilibrium and transition state structures were performed using the M06-2X density functional with the standard 6-31G(d) basis set. In a similar manner to catalysis by bifunctional thiourea-based organocatalysts (Figure 4b), it is also possible to distinguish a few modes of activation with squaramide-based organocatalysts. For the formation of the C–S bond in the sulfa-Michael reaction between **21** and **22**, four distinct modes of activation (A–D) are possible (Figure 24). Mode A is Takemoto's mode of bifunctional activation also observed for bifunctional thiourea-based catalysts; in a similar manner, mode B is Pápai's; mode C was postulated in a joint experimental/theoretical study on a bifunctional cinchona alkaloid-thiourea catalyst by Wang and coworkers, although they also considered it for squaramide-catalyzed reactions [24]; and finally, in mode D, the electrophile interacts with the alkylammonium and one of the N−H groups of the Brønsted acid, while the nucleophile does so with the distal N−H of the acid. All these modes of activation were investigated by Guo and Wong as possibilities for activation of the sulfa-Michael addition reaction between benzyl thiol **32** and *trans*-chalcone **21,** leading to **33**. It has been shown that, since the initial protonation of the catalyst, as well as its final deprotonation in the catalytic cycle, is facile, the C–S bond-forming step is the rate-determining step. The conformations of the protonated catalyst were investigated first. The two N−H groups of the squaramide have a *syn* alignment in the active catalytic conformation. The vinyl group on the quinuclidine moiety has been shown to be *anti* concerning C2−C3 bond in a different study, and it was adopted as such in this study [58]. Since there is free rotation around the C8−C9 and C4′-C9 bonds, six main conformations are possible, *anti*-open, *syn*-open, *anti*-closed, *syn*-closed, plus two hindered conformations, which were ignored since coop-

erativity between the three N−H functionalities of the protonated catalyst is not possible in those cases, and therefore, they are not catalytically active. Previous studies also showed that the protonated catalyst $CatH^+$ favors the open conformations by at least 16 kJ/mol over the closed ones, and therefore, closed conformations were also not examined in this study. The energies of these conformations were calculated, and the lowest energy one was found to have the *anti*-open form. The next lowest conformation is the *syn*-open conformer, which is less stable by 7.0 kJ mol^{-1}. These results agree with a report by Sharpless of epiquinine in solution, for which the *anti*-open form was the only conformer found to be present [59].

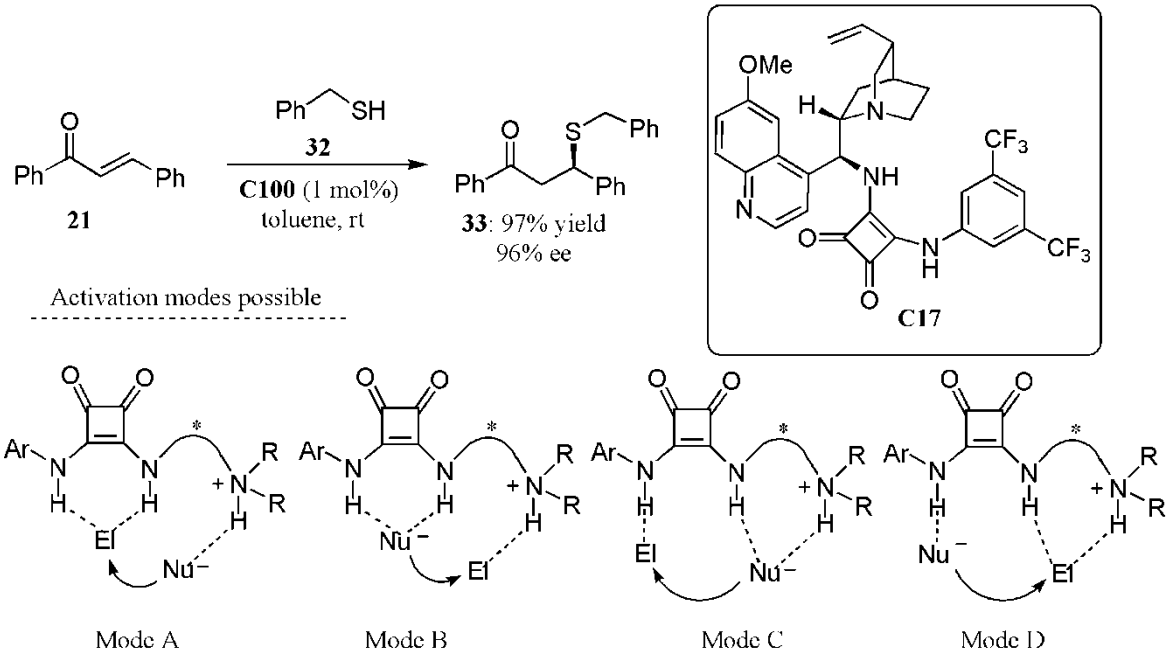

Figure 24. The sulfa-Michael addition reaction between benzyl thiol and *trans*-chalcone catalyzed by cinchona alkaloid-squaramide catalyst **C17** and the four modes of bifunctional activation possible in the C–S bond-forming step [57].

In this conformation, the squaramide ring is coplanar to the 3,5-bis(trifluoromethyl)phenyl group, and this orientation is stabilized by an attractive C−H···O interaction between one carbonyl oxygen of the squaramide moiety and the acidic ortho-proton of the aromatic ring. The 6′-methoxy group of the quinoline moiety is also coplanar to the quinoline ring.

Transition states for the C–S bond-forming step were calculated for each activation mode, with the *anti*-conformation of the protonated catalysts (Figure 25). The lowest energy TS was found to be in mode B, TS-B-R, which gave rise to the major (*R*)-configured product, in agreement with the experimental findings. Both TS's of mode A (TS-A-R and TS-A-S) are less stable by more than 13 kJ mol^{-1}. The TSs with *syn*-open arrangements were much higher in energy (by at least 26 kJ mol^{-1}), and those related to mode C were even higher in energy. Hence, they were all disregarded. TS's for mode D could not be located. To determine the origin of stereo-induction, a distortion−interaction analysis was carried out. The factors that make mode B the preferred conformation are a greater stabilization of the developing alkoxide by the quinuclidinium ion rather than hydrogen-bonding interactions. The excellent stereo-selectivity observed with mode B stems from the more favorable cooperative noncovalent interactions: hydrogen bond, π-stacking, C−H···π interaction, and C−H···F interactions, between the catalyst and the substrates in the major transition state. NCI plots show that the 3,5-bis(trifluoromethyl)phenyl moiety is capable of forming multiple attractive interactions with the substrates to help in differentiating the stereo-controlling transition states. These results are in agreement with Houk's Brønsted acid-hydrogen bonding model for the sulfa-Michael addition reaction with enones, catalyzed by

cinchona alkaloids, in which the enone is activated by the alkylammonium ion, while the thiolate electrophile coordinates with the catalyst's hydroxyl group [60].

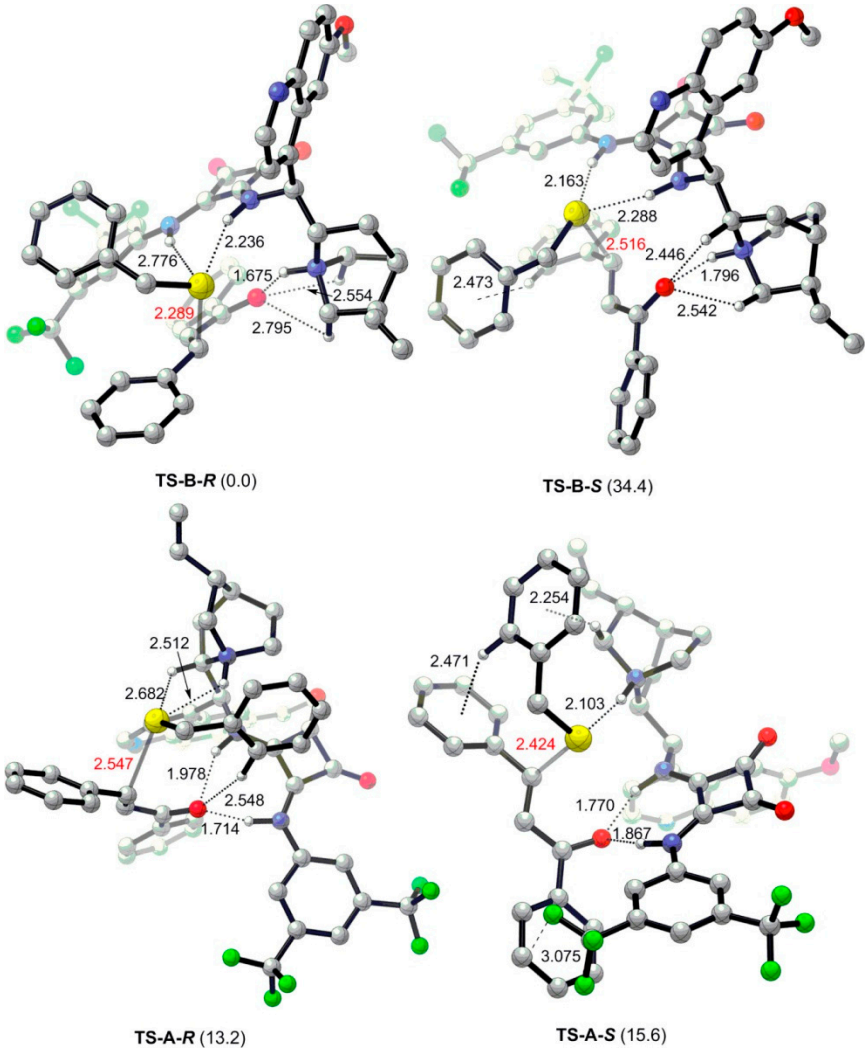

Figure 25. C–S bond-forming transition states for the sulfa-Michael reaction between benzyl thiol and chalcone in modes A and B. Relative Gibbs energies (in kJ/mol) are given in parentheses. Intermolecular distances are given in Å. Nonessential hydrogen atoms are omitted for clarity. Reprinted and adapted from Guo, J.; Wong, M.W. *J. Org. Chem.* **2017**, *82*, 4362–4368, the Journal of Organic Chemistry with permission from the American Chemical Society (Copyright 2017) [57].

Grayson and Houk recently published DFT studies on the asymmetric conjugate addition of aromatic thiols, e.g., **35** to cycloalkenones (**34**) catalyzed by cinchona alkaloid-derived ureas **C20/C21**, a reaction first reported by Singh and coworkers and reported in 2010 [48,61]. This was the first detailed mechanistic study of a cinchona urea-catalyzed reaction [61]. In recent reports on other reactions catalyzed by cinchona-ureas, it was generally found that when comparison data were available, cinchona urea catalysts yielded similar or better levels of enantioselectivity than their thiourea counterparts [48,62], which prompted this study. Since urea is a much weaker acid than thiourea (pK_a = 26.9 and 21.1, respectively, in DMSO), it may happen that cinchona urea and thiourea catalysts operate by different reaction mechanisms.

In these studies, the rate-determining C−S bond-forming step was investigated to determine the preferred mode of catalyst activation and to explain the observed selectivity. The activation modes considered were the same as those described above for thiourea catalyzed reaction, modes A, B and C (Figure 4b) [17,19,24]. The TSs were located at

the M06-2X/def2-TZVPP-IEFPCM(toluene)//M06-2X/6-31G(d)-IEFPCM(toluene) level of theory using Gaussian 09, and a methyl group was used instead of the vinyl group on the quinuclidine ring to simplify the calculations. Of all the major conformations possible for the protonated catalyst, the *anti*-open conformation was found to have the lowest energy, and it was considered for further study (Figure 26). A total of 78 unique pre-reaction complexes were located [48]. In complex **113**, found to have the lowest energy, the thiolate is closely associated with the alkylammonium ions, and there are hydrogen-bonding interactions from the urea group to the thiolate. The alkylammonium ion interacts with the enone too. It was found in this study that the transition states of lowest energy, giving rise to the major and minor products observed experimentally, were obtained via mode B, i.e., TS1 for the major product, Figure 26.

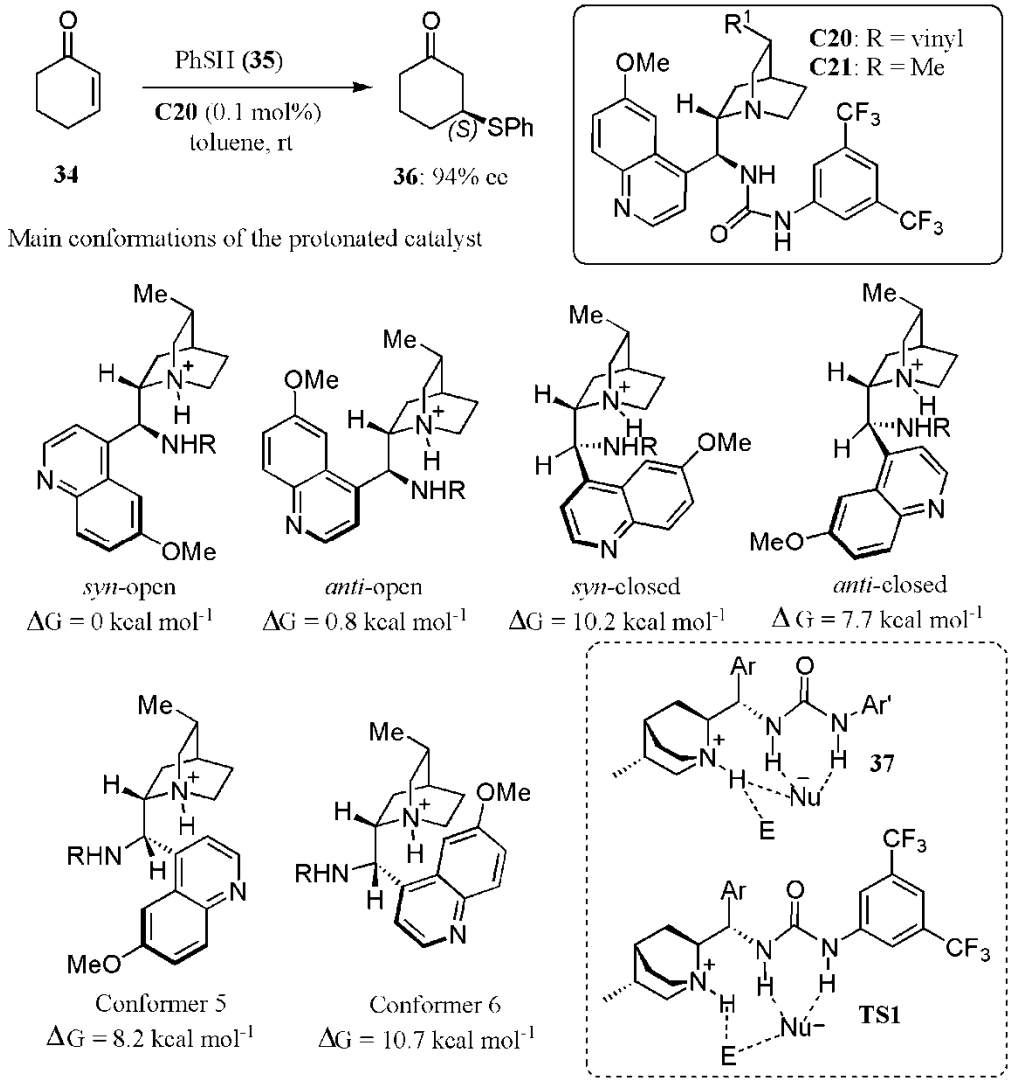

Figure 26. Asymmetric conjugate addition of thiophenol to cyclopentenone catalyzed by cinchona alkaloid-urea **C20** [61] and possible conformations of the protonated catalyst **C21** [48]. All energies are in kcal mol^{-1}.

From **37**, the free energy barrier to TS-B(major) is 10.9 kcal mol^{-1}. The nucleophilic attack takes place axially on the half-chair cyclohexenone, in preference to equatorial attack by 3.3 kcal mol^{-1}. TS-B(minor), which leads to the minor product via mode B, is destabilized relative to TS-B(major) by 3.9 kcal mol^{-1}. No obvious steric interactions were found to contribute to this difference in energy. However, the geometry adopted by enone **34** in TS-B(minor) results in a longer and less directional interaction from the quinuclidinium

ion to the enone oxygen relative to TS-B(major) (N−H···O distance = 1.59 and 1.65 Å and N−H···O angle = 151° and 143° in TS-B(major) and TSB(minor), respectively). It was also found that in TS-B(major), there is a staggered conformation about the developing C−S bond, whereas, in TS-B(minor), there is an eclipsed conformation (CSCH dihedral = 69° and 6°, respectively). In TS-B(major) there is only one NH···S interaction is present, but the other urea NH hydrogen interacts with the π system of the thiolate instead. It was also found in this study that the quinoline ring methoxy group has a strong effect on the TS energy, an effect, which has not been considered in previous mechanistic studies of reactions catalyzed by cinchona alkaloids.

In 2020 Vetticatt, Hirschi, Seidel and coworkers described a new type of bifunctional catalyst, a selenourea-thiourea Brønsted acid catalyst (**C22**), which catalyzed the conjugate addition of cyclic amines **39** to inactivated α,β-unsaturated esters **38** [63] (Figures 27 and 28). β-amino esters **40** were obtained with high *ee*s. DFT calculations and ^{13}C kinetic isotope effect studies helped to throw some light on the reaction mechanism. The catalyst could also be successfully used for the kinetic resolution of cyclic amines.

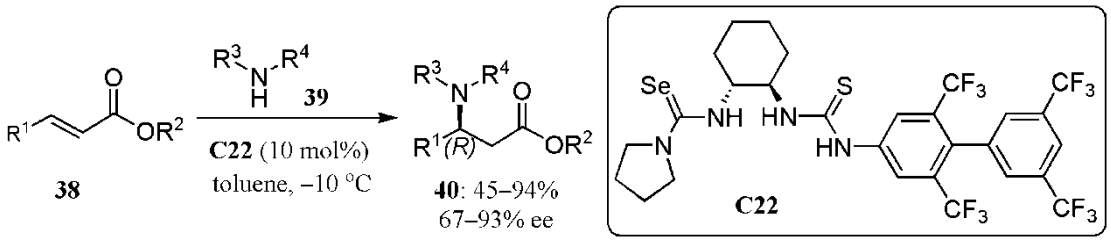

Figure 27. Synthesis of β-amino esters **40** with **C22** as catalyst [58].

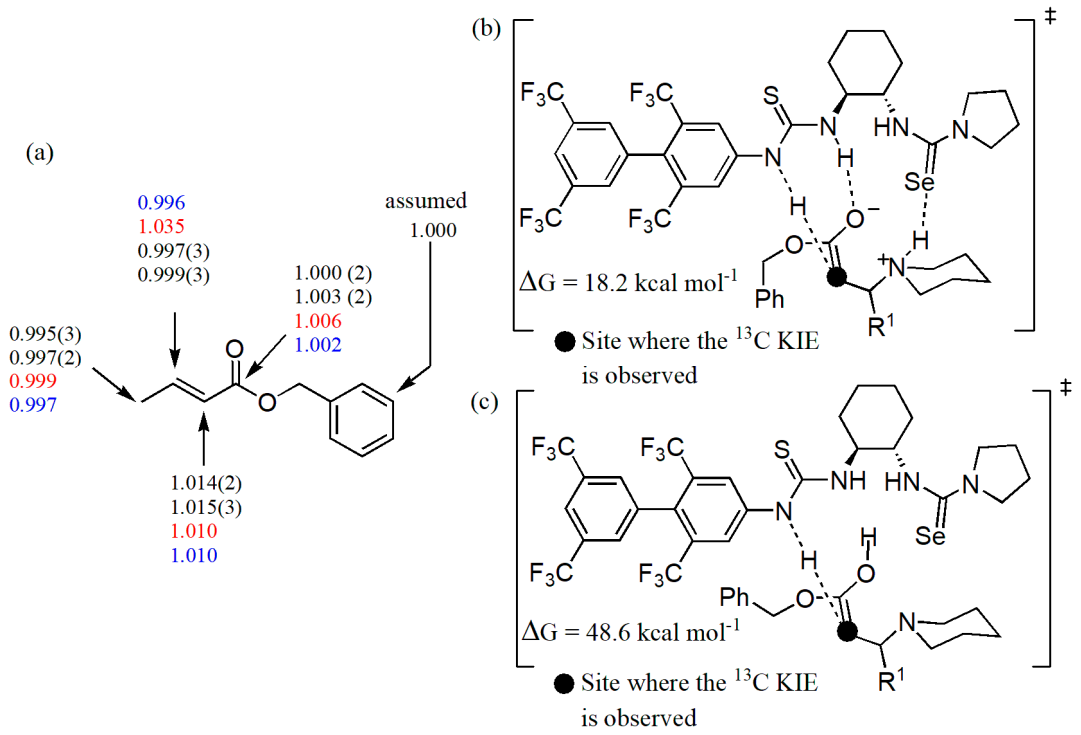

Figure 28. Synthesis of amino esters **40** from compounds **38**. (**a**) Observed KIEs (in black) and calculated KIEs for the C−N bond-forming transition structure R-TS_{C-N} (in red) and for the direct C-protonation transition structure R-TS_{C-prot} (in blue) and the possible transition states according to the experimental KIEs; (**b**) catalyst-mediated C-protonation and (**c**) catalyst-mediated tautomerization [63].

^{13}C kinetic isotope effects (KIEs) were determined for benzyl crotonate using Singleton's ^{13}C NMR methodology for starting materials at natural abundance. Benzyl crotonate and piperidine were reacted and taken as 75 ± 2% and 79 ± 2% conversion concerning the ester. Unreacted benzyl crotonate was reisolated, and the ^{13}C isotopic composition was compared that in samples of crotonate not subjected to the reaction conditions. From the changes in relative isotopic composition and the fractional conversion, ^{13}C KIEs were determined (in duplicate) in the standard way. The values obtained are shown in Figure 28. For confirmation, ^{13}C values of KIEs were also predicted from the scaled vibrational frequencies using the program ISOEFF98 for both R-TSC−N and R-TSC–prot, then applying a Wigner tunneling correction to all values. The most interesting results are the unity KIE observed at the β-carbon and the normal KIE of ∼1.5% on the α-carbon. If C−N bond formation was the first irreversible step in the catalytic cycle, a normal KIE was expected on the β-carbon, not unity, which implies reversible C−N bond formation. A normal KIE on the α-carbon (∼1.5%) suggests that α-protonation is likely to be the first irreversible step in the catalytic cycle. The calculated values are in agreement with these postulates. Therefore, C–N bond formation is a reversible event, and the rate- and enantio-determining step occurs after. These results suggested that the origin of enantioselectivity would be better understood if the transition state analysis were made for the α-carbon protonation step. Since there is no external Brønsted acid, the most acidic proton would be one of the thiourea NHs, which would then be involved in α-protonation. Two situations are possible: an α-carbon−catalyst-mediated tautomerization or catalyst-mediated direct C-protonation. An investigation using DFT calculations showed that catalyst-mediated tautomerization of the enol is prohibitively high in energy (ΔG‡ = 48.6 kcal mol^{-1}), whereas catalyst-mediated C-protonation is energetically accessible (ΔG‡ = 18.2 kcal mol^{-1}) (Figure 29). In the lowest energy TS leading to the R-enantiomer, it was found that there is strong intramolecular H-bonding between the protonated piperidine and the enolate oxygen (1.81 Å). One thiourea NH is loosely bound (2.35 Å), while the other (more acidic) is transferred to the ester α-carbon. Selenium forms a weak nonconventional CH···Se interaction (2.76 Å) with one of the α-CHs of the piperidine moiety. There have been a few scanty reports on the involvement of a thiourea catalyst as a Brønsted acid in mechanisms, and this related behavior of Se represents a new mode of catalysis, which could be used as a guide in future developments.

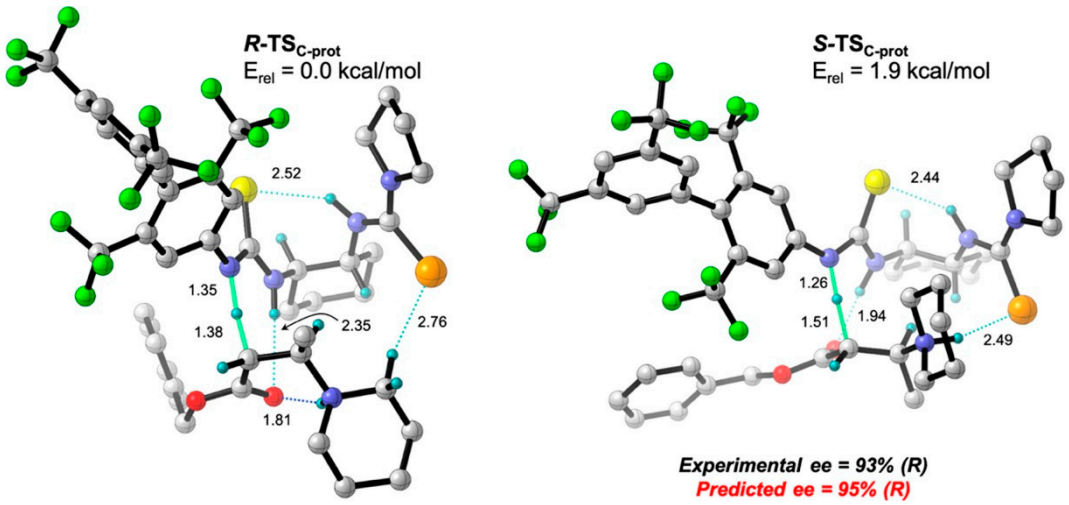

Figure 29. Lowest energy transition structures for C−N bond formation catalyzed by selenourea-thiourea catalyst **C22**. Reprinted and adapted from The Journal of the American Chemical Society with permission from the American Chemical Society [63].

2.3. Cascade Reactions Involving Conjugate Addition

In 2014 Carrillo, Vicario and coworkers reported a stereoselective and diastereodivergent procedure to synthesize functionalized cyclohexanes containing four stereocenters through an asymmetric Michael-initiated ring closure (MIRC) cascade reaction [64]. Two different (*R*,*R*)-configured bifunctional squaramide-based organocatalysts (**C23** and **C24**) made possible the conversion of the same starting materials into products with different absolute configurations. This was possible by the introduction of subtle structural differences in the two catalysts. A wide range of nitroalkenes **7** and α-nitro-δ-oxo esters **41** reacted in a highly diastereo- and enantioselective Michael/Henry cascade giving high yields of products **42** (Figure 30). A gram-scale synthesis was also possible without loss of stereoselectivity.

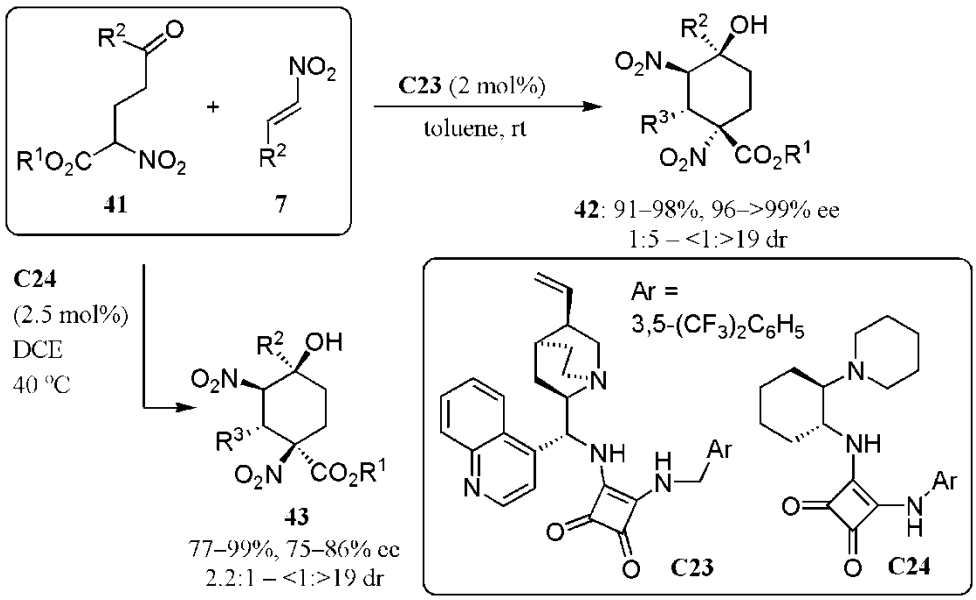

Figure 30. Diastereo-divergent synthesis of functionalized cyclohexanes [64].

Kinetic experiments were performed to find the rate-determining step, and DFT calculations were performed at the B3LYP/6-31G(d) level of theory using the PCM model to explain the reaction process and the origin of stereo-divergence. The initial Michael reaction, in which the initial two stereocenters are formed, was considered as the stereo-defining step. It is in this step that the diastereo-divergency of the reaction occurs when the two different C-1 epimers are formed with each catalyst. It was observed that the reaction was first-order for all reagents: both catalysts, nitronate **41a** (**117**, R^1 = Et, R^2 = Me), and nitrostyrene. The fact that the rate of the reaction was strongly dependent on the electronic nature of the aryl substituent of the nitroalkene also suggested that the initial Michael reaction is the rate-limiting step. Among others, an experiment was performed with a preprepared Michael intermediate, which, when stirred with either catalyst, provided the same product in comparable yields. This is a strong indication that although the configuration of the two stereocenters generated during the initial Michael reaction step is controlled by the catalyst, the diastereoselectivity of the intramolecular Henry reaction is strictly governed by the substrate. Hence the DFT analysis was performed for each catalyst on a simplified Michael reaction between **44** and **7b**. The optimized transition state structures (TS1 and TS2) found by FDT analysis leading to the major isomer formed by each catalyst are shown in Figure 31.

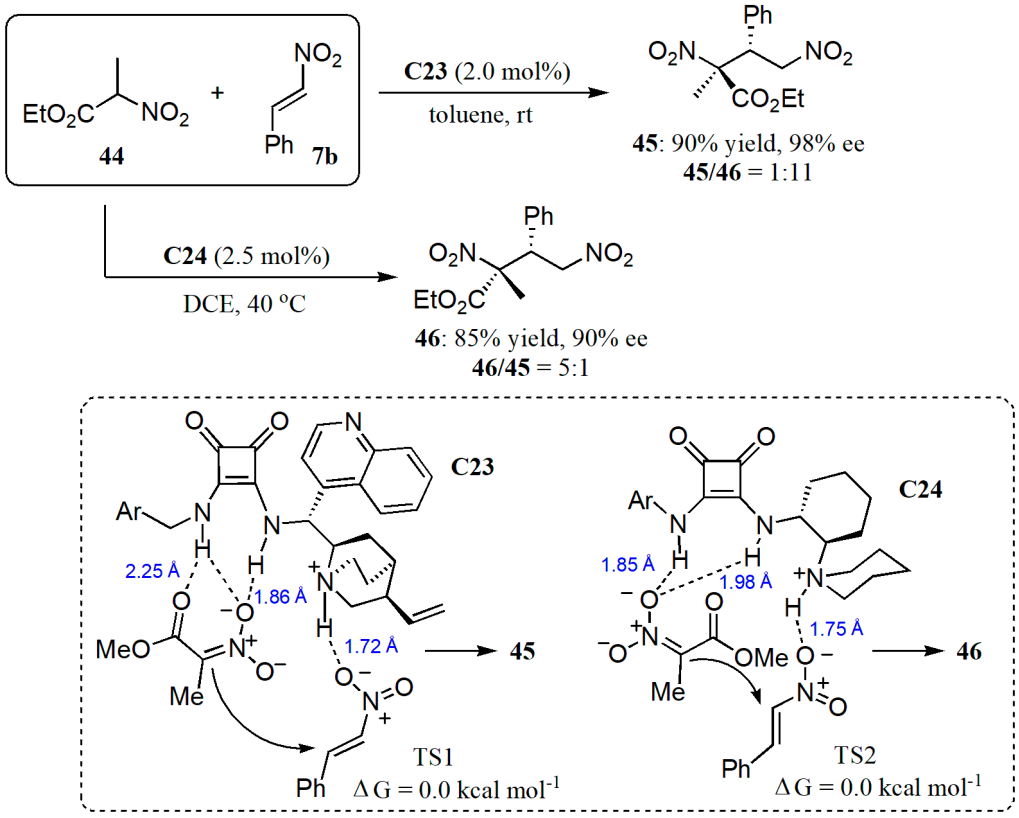

Figure 31. Model of the initial diastereo-divergent Michael addition in the cascade reaction leading to functionalized cyclohexanes **42** and **43** and TSs leading to the major products **45** and **46** determined by DFT calculations [64].

From the DFT experiments, it could be concluded that the mode of activation of the catalysts involves activation of the nucleophile by the squaramide unit through multiple H-bonding interactions, while the nitroalkene stays bound to the ammonium salt (formed after the initial deprotonation of the pronucleophile) via a single H-bond. The different simple diastereo-selections provided by each catalyst depend on their ability to form two different H-bonded complexes with the nitroacetate enolate, with the nitronate moiety exposing a different reactive prochiral face depending on the catalyst used.

Meninno, Lattanzi and coworkers reported the first enantioselective catalytic approach to *cis*- and *trans*-2,3-diaryl-substituted 1,5-benzothiazepines in 2018 [65]. The one-pot two-step sulfa-Michael/lactamization sequence between compounds **47** and **48**, promoted by thiourea-based bifunctional catalyst **C25** and *p*-toluenesulfonic acid, afforded products **49** in good to high yields and very high *ee*s (Figure 32). Mechanistic studies were performed on the reaction. An uncatalyzed reaction monitored by ^{1}H NMR in toluene-d_8 over time revealed that small amounts of *cis*-Michael adduct **50**, as well as cyclized product **49a** (R^1 = R^2 = Ph, R^3 = H), are formed during the reaction, which contributes to lower the *ee* of the *cis*-benzothiazepine. A similar experiment in the presence of the catalyst showed the formation of an increasing amount of Michael adduct over time, but not a cyclic product. It was found that the organocatalyst promoted a competitive 1,2-addition/elimination reaction, confirmed by detecting 30% of free pyrazole at the end of the reaction. The mixture of *cis*/*trans*-**49a** was recovered with the same level of diastereo- and enantioselectivity of the starting adduct **50**, which suggests that a retro-sulfa Michael/sulfa-Michael process does not happen since that would lead to epimerization/racemization. A racemic mixture of adduct treated with the catalyst afforded <10% of the *trans*-benzothiazepine after two days, showing that the lactamization reaction is negligible within the overall reaction times for the method developed. Overall, although the uncatalyzed Michael reaction, lactamization, as well as catalyst promoted lactamization, may influence the diastereo- and

enantioselectivities observed at the end, they were nevertheless predicted to be poorly effective during the overall reaction times taken by both sequential steps.

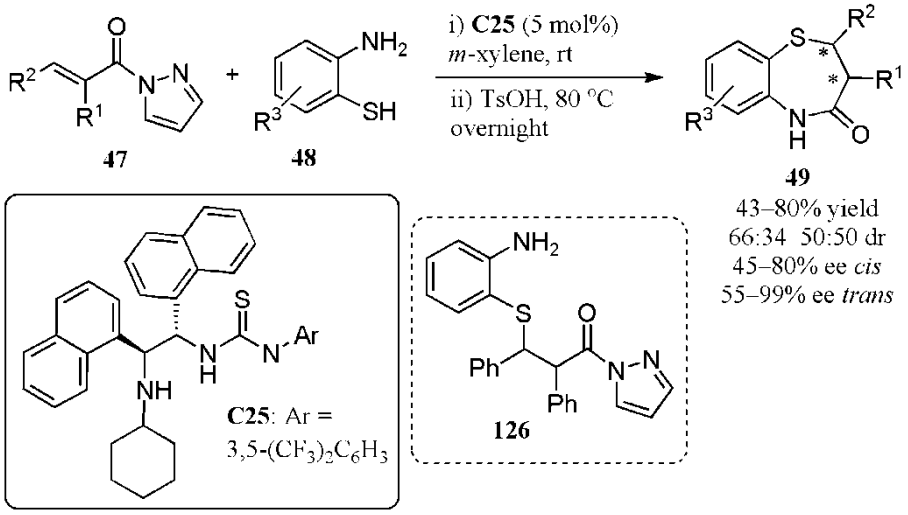

Figure 32. One-pot synthesis of chiral 1,5-benzothiazepines **49** [65].

Recently, Liu, Li, Song, Ban and coworkers described a thiosquaramide (**C26**)-catalyzed cascade Michael−Henry elimination reaction for synthesizing cyclopentenes [66]. In this reaction, phenacylmalononitriles **51** and nitroolefins, **7** reacted with very high diastereoselectivity, giving high yields of products **52** with moderate to high *ee*s, which could nevertheless be as high as 98% (Figure 33). Previous approaches to cyclopentenes from the same substrates were reported previously, but in the racemic series, the latest one using TBAF as catalyst [67]. The products contain a chiral quaternary center as well as an internal double bond, with many possibilities for derivatization. Based on experimental data and preliminary theoretical analysis (Hartree−Fock calculations), a mechanism was proposed involving an organocatalyzed asymmetric Michael addition (with TS1) and catalyst-assisted E2 elimination (with TS3) (Figure 34). Although an alternative path exists via non-catalyzed E_1 elimination (path A), this route would give rise to two isomers, the product observed, **52a** and **E**. However, **E** was not observed. Therefore, it was concluded that the reaction proceeds via the catalyzed E_2 elimination path.

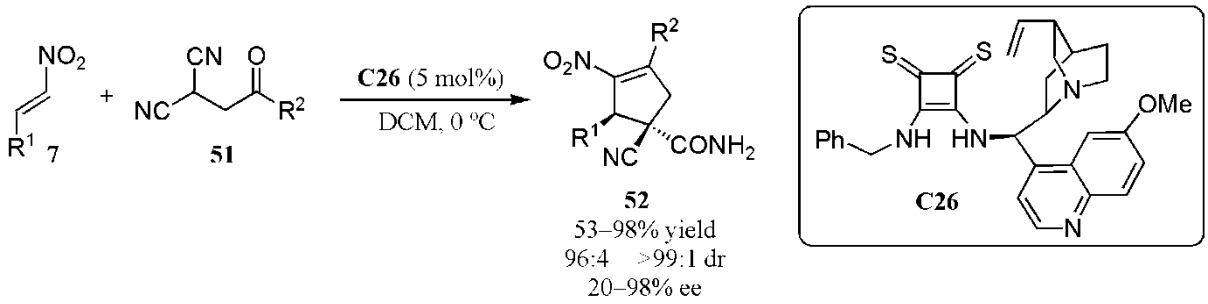

Figure 33. Enantioselective synthesis of cyclopentenes **127** [66].

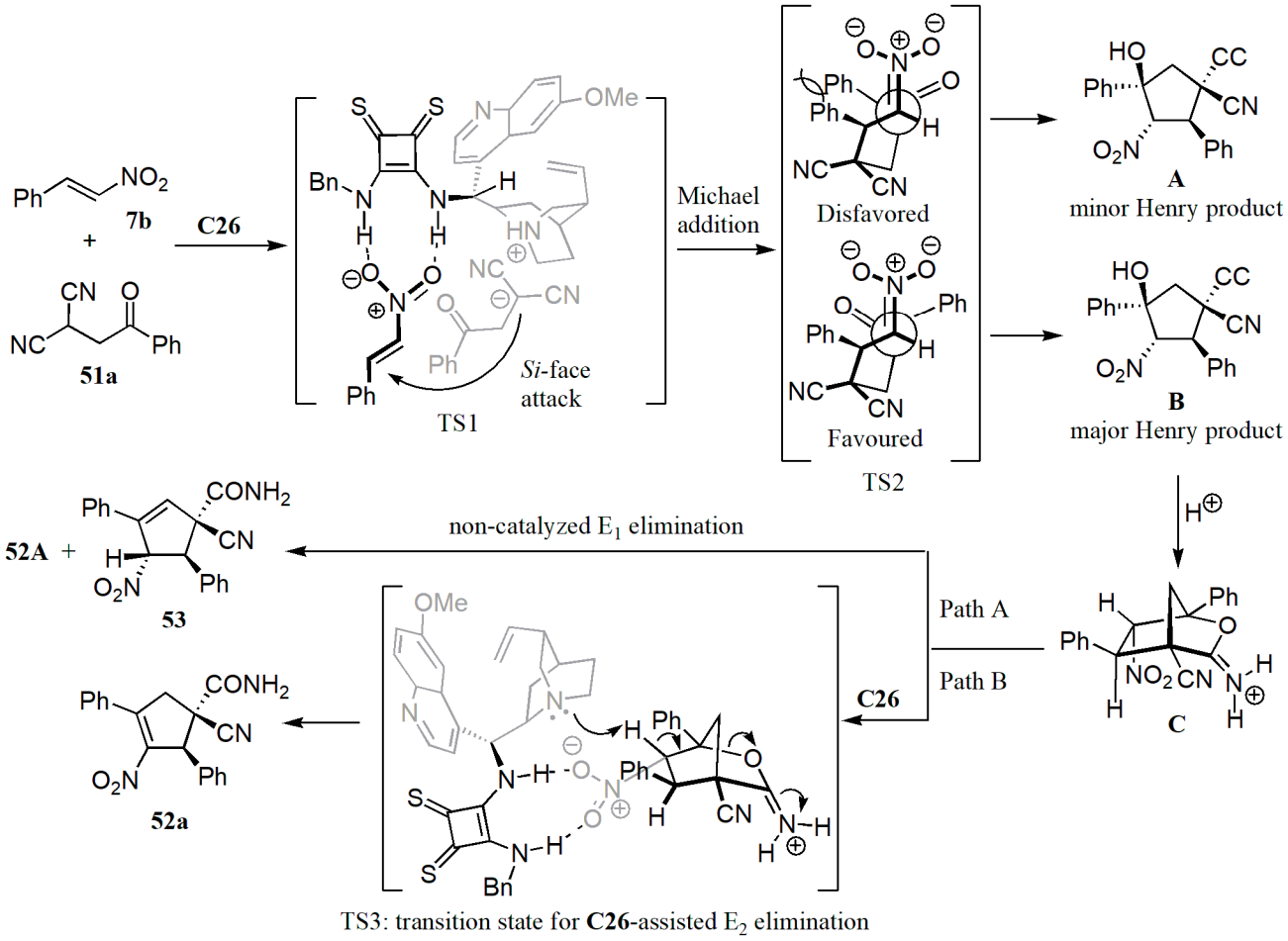

Figure 34. Mechanism proposed for the Michael–Henry–elimination cascade leading to cyclopentenes [66].

3. Cycloaddition Reactions

Another class of reactions that have been shown to benefit from developing hydrogen-bonding catalysis with bifunctional catalysts is cycloaddition reactions. [4 + 2] Cycloadditions as well as [3 + 2], i.e., formal [3 + 2], formal [3 + 3], [5 + 2], 1,3-dipolar cycloadditions and Tamura cycloadditions have been successfully achieved. This topic was reviewed by Held and Tsogoeva in 2016 [68]. Some interesting kinetic and theoretical studies have been reported recently. Wang, Wang and coworkers described a formal thio [3 + 3]-cyclization catalyzed by a thiourea-based bifunctional catalyst (**C27**) in 2014 [69]. Starting from 2-benzylidenemalononitrile (**54**) and indoline-2-thiones **55**, optically active thiopyrano-indole annulated heterocyclic compounds **56** were obtained in high yields and excellent *ee*s. The authors also attempted to react the less acidic indolin-2-ones **57** with 2-benzylidenemalononitrile in a similar way, but these attempts were unsuccessful, and no reaction was observed. To explain the differences in reactivity between the two indoline substrates, DFT calculations were performed at the B3LYP/6-311++G(d,p) level using the CPCM solvent model. Based on previous transition-state models for thiourea-catalyzed reactions, it was assumed that both reactants are activated simultaneously by the catalyst, as shown in Figure 35. According to the theoretical results obtained, enolization of the indolin-2-one (**57**) is much more difficult than that of indoline-2-thione (**55a**). Catalyst protonation by the enol forms is facile according to the Pápai and Wong models. The enantioselectivity obtained is dependent on the way the substrates coordinate to the catalyst. Complex **S-M1** (3.75 kcal mol^{-1}) is more stable than **O-M1** (8.80 kcal mol^{-1}), in agreement with the experimental observations that **55** is much more reactive than **57**. The energy

barrier for C–C bond formation is 1.34 kcal mol^{-1} lower for the indoline-2-thione, which also explains why the thiopyrano-indoles are easier to obtain.

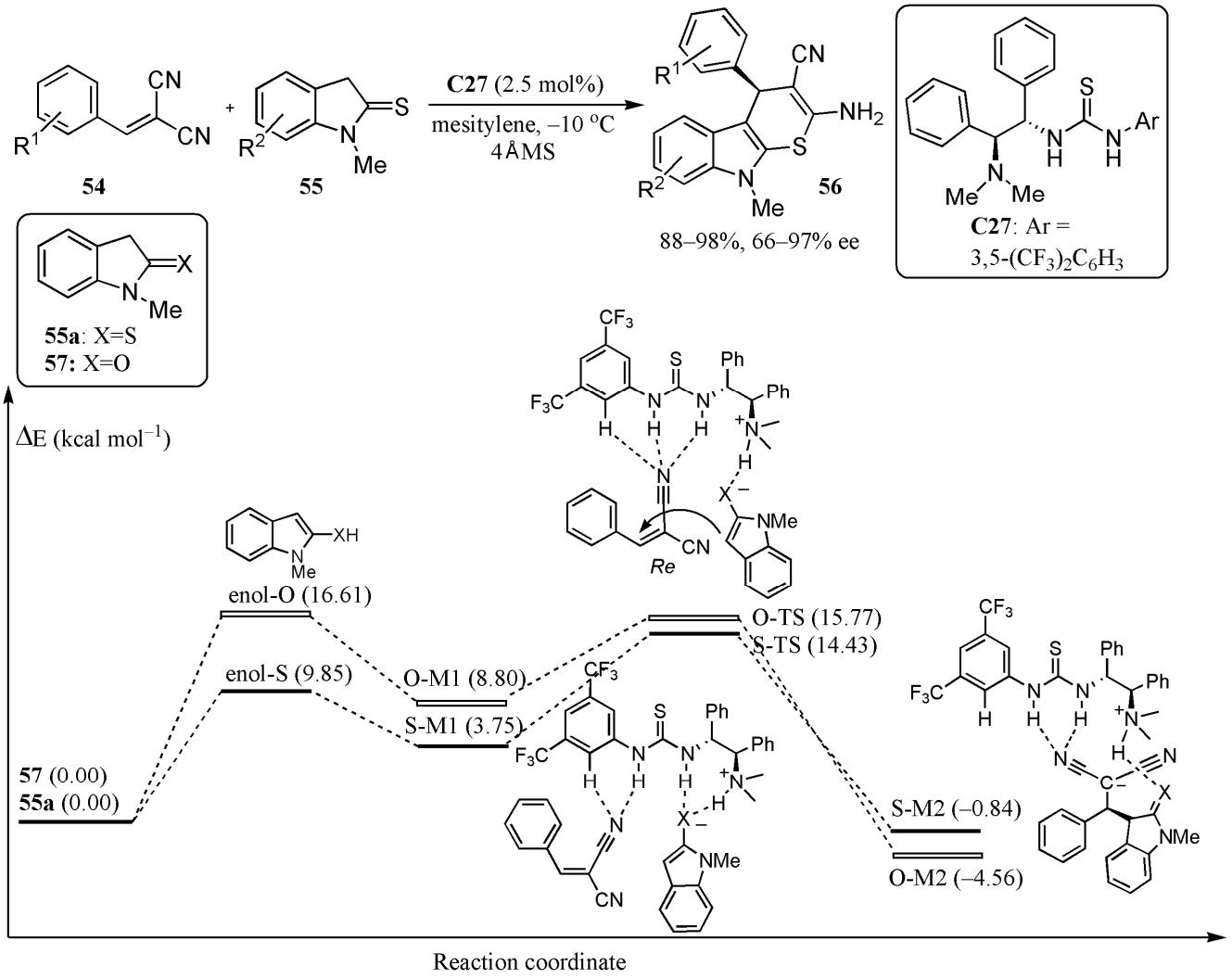

Figure 35. Enantioselective synthesis of thiopyrano-indole-annulated heterocycles via a formal thio [3 + 3]-cyclization [69].

In 2017 Jacobsen and coworkers introduced a new concept in H-bond donor catalysis [70]. To overcome the fact that small-molecule dual hydrogen-bond donors, such as ureas, thioureas, squaramides, and guanidinium ions are only weakly acidic and, therefore, favor reactions with highly reactive electrophilic substrates, they developed a way to activate them through by associating them with Lewis acids. Silyl triflates (**58**) were found to be ideal for this purpose since they are readily available, have broad applicability in organic synthesis, and when they coordinate with weakly coordinating anionic ligands, e.g., disulfonimides, their reactivity is increased [71,72]. Association with a chiral H-bond donor catalyst, as in **59**, can give rise to a charge-separated complex, by anion abstraction, with higher Lewis acidity than that of the silyl triflate alone (Figure 36a).

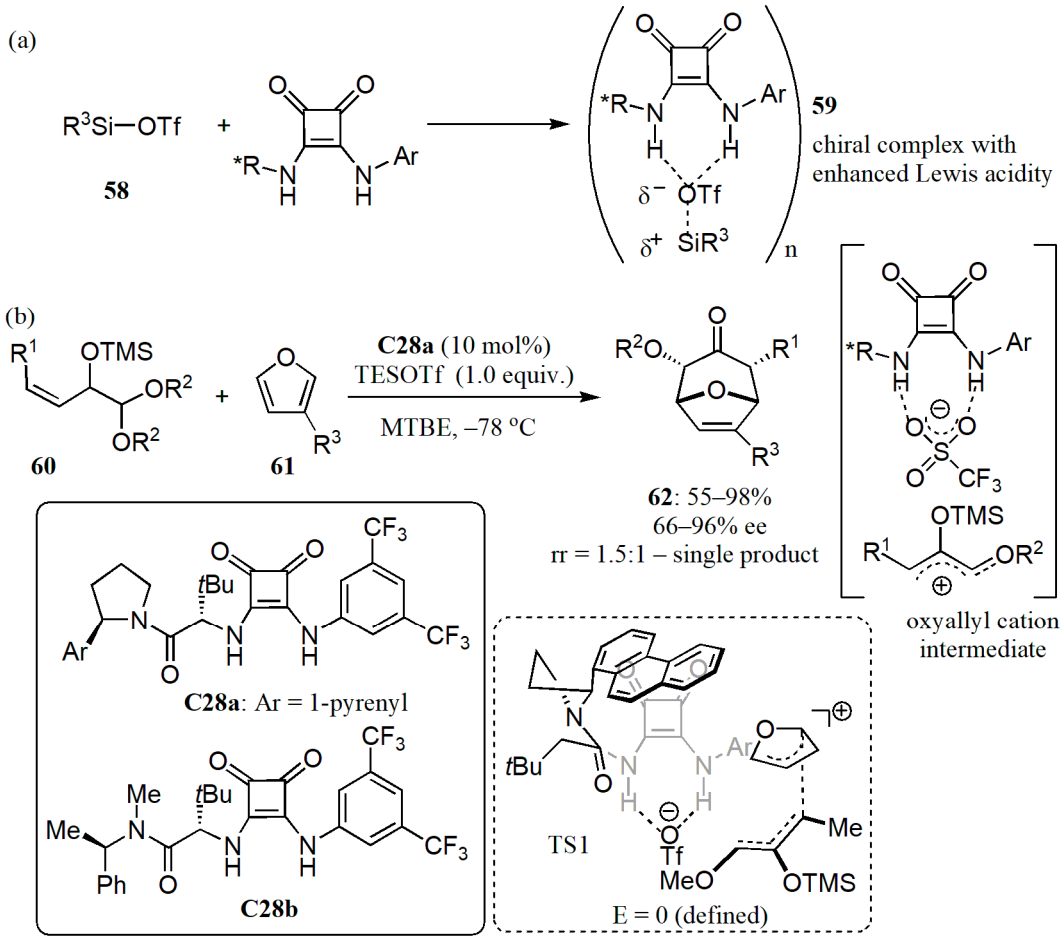

Figure 36. (**a**) Activation of a silyl triflate (**58**) via anion abstraction by a squaramide catalyst; (**b**) Application of the type of activation shown in (a): Cooperative reactivity of squaramide-based catalyst **C28a** and TESOTf in enantioselective [4 + 3] cycloadditions via oxyallyl cation intermediates; r.r. is the regioisomeric ratio [70].

One of the systems utilized to investigate the H-bond donor–silyl triflate cooperativity was a [4 + 3] cycloaddition reaction, which gives rise to functionalized seven-membered carbocyclic frameworks, a reaction which had proved previously to be challenging to perform in an enantioselective manner. Silyl enol ethers capable of acting as oxyallyl cation precursors (**60**) were reacted with furans (**61**) to generate bicyclic [4 + 3] cycloadducts (**62**) in good yield and high *ee*s, as single diastereomers in some cases in the presence of **C28a** (Figure 36b).

Kinetics and theoretical studies were performed on this reaction. For the kinetics studies, Burés' method was utilized [73]. A first-order kinetic dependence on the acetal, zero-order dependence on the furan and a first-order dependence on the catalyst were observed, as well as saturation kinetics concerning triethylsilyl trifluoromethanesulfonate (TESOTf). The data are consistent with a pre-equilibrium formation of a resting-state complex between the catalyst and TESOTf, and a rate-limiting reaction of this complex with the acetal. It was found that there was a 1:1 binding interaction between the simpler squaramide **C28b** and different triflate sources, and the bonding constants were determined from titration experiments by ^{1}H NMR spectroscopy. TESOTf was found to bind 4000 times as tightly as NBu_4OTf, which suggests that there is the simultaneous binding of both the triflate and the trialkyl silyl component in the complex formed. Taking into account the combined results, it appears that there is a formation of an unexpectedly strong 1:1 complex between TESOTf and 5 as the resting state of the catalyst in the reactions described.

The kinetics and DFT studies suggest that in this resting state, the complex acts as a potent Lewis acid that promotes acetal ionization. Post-rate-determining reaction of the

oxyallyl cation intermediate with the furan gives rise to the [4 + 3] cycloadduct. Since similar *ee*s were obtained with different trialkyl silyl triflate promoters tried, it appears that the enantioselectivity-determining step occurs after the formation of the oxyallyl cation and involves the reaction with furan. Single-point calculations at the M062X/6-31+G(d,p) level of theory could reproduce both the sense and magnitude ($\Delta\Delta E^{\ddagger}_{calc}$ = 1.28 kcal mol^{-1}) of enantioinduction determined experimentally. The structure corresponding to the lowest-energy TS (TS1) for the first, enantioselectivity-determining C–C bond-forming step, towards the major enantiomer of product, is shown in Figure 36. Besides a network of hydrogen-bonding interactions between the different reacting components, there seems to be a stabilizing interaction between the furan and the catalyst in the TS leading to the major enantiomer, absent in the TS leading to the minor enantiomer, which can be deduced from the position of the furan ring close to the aromatic substituent of the catalyst. This may be a key factor responsible for enantioselectivity.

When homophthalic anhydrides **63** are reacted with imines **64,** chiral lactams **65** can be obtained in a highly enantioselective manner in the presence of bifunctional squaramide–based catalysts (Figure 37). This was discovered by Vetticatt and Seidel, who proposed a novel ion-pairing mechanism to achieve a formal [4 + 2] cycloaddition [74]. Although this reaction had been previously used in synthesis and even been applied to alkaloid synthesis, no asymmetric versions had yet been developed [75,76]. The new mode of activation, an anion-binding/ion-pairing approach, was based on the concept that the hydrogen-bonding catalyst, which itself remains neutral throughout the reaction, can convey enantioselectivity by interacting with an anionic nucleophile and a cationic electrophile at the same time. The interaction of the hydrogen-bonding thiourea with the anhydride increases the acidity of the substrate, facilitating ion-pair formation. The result is an increased equilibrium concentration of the ion pair intermediate. The iminium ion generated can then interact with another binding site on the catalyst, which results in creating a well-defined ion pair, which then undergo the enantioselective Mannich reaction. Catalyst **C29** was found to be the best out of a range tried. The reaction mechanism was investigated, and it was observed that there were no nonlinear effects, which suggested that the rate-limiting step involves only one catalyst unit. The nature of the transition state of the rate- and stereo-determining step, the Mannich addition for the reaction between **63** and *N*-phenyl benzimine catalyzed by **C29** was investigated using B3LYP-GD3[22]/6-311+G** PCM [23] (diethyl ether)//B3LYP/6-31G* calculations as implemented by Gaussian 09. The lowest-energy transition structures found leading to the major and minor enantiomers of the product are shown in Figure 37.

The results show an early C–C bond formation step. In the TS structure leading to the major enantiomer (*SS*-TS), the enolate is bound to the catalyst through two strong H-bonds via the thiourea NH groups (Figure 37). The protonated imine is directed to the *Re* face of the enolate through a strong H-bond with the carbonyl oxygen of the amide moiety of the catalyst. Similar H-bonding interactions exist in TS leading to the minor enantiomer (*RR*-TS), but this TS is higher in energy by 2.0 kcal mol^{-1}, which agrees with the experimentally observed value of ee.

Thiourea-based bifunctional catalysis was also responsible for an enantioselective 1,3-dipolar cycloaddition of salicylaldehyde (**66**)-derived azomethine ylides with nitroalkenes **67** that proceeded with excellent exo/endo selectivity [77]. An intramolecular hydrogen bond involving an *o*-hydroxy group allowed the reaction with azomethine ylides bearing only one activating group. In methods previously developed, two activating groups (two EWGs or one EWG and one aryl group) were required at the dipole to increase the acidity of α-protons. As a result, the substitution pattern of the final products was restricted.

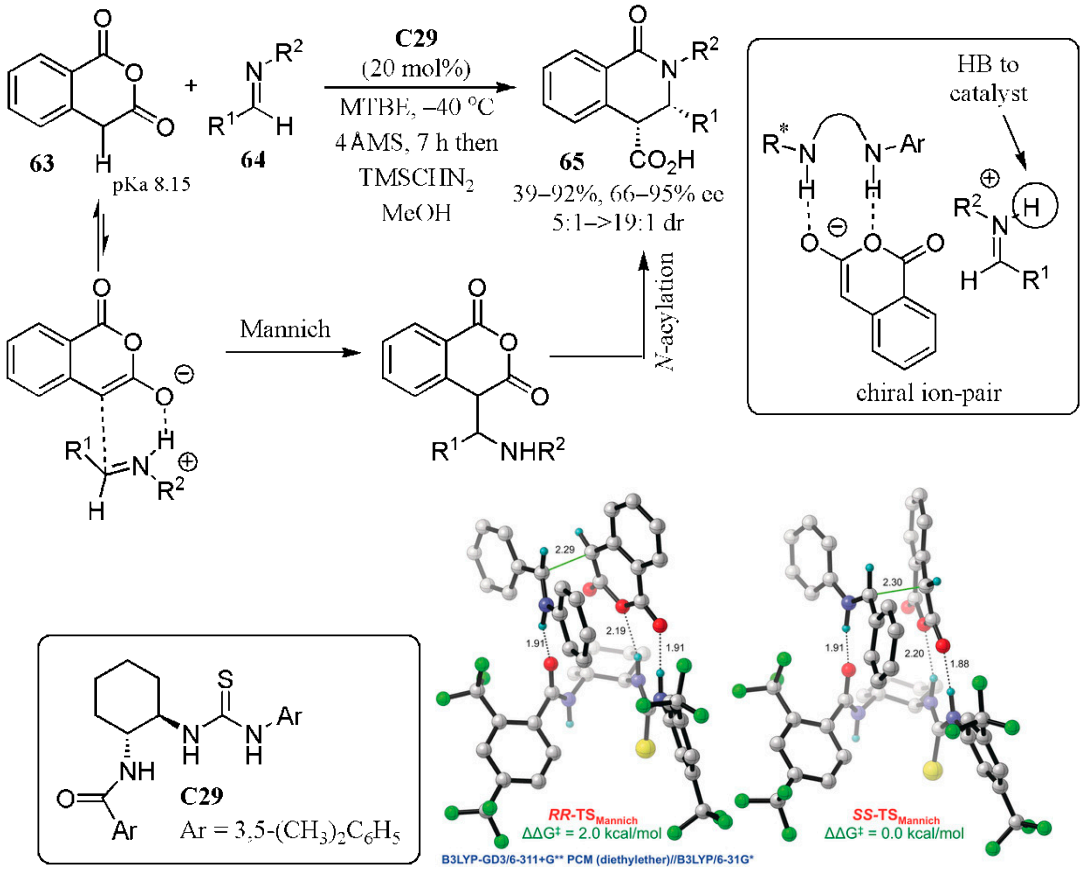

Figure 37. Enantioselective synthesis of lactams by [4 + 2] cycloadditions catalyzed by **C29,** including the lowest-energy transition structures leading to the major and minor enantiomers of product **65a** (**65**, R^1=R^2=Ph). Distances are in Å, and some hydrogen atoms are omitted for clarity [74]. Reprinted and adapted from Angewandte Chemie International Edition with permission from Wiley.

In this work, the activation of the azomethine ylide by intramolecular bonding, as well as the intermolecular hydrogen bonding with the catalyst, was demonstrated by DFT calculations to be crucial for the reaction. For these studies, β-nitrostyrene, Takemoto's catalyst **C1** and azomethine ylide **69**, formed by deprotonation of **66** by the catalyst, were considered as the reacting species. Three different coordination points of the reactants with the catalyst with both endo and exo approaches were considered, according to the Takemoto, Pápai and Zhong's models discussed above. The pre-association complex, the intermediates, and the catalyst-bound products were computed, as well as the corresponding TSs. The first TS, TS1, gives rise to the formation of the C–C bond, whereas the second, TS2, to the intramolecular attack of the imine leading to ring closure. Calculations for the Zhong´s model (Figure 38) showed that the energy first barrier (TS1 = 3.35 kcal mol^{-1}) was higher than in the case of Pápai's model (TS1 = 1.84 kcal/mol), but the second lower (TS2 = 14.48 and 16.47 kcal mol^{-1}, respectively). The intermediate and the catalyst-bound product, according to Zhong´s model, were thermodynamically more stable. Altogether the results suggest that Zhong's mechanism is in operation. An intermolecular hydrogen bond between the thiourea and the OH group of ylide is observed only in Zhong's model. While it provides additional stabilization to the PAC, it also increases the reactivity of the azomethine ylide, and it is one of the factors that favor Zhong's approach to the others.

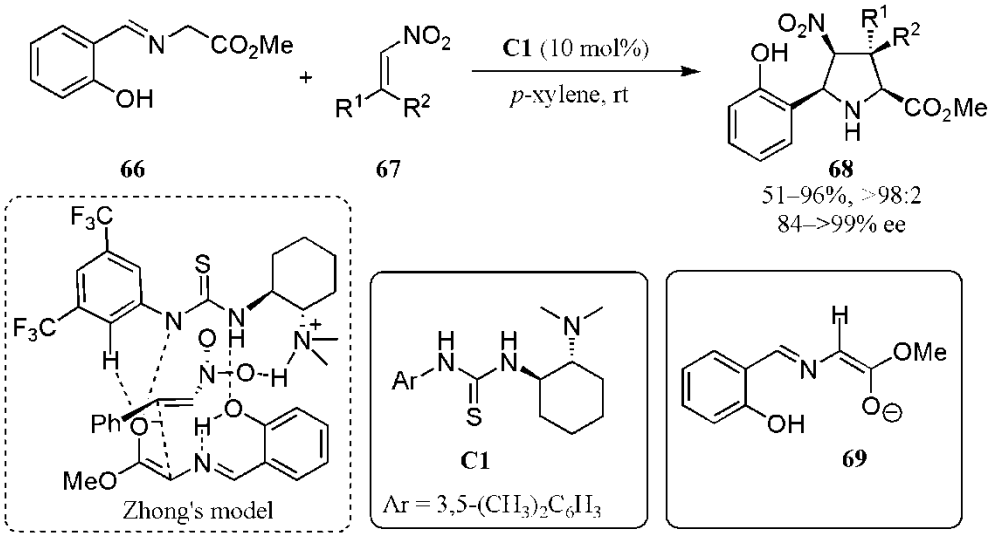

Figure 38. Synthesis of pyrrolidines by 1,3-dipolar cycloaddition of **66** with nitroalkenes **67** under bifunctional catalysis [77].

Cinchona thiourea catalysts have also been used to induce axial chirality. In a recent work described by Yan and coworkers, an atroposelective intramolecular [4 + 2] cycloaddition was used to convert in situ generated vinylidene ortho-quinone methides (VQM), formed by the intramolecular reaction of 2-ethynylphenol derivatives with alkynes, into axially chiral heterobiaryls, i.e., naphthalenylpyran **71** [78]. Several products could be obtained in very high yields and *ee*s (96–>99% *ee*) at rt. Subsequently, Yan, Bai, Lan and coworkers performed theoretical studies, i.e., DFT calculations, on the reaction shown in Figure 39 to investigate the mechanism and origin of enantioselectivity [79]. All DFT calculations were performed with the Gaussian 09 series of programs, and the B3-LYP functional with the standard 6-31G(d) basis set was used for geometry optimization. The results obtained led to the proposal of the mechanism shown in Figure 39. The reaction starts with deprotonation of the naphthol moiety by the quinuclidine, facilitated by the formation of two hydrogen bonds with the thiourea moiety, which enhances the acidity of the alkynyl naphthol. Conjugation with the naphthalenoate enhances the basicity of position C2 in the alkyne moiety, facilitating protonation. Intramolecular proton transfer of ammonium naphthalenolate salt **B** gives rise to the VQM intermediate **C-*R*** with dearomatization. This process is endergonic by 15.3 kcal mol^{-1}. The conjugative allene and carbonyl moieties act as an enophile in the ensuing [4 + 2] hetero-Diels–Alder cycloaddition. The axial chirality of the VQM intermediate is created in the protonation step and the enantioselectivity of the reaction. The enantioselectivity is controlled by steric repulsions with the cinchonine framework, leading to an *R*-axial chiral VQM as the major intermediate. The enantioselectivity for the axial chirality of the product is controlled in the cycloaddition step. An additional hydrogen bond between the naphthalenol and quinuclidine moieties makes the generation of an S-axial chiral naphthopyran the most favorable (Figure 40). The calculated energy barrier for this step is only 6.8 kcal mol^{-1}, whereas the energy barrier for the formation of its enantiomer was calculated to be 13.1 kcal mol^{-1}. The difference in energy (6.3 kcal mol^{-1}) predicts >99% *ee* for the *S*-axial enantiomer, which corresponds with the experimental observations.

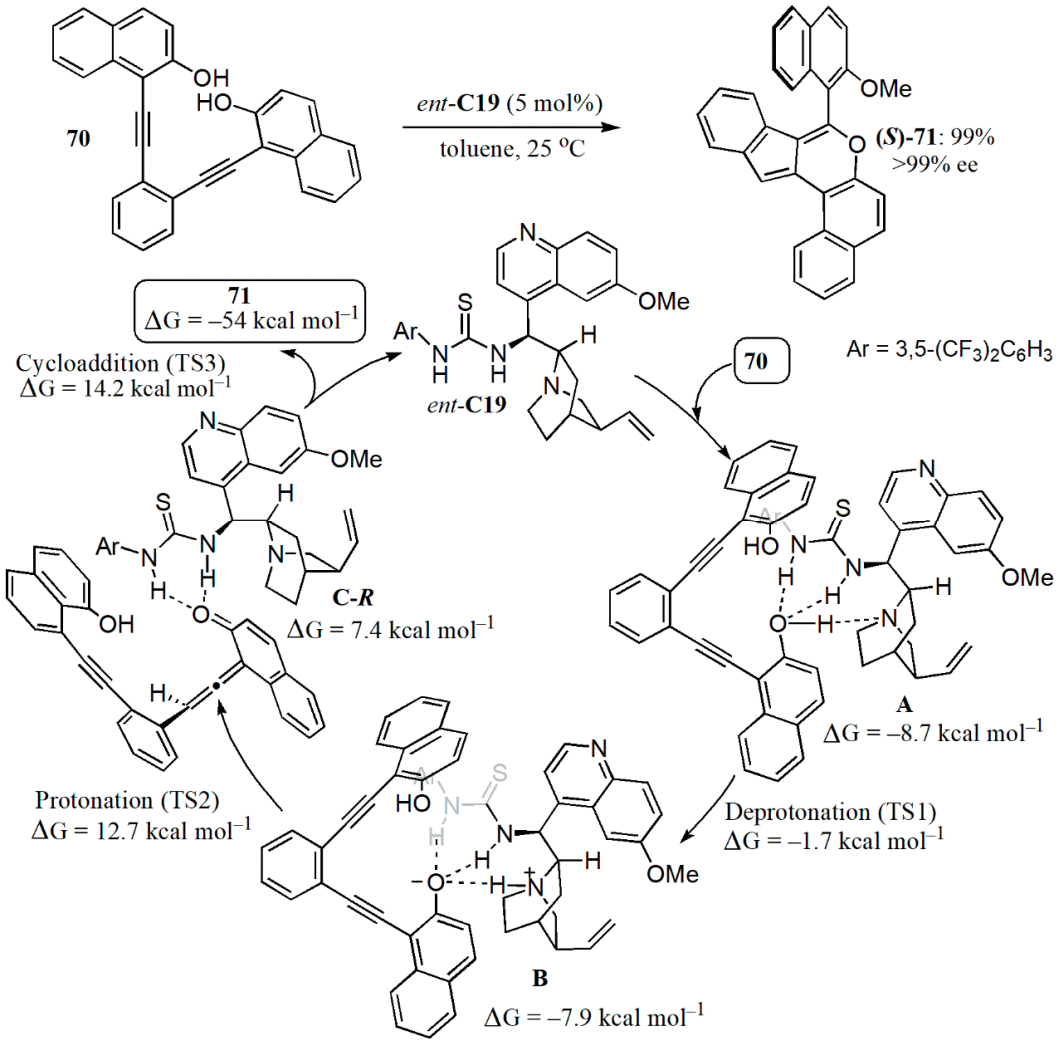

Figure 39. Intramolecular [4 + 2] cycloaddition of 2-ethynylphenol and the proposed catalytic cycle; the relative energies are given concerning catalyst *ent*-**C19** with substrate **70** [79]. The free energies were obtained by adding DGcorr (the thermochemical correction for the Gibbs free energy calculated at the B3-LYP/6-31G(d) level in the gas phase) to DEM11/solvent (the single-point energy calculated at the M11/6-311+G(d,p) level in toluene-based on the gas-phase stationary point).

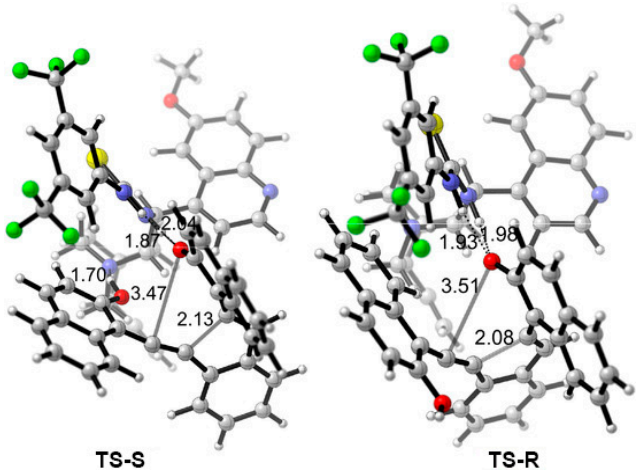

Figure 40. TSs for the cycloaddition step of the ent-**C19**-catalyzed intramolecular [4 + 2] cycloaddition reaction. Bond lengths are in Å. Reprinted and adapted from Chemistry—An Asian Journal with permission from Wiley [79].

The Tamura reaction, the cycloaddition between activated alkynes or alkenes and enolizable anhydrides, such as homophthalic anhydride, was studied by Connon and coworkers. They reported the first examples of asymmetric Tamura cycloaddition reactions involving singly activated alkenes in 2016 [80]. Homophthalic anhydride (**63**) was reacted with α-methyl nitrostyrenes (**72**) in the presence of squaramide-based catalyst **C30** to produce bicyclic aromatic ketones **73/74** with three new stereocenters in 12–99% *ee*. It was found that the products were susceptible to equilibration, **74** equilibrated to **73**, which was observed even during evaporation of the solvent during purification. To obtain products under reproducible conditions, the reaction conditions described in the equation in Figure 41 had to be followed carefully, and also the purification, with a concentration of the solvent performed at low temperatures (not higher than 30 °C). It was also observed with **73a** (**73**, R = Ph) that when the pure diastereoisomer was subjected to epimerization conditions in the presence of CD_3OD, i.e., heating to 55 °C for 55 h in MTBE (0.1 M), that there was 60% incorporation of deuterium at the ester's α position. It was also found that **73a** epimerizes faster than **74a** and that **74a** is the more stable isomer in the presence of MeOH. This experiment showed that even the more stable diastereoisomer undergoes proton transfer. This unusual equilibration, which occurs in a methanolic solution in the absence of a recognizable base via proton transfer at the α-carbon of the ester, was subsequently investigated computationally. These calculations, as well as XRD data, indicated that the nitro group and the proton involved in the epimerization are ca. 2.74 Å apart, and hence it was proposed that proton transfer is mediated by the proximal nitro functional group. However, such mechanism is thermodynamically unfavorable (relative energy >50 kcal mol^{-1} with respect **74a**), and another mechanism was considered solvent-assisted proton transfer. The involvement of two MeOH molecules was found to be kinetically more favorable than one only. It was, therefore, proposed that two molecules of MeOH interact with the product; subsequently, a shuttle (concerted) deprotonation/protonation takes place with the participation of both MeOH molecules bound to both each other and to the substrate, leading to intermediate **75**. The energy barrier for this process was calculated to be 18.7 kcal mol^{-1}. The corresponding reaction involving the other diastereoisomer (**74**) has a slightly higher energy barrier (21.5 kcal mol^{-1}). **74·2MeOH** was found to be 1.6 kcal mol^{-1} more stable than **73a·2MeOH**, consistent with the findings from deuteration experiments, that **73a** epimerizes faster than **74a**, and that **74a** is the more stable diastereoisomer.

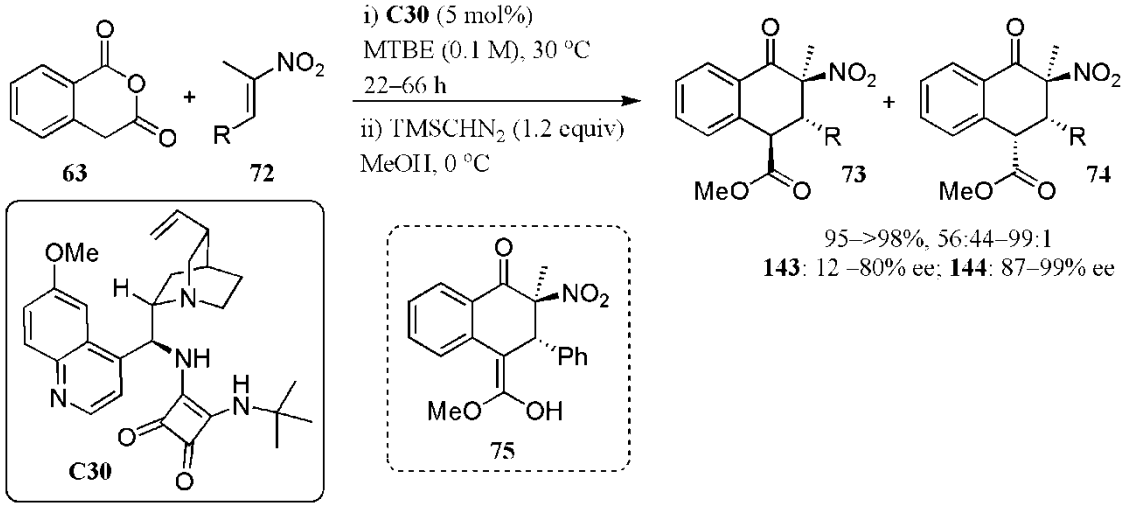

Figure 41. Asymmetric Tamura cycloaddition reaction catalyzed by **C30** [80].

The Connon group also showed that a wide range of aldehydes undergoes cycloaddition with homophthalic anhydride (**63**) in the presence of organocatalyst **C31** to yield substituted lactones **77** in excellent yield and *ee*s (Figure 42) [81]. In 2016 Rozas, Connon and

coworkers reported the first DFT mechanistic study on the cycloaddition of benzaldehyde (**76a**) with homophthalic anhydride [82]. The reaction was found to follow a mechanism in which the catalyst binds to the anhydride, a highly energetically favorable process (ca. 40 kJ mol^{-1}), which then deprotonates it, leading to a squaramide-bound enolate. This reaction is thermodynamically favorable, with the catalyst-bound enolate found to be 21.1 kJ mol^{-1} more stable than the substrate–catalyst complex. This reaction is followed by C–C bond formation. An atoms in molecules (QTAIM) analysis revealed the existence of a web of HB interactions between enolate oxygen atoms not involved in squaramide binding and both the catalyst's quinoline ring and the C-2 phenyl substituent, shown in previous studies to be beneficial for product dr and ee. Therefore it seems that this unit facilitates face-selective binding of the enolate, which then adds to the aldehyde, which is at the same time being activated by the catalyst's ammonium ion. In the C–C bond-forming step, in which the stereocenter is established, the binding interaction between **C31** and the anhydride is mostly unaffected by the aldehyde. This implies that as a result of the location of the ammonium ion, only one enolate face is available to attack the aldehyde, which leads to the high enantioselectivity observed. It also appeared from the results that the face-selective addition to the aldehyde was primarily directed by the HB to the ammonium ion. A computational analysis of all available pathways revealed that the pathway leading to *trans*-(R,R) was clearly favored. C–C bond formation is followed by acylation to give the lactone in a concerted and general-base/hydrogen bonding catalyzed step. The web of attractive interactions between the catalyst's quinoline/quinuclidine ring and the anhydride O-atoms was found to be absent in the TSs/intermediates leading to minor stereoisomers. The calculated *ee* value agreed well with the experimental results.

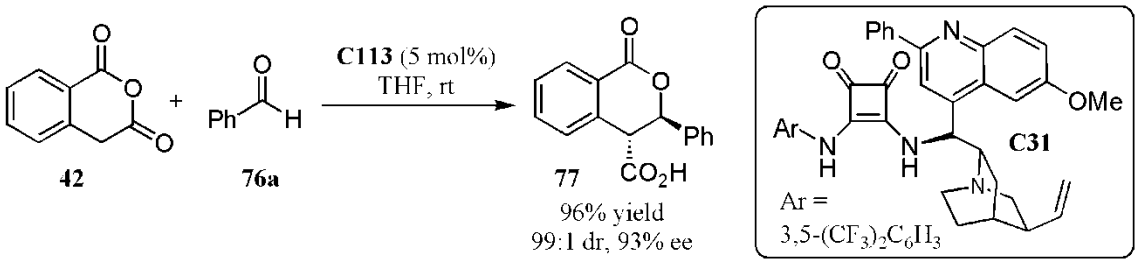

Figure 42. The organocatalytic asymmetric reaction of benzaldehyde and homophthalic anhydride [82].

4. Aldol and Henry Reactions

In 2017 an organocatalytic decarboxylative aldol reaction of β-ketoacids with α-ketophosphonates allowed the enantioselective synthesis of tertiary α-hydroxyphosphonates was described by Chowdhury and coworkers for the first time (Figure 43) [83]. α-Hydroxyphosphonates have been shown to exhibit many kinds of useful biological activities, including in reports by one of us, and they are the object of much research [84–86]. Recent accounts on the synthesis of tertiary α-hydroxyphosphonates include cross aldol reactions at low temperatures, but long reaction times are required. Up to this report from the Chowdhury group, cross aldol reactions of α-ketophosphonates (**79**) with acetone or acetaldehyde were reported, but reactions with aromatic ketones, e.g., acetophenones, not. In this report, β-aryl β-ketoacids **78** were employed as surrogates of the acetophenone enolate to fill this gap. In this quinidine-derived urea (**C32**)-catalyzed process, the products **80** were obtained in high yields and *ee*s.

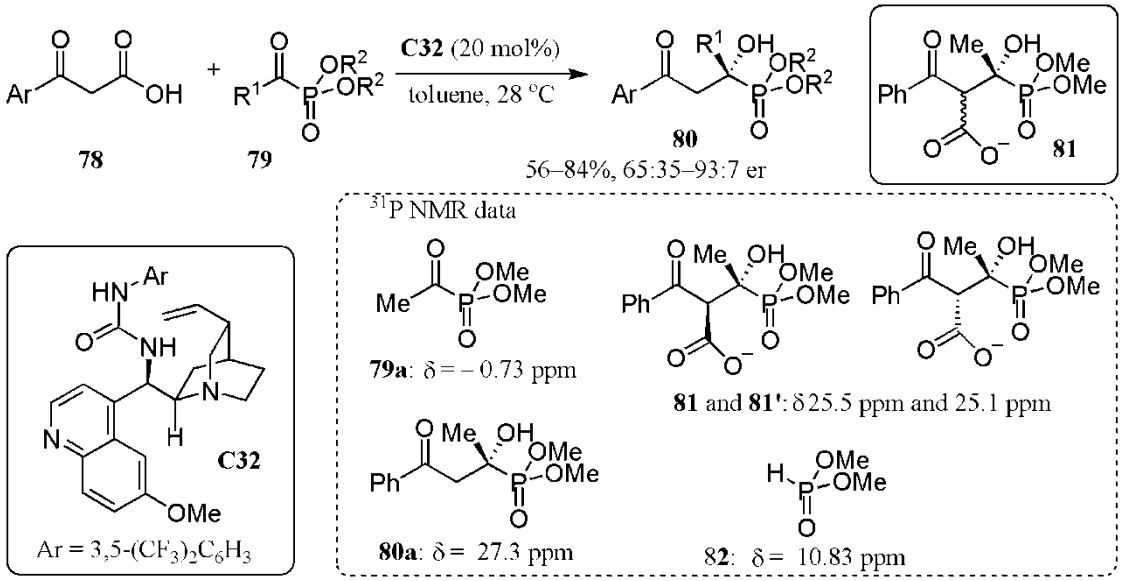

Figure 43. Organocatalytic synthesis of tertiary α-hydroxyphosphonates [83].

Control experiments were performed to investigate the mechanism. The reaction was thought to proceed via the formation of an intermediate of type **81**, which can lose CO_2 to yield the desired product. ^{31}P NMR studies of a reaction between α-ketophosphonate **79a**, benzoylacetic acid **78a** and the catalyst showed that, soon after **78a** and the catalyst are added to a solution with **79a**, a few signals appear in the spectrum, due to the product, to two diastereoisomers of intermediate **81** and also to dimethylphosphite (**82**), due to the decomposition of **79a**. An additional signal at 22.54 ppm, possibly due to a complex formed between **79a** and the catalyst **C32**, was also observed. After some time, the intensity of the signal due to product **80a** increased, while all those of the signals at δ 25.46 ppm and 25.1 ppm decreased, which is consistent with the mechanism proposed.

The Henry or nitroaldol reaction, mechanistically similar to the aldol reaction, is another important tool for carbon–carbon bond formation. Several studies have shown that cinchona alkaloids bearing a hydrogen bonding group at the C-6′ position can catalyze the Henry reaction in high yields and *ee*s [87]. The first theoretical studies aiming to clarify the mode of action of thiourea-cinchona alkaloid bifunctional catalysts (e.g., C**33**) were reported by Himo and coworkers in 2007 [88]. In the reaction between nitromethane and benzaldehyde (**76a**), with simplified catalyst **C34**, the results supported a mechanism involving initial nitromethane deprotonation and aldehyde complexation (Figure 44a). Two pathways with comparable energy barriers are then possible for C–C bond formation. They differ in the way the reactants bind to the catalyst. Either nitromethide binds both to the quinuclidinium and one thiourea NH, while the aldehyde binds to one thiourea NH only (path A), or nitromethide binds to both thiourea NH hydrogens and benzaldehyde to the quinuclidinium unit (path B). A small preference for path A was found to exist. Experiments have shown that the results are strongly dependent on the nature of the solvent and not simply a polar, nonpolar distinction, often observed in some organocatalyzed reactions. This type of correlation is not possible with the Henry reaction. *Ee*s correlate roughly with the Lewis basicity of the solvent, so that the higher the Lewis basicity, the higher the *ee*. This suggests that the energies leading to both TSs are similar. In this study, TSs states leading to both enantiomers were located for the two pathways (Figure 44b); for path A, three TS rotamers were found for each enantiomer, corresponding to the different Newman projections for C–C bond formation, as shown in Figure 44b. For path B, since there is bidentate coordination between both NH groups of the thiourea and the nitro group, only one TS is possible for the formation of each enantiomer (*R* and *S*). It was found that the lowest energy TS (TS-S) corresponds to the *S*-product as observed experimentally, and the calculated energy difference between TS-S and TS-R was quite small, only 1.1 kcal mol^{-1},

which is also in agreement with the experimental observations from solvent effects. The energies calculated for the six lowest-lying transition states are shown in Figure 44b. Slight differences in the interaction of the solvent with the TSs leading to the *S* and *R*-enantiomers cause small differences in energy, which result in the changes in ee observed.

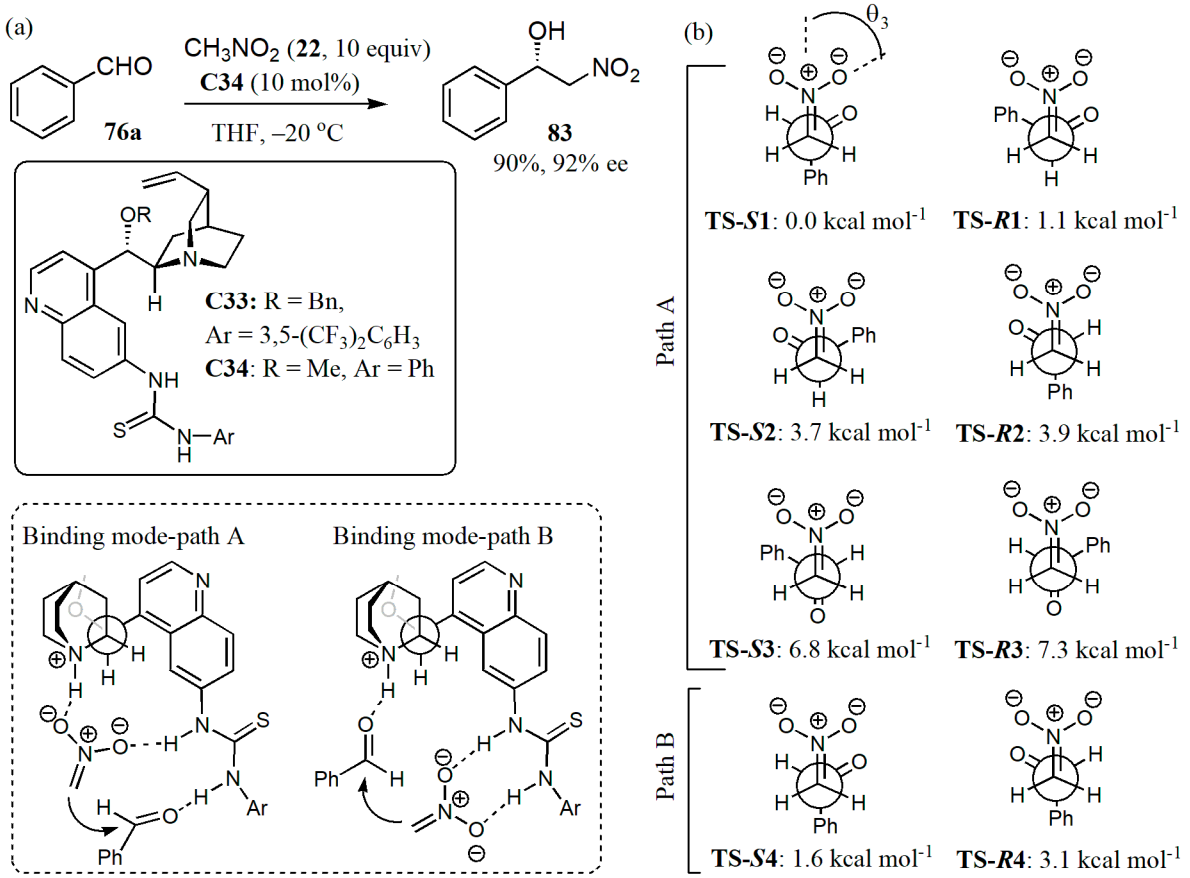

Figure 44. (**a**) Cinchona thiourea-catalyzed enantioselective Henry reaction; (**b**) Calculated relative transition state energies for C–C bond formation. Values include solvation effects [87,88].

More recently, Otevrel and Bobal developed a novel multifunctional *C2*-symmetric biphenyl-based diamine-tethered bis(thiourea) organocatalyst (**C35**), which was tested in the Henry reaction and also applied with success to the catalytic enantioselective syntheses of the enantiopure drug (*S*)-econazole and (*R*)-mirabegron, a late-stage intermediate (Figure 45) [89]. Under optimized conditions, the catalyst provided excellent yields and *ee*s, particularly with electron-deficient aromatic and heterocyclic substrates, although moderate drs. Preliminary kinetic and spectroscopic experiments were also performed to study the reaction. Among other parameters, the effect of temperature was probed. A plot of temperature vs. stereoselectivity of nitroaldol **86a** exhibited a linear trend intersecting at a value of the reciprocal inversion temperature (T_{inv} = −5 °C). The *syn* diastereomers prevailed only at reaction temperatures lower than T_{inv}. This unusual temperature effect on the *ee* and dr values was attributed to catalyst-mediated reversibility of the reaction at $T > T_{inv}$. On the contrary, temperature variations were less pronounced on the formation of **86b**, which displayed a simple temperature effect. No nonlinear effects were found, suggesting that the active form of the catalyst is monomeric. Kinetic studies revealed first-order kinetics concerning the model aldehyde, 2-nitrobenzaldehyde, and the catalyst. Similar experiments to determine the reaction order of the nitroalkane were not possible due to solubility problems and volatility. Instead, the role of nitromethane was investigated by isotopic substitution with $MeNO_2$-d_3. Proton abstraction of the nitroalkane was identified as the rate-limiting (or a partially rate-limiting) step in the overall reaction.

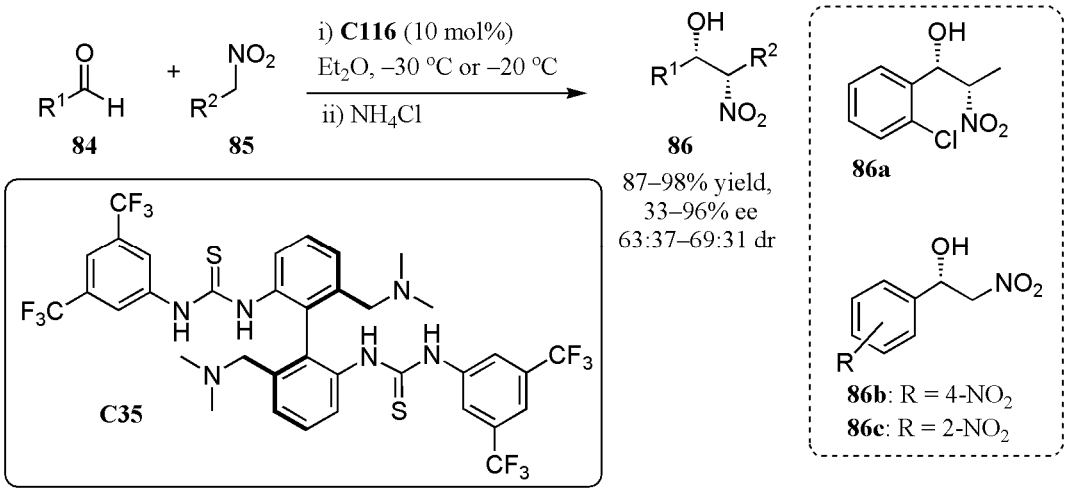

Figure 45. Asymmetric Henry reaction catalyzed by **C35** [89].

In 2017 Herrera and coworkers performed a study to test the accuracy of different combinations of DFT methods and basis sets in squaramide catalysis [90]. The Henry reaction between 4-cyanobenzaldehyde and nitromethane was selected as a model reaction. This was a complex reaction of about 100 atoms and many diverse non-covalent interactions. Eighteen different computational approaches were compared to find an accurate one that required the least possible amount of calculation time. Functional wB97X-D provided the best results when used with different versions of the 6-311 basis sets. Highly accurate calculations of the outcomes were obtained when the method was tried on nine aldehydes with different structural characteristics. It was also found that for relatively large systems, such as this, using a split-valence triple-zeta basis saves much time compared to using larger basis sets sometimes employed in organocatalytic studies, as, for example, the TZV and Def2TZV basis set families.

5. Miscellaneous Reactions Involving Anion-Binding Catalysis

Besides the synthesis of chiral lactams described by Vetticat and Seidel (Figure 37, Section 3), other examples of anion-binding catalysis have been described [74]. Those which do not fit in the categories covered in the previous sections have been grouped in this section. Anion-binding catalysis by dual H-bond donors may take place via different activation modes (Figure 46): there may be an association of the H-bond donor to a preformed ion pair, as in A; there may be Brønsted acid co-catalysis, with the H-bond donor enhancing the acidity of a weak acid by stabilizing its conjugate base, as in B or they may be anion abstraction from a neutral substrate as in C [91]. Mode C has been used to explain many enantioselective reactions, but until 2016 it remained still a mechanism poorly understood. In 2016 Jacobsen and coworkers published a study on the amido-thiourea (**C36**)-catalyzed alkylation of racemic α-chloroisochroman **87** with silyl ketene acetal **88**, which sheds some light on this topic [92]. This study followed mechanistic studies performed on this reaction by the group, which suggested that an unusual cooperative mechanism was in operation, with the catalyst resting as a dimeric aggregate under typical reaction conditions (0.1 M in the substrate, 10 mol% of catalyst). For the catalyst to react with the substrate and drive the rate-determining C−C bond formation step, deaggregation was necessary. This can limit efficiency. Catalytic loadings of 5–20 mol% and long reaction times (>24 h) are often required by H-bond donor-catalyzed reactions, and in many cases, they have the limitation of working better under dilute reaction conditions (≤0.1 M in the substrate). These studies aimed to help the design of more efficient catalysts.

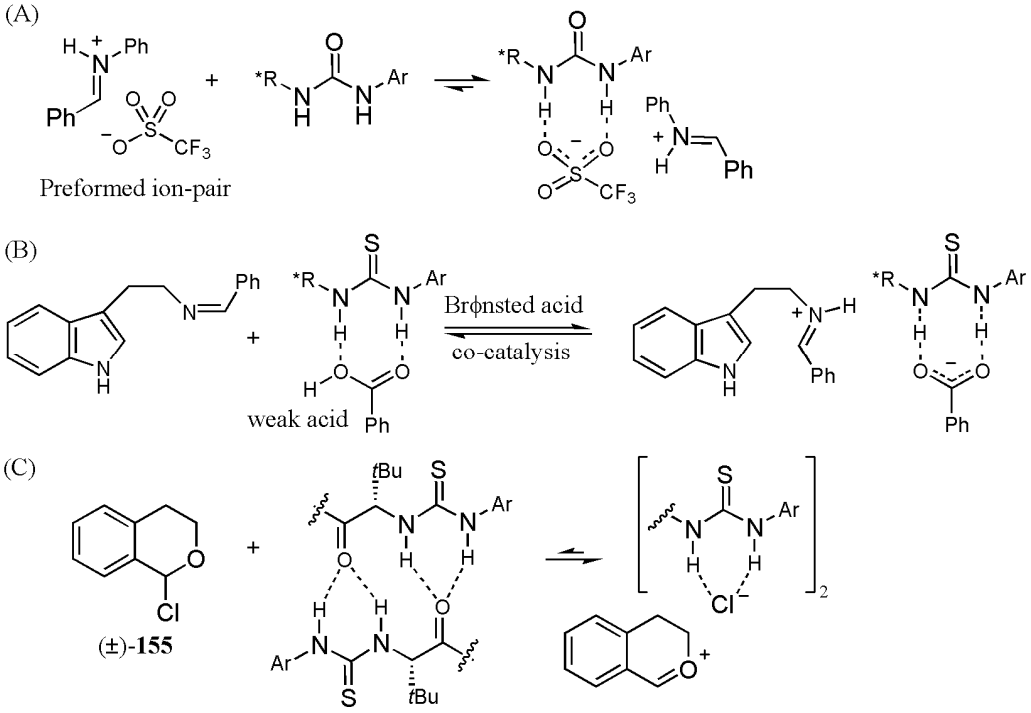

Figure 46. Activation modes in anion-binding catalysis by dual H-bond donor catalysts: (**A**) Binding involving pre-formed ion pairs; (**B**) Brϕnsted acid co-catalysis; (**C**) Anion abstraction catalysis [91].

Epimerization rate data alone did not allow a distinction to be made between an S_N2 and an S_N1 mechanism. However, whereas racemization of **89** through an S_N1 mechanism should be inhibited by exogenous chloride sources, racemization via an S_N2 mechanism should be promoted by an increased concentration of an exogenous chloride nucleophile. SIR experiments with the addition of tetraoctylammonium chloride or hydrogen chloride (such that [Cl−] = [**C36**]T) were performed. It was found that epimerization was completely suppressed in both cases, consistent with an S_N1 mechanism for substrate racemization. Ionization promoted by the catalyst affords the oxocarbenium−chloride ion pair. Substrate epimerization and alkylation share the same kinetic dependence on catalyst and α-chloroether, which means that the two processes have a common transition-state stoichiometry. Comparing the rate laws reveals that epimerization catalyzed by **C36** or **C37** is 101–103 times faster than alkylation, which would be needed for alkylation via either dynamic kinetic resolution or a stereoablative S_N1 mechanism. Since the oxocarbenium−chloride ion pair is generated in the epimerization, it must also be an intermediate in the alkylation. Alkylation proceeds via an anion-abstraction ion-pairing mechanism, as shown in Figure 47, involving the cooperative action of two catalyst molecules. The racemization is catalyst-mediated and Cl^- inhibited.

Catalyst aggregation is counterproductive. In further studies by the Jacobsen group, a linkage was introduced between two catalyst monomers, aiming to improve stabilization of the dominant TS complex and hence to improve catalytic activity [93]. Although preliminary DFT analysis did not distinguish whether catalyst activation proceeds by a 4H- or a 2H-Cl^--binding geometry, i.e., via I or II (Figure 48), in the solid-state, a 4H-geometry was observed, a fact, which guided the choices of structural changes [90,91]. A methyl substituent, shown previously to minimize competing reaction pathways and improve reactivity and the *ee*s, was introduced [94]. The bisthioureas were also linked in a way that disfavored aggregation while still resembling the structures of the untethered monomers. Of all the catalysts prepared, the best results were obtained with *ent*-**C38,** which, when applied to the enantioselective alkylation of racemic isochroman **87** (Figure 47a), afforded the product in 96% yield, 92% *ee*, in 3 h at −78 °C with a catalytic load of 0.1 mol% only,

i.e., with 100 times lower catalyst loading, 8 times shorter reaction time and a 5 times more concentrated solution.

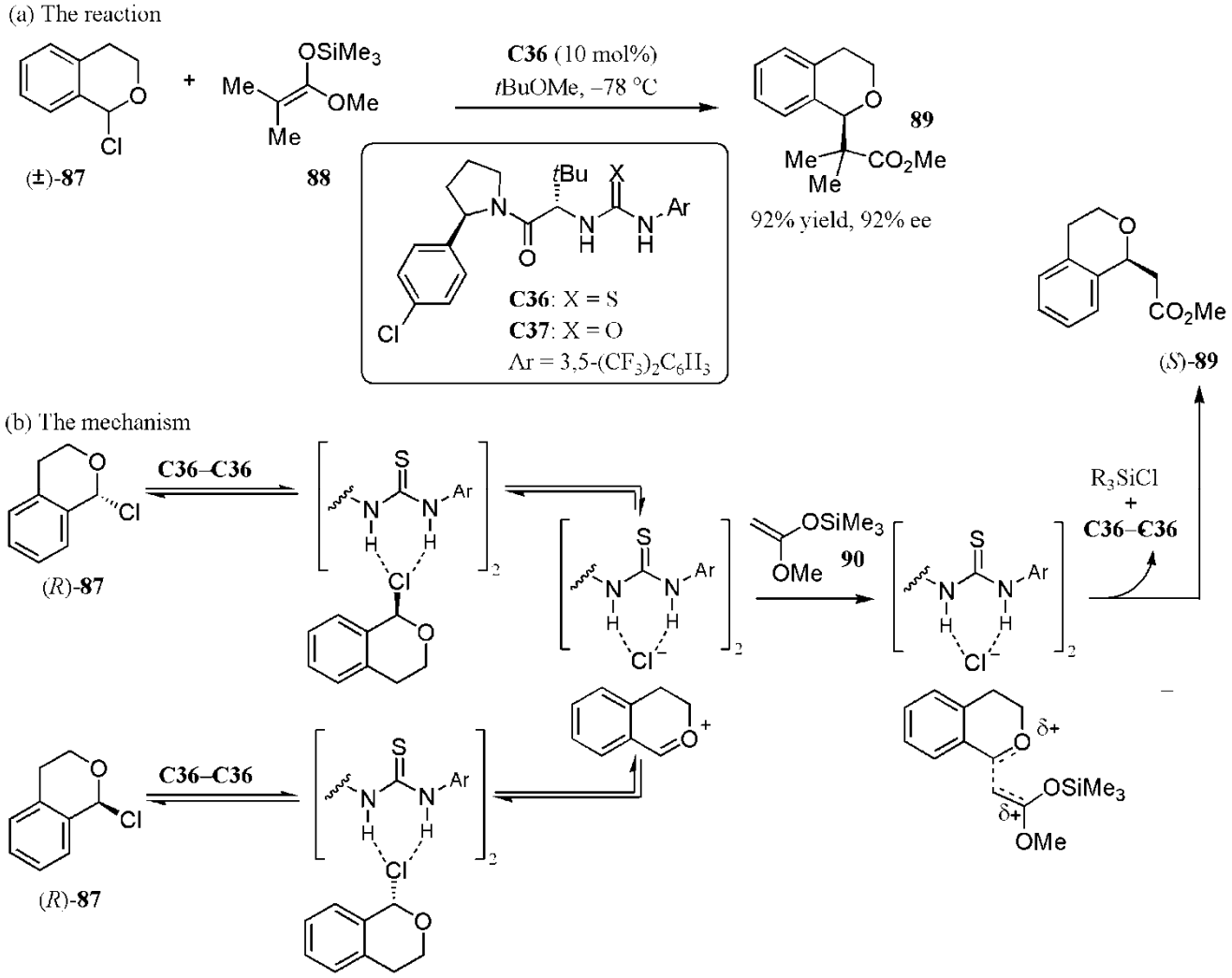

Figure 47. Enantioselective α-chloroisochroman alkylation via anion-abstraction catalysis (**a**) and its mechanism (**b**) [91].

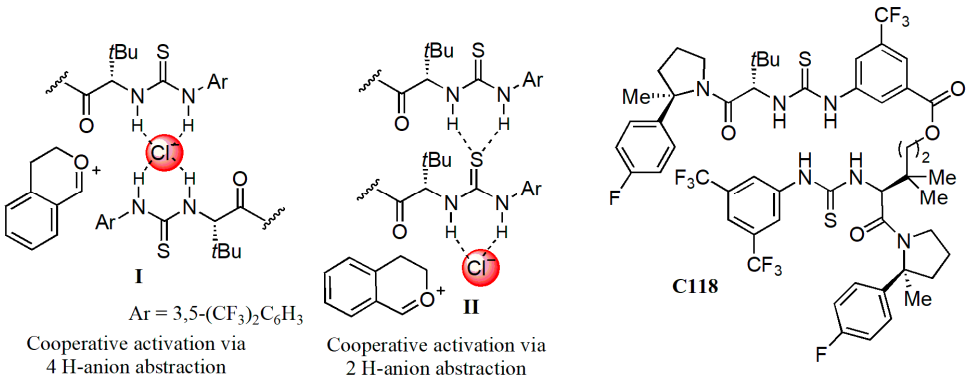

Figure 48. Anion-abstraction catalysis via the cooperative action of two amido-thioureas and catalyst **C38** [93].

The kinetic resolution of racemic amines via acylation and other methods is an important means to obtain chiral amines for various applications. The utilization of small-molecule catalysts for resolution is still challenging, in contrast to enzymatic methods, and only recently have solutions started to appear, which nevertheless, are not as advanced as

the corresponding methods for kinetic resolution of alcohols [95,96]. The kinetic resolution of various classes of amines has been achieved by the Seidel group, with asymmetric nucleophilic catalysis, using an in situ generated chiral acylating reagent [97]. Three components are involved: 4-dimethylaminopyridine (DMAP, a nucleophilic catalyst), an achiral acylating reagent (**91**), and a chiral anion receptor/hydrogen bonding (HB) catalyst (Figure 49). DMAP, which exists in equilibrium with the corresponding acylpyridinium salt (e.g., ion-pair I), is converted into a chiral species through the interaction of the counteranion with a chiral anion receptor, e.g., a thiourea catalyst, forming ion-pair II. This has an impact on the DMAP/acylpyridinium salt equilibrium. Since ion-pair II is more electrophilic and/or soluble than ion-pair I, reactions with amines should occur more readily with ion-pair II than with ion-pair I, a fact that has been applied in the kinetic resolution of amines. In a recent study, the Seidel group investigated the role of ion-pair II and other reaction components in the enantioselectivity of the kinetic resolution shown in Figure 49a as a model reaction [90]. Computational studies at the M06/6-31G(d,p) level of theory, including solvent modeling utilizing a polarized continuum model, provided new information on the nature of the ion pair and revealed a range of important secondary interactions responsible for enantiodiscrimination. Catalyst **C39** was found to be the most efficient. Toluene was the best solvent, and it has been generally observed to be a privileged solvent for enantioselective reactions preceding via catalyst−substrate ion pairing, which agrees with the fact that the nature of the ion pair is influenced by the reaction medium, with nonpolar solvents favoring tight (contact) ion pairs and the more polar ones leading to solvent-shared or solvent-separated ion pairs. NMR studies at different concentrations suggested that the catalyst is present in a nonaggregated form at the concentrations used for catalysis. A 1:1 binding stoichiometry of benzoate by the catalyst was inferred by titration studies with tetrabutylammonium benzoate (TBAB) monitored by NMR and UV-vis titration. This information confirms the idea that the key ion pair involved in catalysis consists of a catalyst with a thiourea subunit binding to the benzoate counteranion of the DMAP-derived *N*-benzoylpyridinium salt. Deprotonation of the catalyst and involvement of a neutral acylating agent in the reaction could be ruled out by comparison of NMR data with spectra obtained when the catalyst was treated with different bases. Evaluation of two diastereomeric quaternary complexes helped to rationalize the experimental observation that the *R*-enantiomer of **92** is benzoylated preferentially over the corresponding *S*-enantiomer. In the case of both the bis-thiourea **C39** and the amide-thiourea catalyst **C40**, dual intramolecular hydrogen bonding to the sulfur atom of a thiourea subunit was found to occur, and the result was activation of this moiety for anion binding since the two N−H bonds become more acidic.

A recent example of anion binding catalysis involves the nucleophilic addition of *N*-*tert*-butylhydrazones to isoquinolinium ions (from **95**) (Figure 50). This reaction, which leads to the dearomatization of the isoquinoline, proceeded in a highly enantioselective manner in the presence of bifunctional thiourea-based catalyst **C41**. Two chiral centers were formed in the reaction, and the diastereoselectivity was >20:1 in all cases studied [98]. If the reaction proceeds by anion-binding catalysis, it is expected that the geometry, size and coordination ability of the counteranion should have a marked effect on the results. As a test, anion exchanges (Cl!TFA, BF_4, BARF) were performed before the addition of hydrazone **97a**. Poorer reactivities and *ee*s were observed in all cases, as expected when the spherical, small chloride anion was replaced by the new anions. In addition, an experiment with pyrrolidine-derived hydrazone **97b** yielded low amounts of product, but racemic, which confirms that the chloride-binding ability of the hydrazone is essential. Further, the evidence available pointed to the formation of a 1:1 complex: the absence of a significant nonlinear effect suggests that a 2:1 complex may not be operating, information, which was also confirmed by the method of continuous variation, for which the data obtained fits with a 1:1 complex.

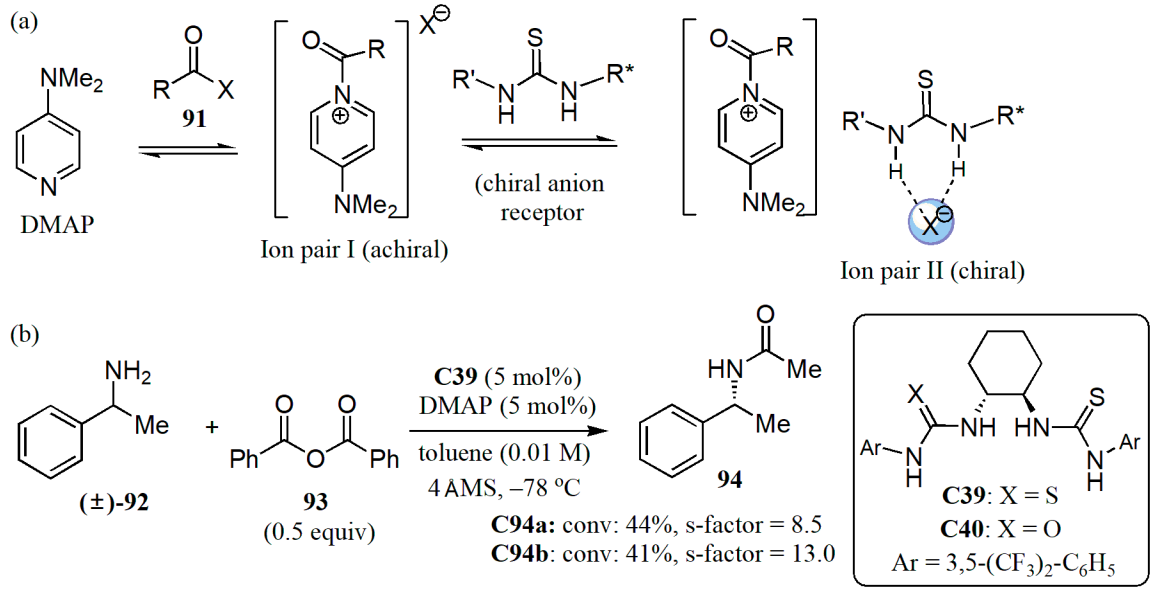

Figure 49. (**a**) The concept of anion binding and the formation of a chiral ion pair in an asymmetric acyl transfer reaction; (**b**) Kinetic resolution of amines by a dual-catalysis anion-binding approach [95].

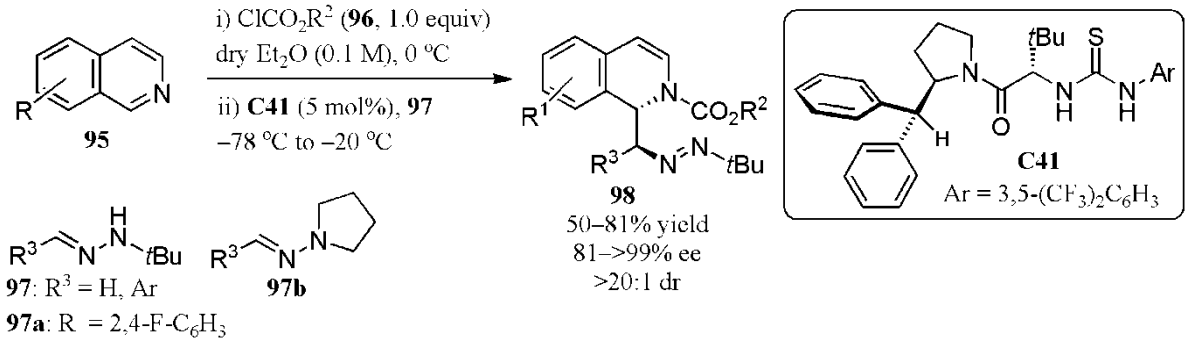

Figure 50. Asymmetric addition of *N-tert*-butylhydrazones to isoquinolinium ions [98].

Computational studies revealed that in the most favored TS, the azomethine carbon approaches the *Si* face of the isoquinolinium C(1)=N bond (Figure 51A). A difference of 10.5 kcal mol^{-1} was found concerning the most stable transition structure leading to the *R* enantiomer of **97c**. NCI analysis of the lowest energy transition structure showed the presence of stabilizing Cl–π, CH–π and π–π interactions [99]. A new tool for NCI quantitative analysis showed that noncovalent interactions of the chloride ion with the NH's of the thiourea moiety and hydrazone, as well as with the azomethine hydrogen atom, are stronger in the preferred TS (Figure 51B, bottom square). These interactions fix the orientation of the reagents in a highly ordered [**120**]-Cl-hydrazone complex as the key intermediate, from which there is the preferential approach of the azomethine carbon to the Si face of the isoquinolinium C(1)=N bond. This mode of reaction is responsible for the high stereoselectivity observed, as well as the *S*,*S* absolute configuration of the product.

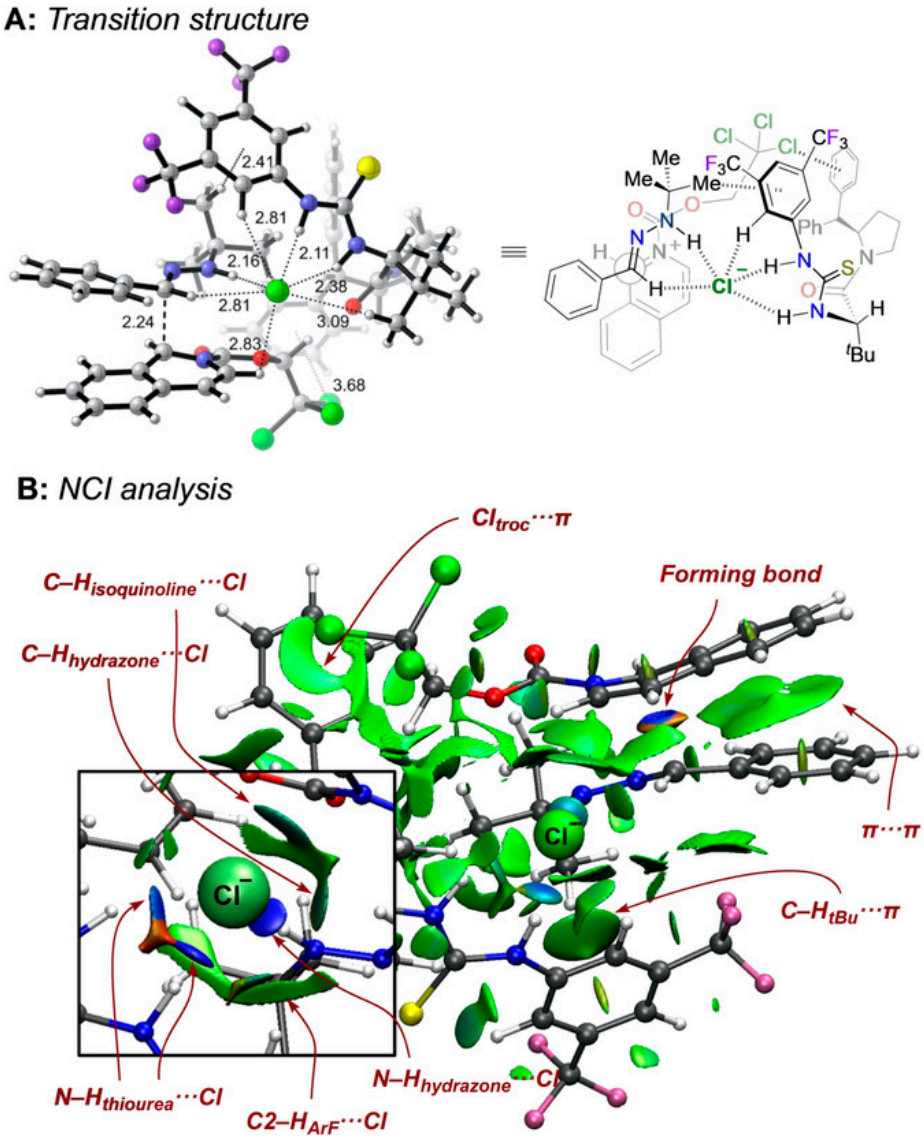

Figure 51. (**A**) TS structure and (**B**) NCI TS analysis of the asymmetric addition of *N-tert*-butylhydrazones to isoquinolinium ions. Reprinted and adapted from *Angewandte Chemie International Edition* with permission from Wiley [98].

6. Miscellaneous

Enantioselective transfer hydrogenation is another reaction that has benefited from developing bifunctional dual hydrogen donor catalysts [100]. The reduction of nitroalkenes is an example. In 2015 Benaglia and coworkers developed a procedure for the reduction of β-trifluoromethyl-substituted nitroalkenes **99** with Hantzsch esters **100** as hydrogen sources (Figure 52) [101]. A multifunctional thiourea-based (*S*)-valine derivative (**C42a**) was found to be a good catalyst, affording very good yields and *ee*s of amines in the case of trisubstituted olefins. Tetrasubstituted olefins reacted with lower stereoselectivity. Computational studies were performed to investigate the reaction further. The transition states leading to the formation of both (*R*)- and (*S*)-**101a** (**101**, R^1 = Ph), TS-*R* and TS-*S*, for the reaction with catalyst **C42b**, located at a B3LYP/6-31G(d) level of theory are shown in Figure 52; finer electronic energies were obtained increasing the basic setup to 6/311+(2df,2pd) with two different functionals: B3LYP and M062X. A methyl-substituted Hantzsch ester was used instead of **100** for simplification. A preliminary conformational analysis revealed a very rigid structure, and only three conformations were found. It was assumed that there was the coordination of the nitro group to the thiourea moiety

and of the Hantzsch ester NH group to the catalyst carboxyamide group. At a first inspection, it may be seen that the pyrrole moiety plays an important role. In TS-*S*, there is a repulsive interaction between the pyrrole ring and phenyl group of the nitroalkene, which disfavors the formation of the *S* enantiomer. In addition, with the substrate coordinated to the thiourea, the nitroolefin C2 electrophilic carbon atom in TS-*S* is closer to the bulky diaminocyclohexane moiety than in TS-*R*. This forces the Hantszch ester, in releasing the hydride, to a hindered area with the ester group repulsively interacts with the 2,5-methyl pyrrole substituents, thus further favoring TS-*R*.

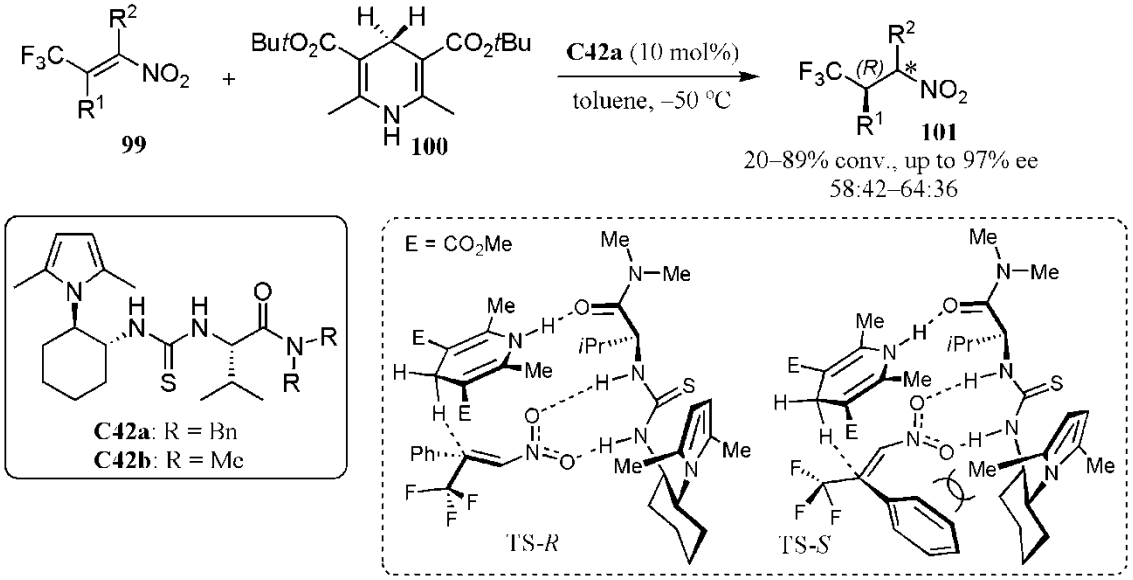

Figure 52. Enantioselective organocatalytic reduction of β-trifluoromethyl nitroalkenes **99** [101].

Qiu, Zhao and coworkers described a Morita–Baylis–Hillman reaction of *N*-alkyl isatins **102** with acrylates **103** catalyzed by a bifunctional phosphine–squaramide (**C43**) in 2015 (Figure 53) [102]. The catalyst was part of a series synthesized from inexpensive and commercially available β-amino alcohols. The products, chiral 3-substituted 3-hydroxy-2-oxindoles (**104**) bearing an exocyclic double bond, were obtained in very high yields and *ee*s and the reaction mechanism was probed by means by ^{31}P NMR, ESI-MS and KIE studies. KIE studies with *N*-methylisatin and butyl acrylate revealed a carbon isotope effect on the 3-carbon when the ^{13}C ratio of recovered *N*-methyl isatin was compared to that of the original sample (C3 = 1.021). This suggests that C–C bond-formation is the rate-limiting step of the MBH reaction. A mechanism was proposed, as shown in Figure 53, with the support of MS since some of the intermediates could be detected.

The Pictet–Spengler reaction allows the efficient construction of important heterocycles of interest for the pharmaceutical industry. In nature, this reaction gives rise to monoterpene indole alkaloids, as well as many secondary metabolites. The reaction mechanism was investigated by Jacobsen and coworkers recently [103]. Initially, there is a condensation of a β-arylethylamine with an aldehyde, C–C bond formation by addition of the pendant arene to the resultant iminium ion and subsequent rearomatization (via deprotonation). In tryptamine derivatives, the C−C bond-formation may take place by direct electrophilic aromatic substitution at C2 or by alkylation at the more nucleophilic C3 position, followed by C−C migration. Although both pathways had been shown to be viable, some questions remained unknown, such as how rearomatization occurred in the nonpolar media commonly used in asymmetric synthesis, and the studies by the Jacobsen group aimed to clarify those issues. Based on a system previously shown by the group to have broad applicability, with **105** and **76**, and to afford chiral tetrahydro-β-carboline products **106** with high *ee*s thanks to the cooperative action between a bifunctional chiral thiourea-based catalyst (**C44**) and weak achiral Brønsted acids, such as benzoic acids,

new studies were undertaken (Figure 54) [104]. It was found by applying kinetic studies, isotope effects, structure−enantioselectivity relationships, and computational analyses that rearomatization (the deprotonation) is the rate- and enantioselectivity-determining step. The indole N-H was found to be important for enantioinduction since the reaction of a methylated substrate yielded a nearly racemic product. In addition, it was also observed that the co-catalysts play key roles in several steps leading up to and, including the deprotonation step. Coordination to the thiourea increases the acidity of benzoic acid leading to substrate protonation. Anion-binding to the conjugate base helps to stabilize the pentahydro-β-carbolinium ion intermediate. These interactions contribute to rate acceleration. Enantiodifferentiation is due to differential π···π and C−H···π interactions in the TSs leading to the two enantiomers, which are organized by hydrogen-bonding interactions. On the whole, catalyst **C44** displays many of the features of enzymatic Pictet−Spengler catalysts.

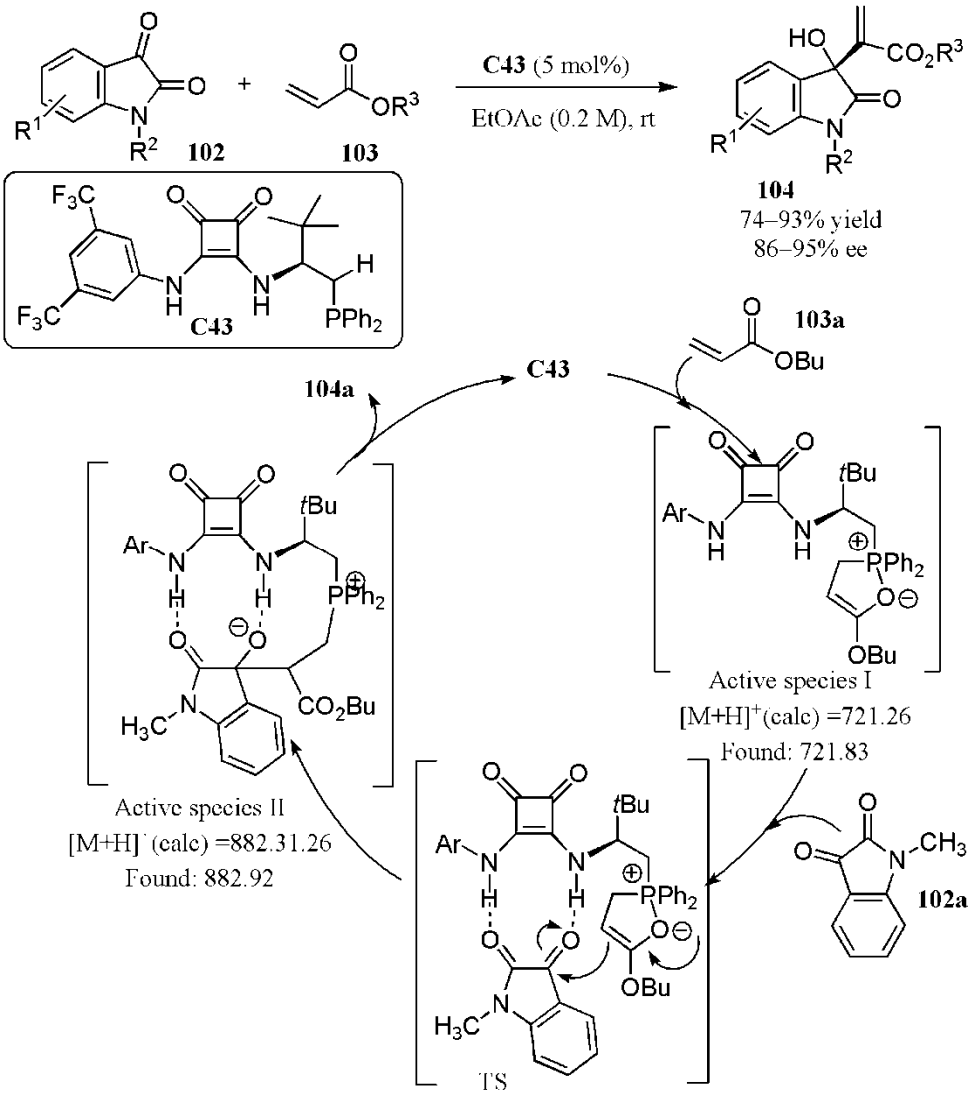

Figure 53. Enantioselective Morita–Baylis–Hillman reaction of *N*-alkyl isatins with acrylates and the mechanism proposed [102].

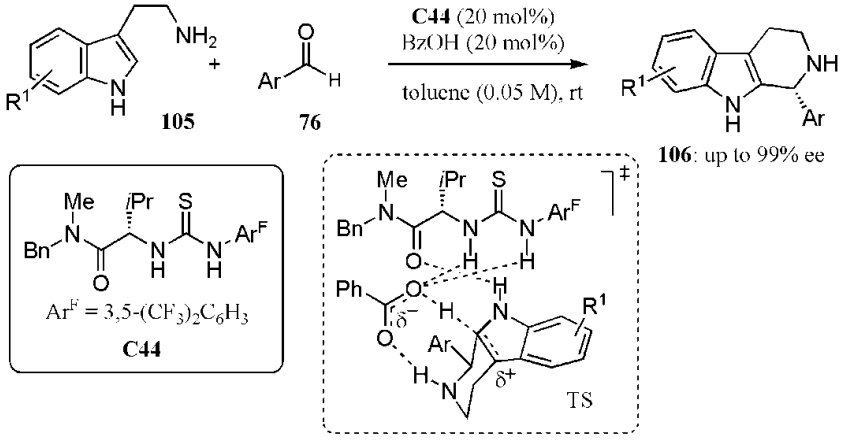

Figure 54. Enantioselective Pictet–Spengler reaction catalyzed by **C44** [103,104].

In 2018 Zhong and coworkers did a related study on a cinchona alkaloid squaramide-catalyzed asymmetric Pictet–Spengler reaction [105]. DFT calculations were also performed to clarify the reaction mechanism. The products were obtained with very high yields and moderate to very high *ee*s when quinidine-derived squaramide catalyst **C44** was employed to promote the reaction. In this process, there was no need for the addition of a co-acid catalyst. The *ee*s were found to be highly dependent on the nature of the aldehyde used. They were as high as 99%, but generally, when a 2- or 4-electron-withdrawing substituent was present in an aryl aldehyde, the *ee*s were low.

Bifunctional dialkyl sulfide catalysts are still rare. However, in 2018 Yamanaka, Shirakawa and coworkers described the synthesis of some novel catalysts with these features that could promote regio-, diastereo-, and enantioselective bromolactonization of **107** to yield compounds **109** [106]. **C45** was the best. The presence of the urea functionality was found to be critical since an analogous catalyst bearing a methyl group instead of SBu afforded racemic product only. Hence, was the nature of the brominating agent **108**. The results for a few regents **108** tried are shown in Figure 55. DFT calculations were performed to provide some insight into the origin of stereoselectivity. An associative TS model involving monocoordinated succinimide anion fitted best. The structures of the most promising TS models are shown in Figure 56. A 4.3 kcal mol^{-1} difference between TS_{major} and TS_{minor} agrees with the experimental results. The succinimide anion is found to be coordinated with both the urea and the sulfide moieties in TS_{major}, but only with the urea moiety in TS_{minor}, and additional NH/π interaction between a portion of the NH residue of the urea moiety and the naphthyl moiety in TS_{major} account for the higher stability obtained.

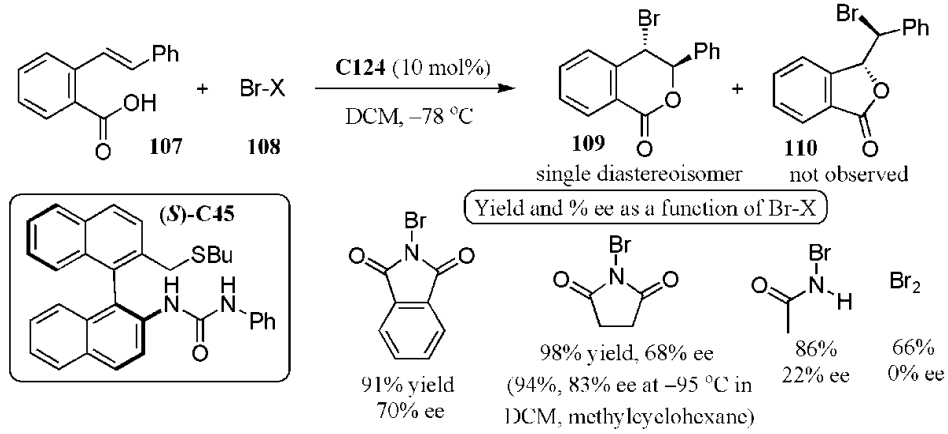

Figure 55. Synthesis of 3,4-dihydroisocoumarin **109** via an asymmetric bromolactonization reaction [106].

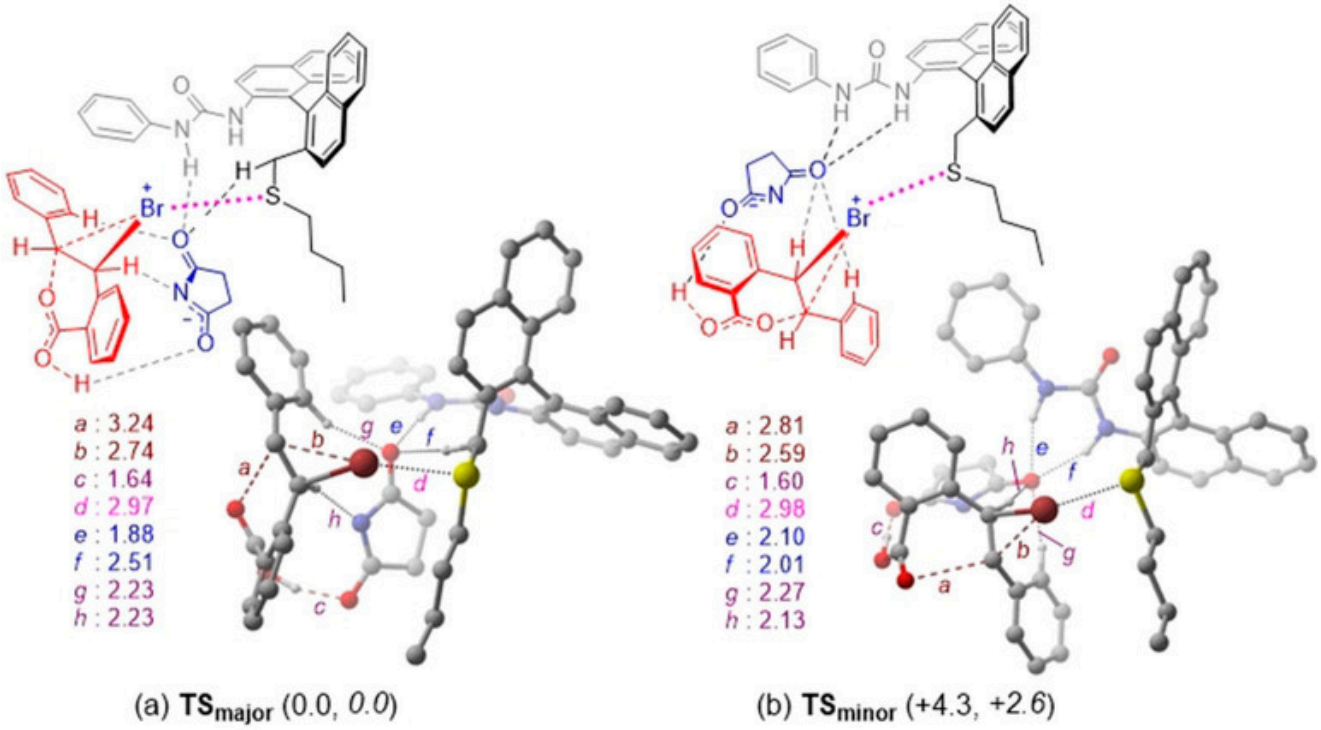

Figure 56. Asymmetric bromolactonization of alkenes **107** catalyzed by a urea-sulfide bifunctional catalyst. 3D structures and the relative Gibbs free energies (kcal mol^{-1}) of TS_{major} (**a**) and TS_{minor} (**b**). Bond lengths are in Å. Reprinted and adapted from Chemistry—A European Journal with permission from Wiley [106].

A recent development in this field is using multivariate linear regression analysis to help the design of new catalysts. One of these works was recently published by Werth and Sigman [107]. By connecting catalyst and substrate structural features, the proposed transition states and the noncovalent interactions responsible for asymmetric induction, using an iterative statistical modeling process, this research aimed to provide a basis for extrapolation to new reactions and/or catalysts so that more accurate predictions could be made in future developments rather than utilizing a totally empirical approach.

7. Conclusions

Dual H-bond donor bifunctional catalysts have become in recent years a very popular and efficient means to perform both new and old reactions in a highly stereoselective manner. Understanding the mechanisms of these reactions and the origin of stereoinduction can help the rational development of new powerful catalysts for future applications. Computational tools and DFT calculations have helped to elucidate mechanisms and reveal nonbonding interactions, which are responsible for the stabilization of transition states and selectivity. Additional studies, such as the determination of acidity scales and kinetic isotopic effects, have had important contributions too. Catalytic loadings are becoming lower, with successful transformations being achieved with even less than 1 mol% of catalysts of interest for large-scale applications. Given the easy-to-assemble modular nature of these catalysts, the large number of reactions that they have made possible with high stereoselectivities, and the mild reaction conditions under which they operate, a bright future is expected for further developments in this area.

Author Contributions: All authors contributed to this work. All authors have read and agreed to the published version of the manuscript.

Funding: This research received no external funding.

Acknowledgments: This work was supported by Fundação para a Ciência e a Tecnologia (FCT), Portugal, in the form of project UIDB/00100/2020 of Centro de Química Estrutural and by the RUDN

University Strategic Academic Leadership Program. Furthermore, the Deutsche Forschungsgemeinschaft (DFG) is acknowledged.

Conflicts of Interest: The authors declare that there are no conflicts of interest.

References

1. Zhao, B.-L.; Li, J.-H.; Du, D.-M. Squaramide-catalyzed asymmetric reactions. *Chem. Rec.* **2017**, *17*, 994–1018. [CrossRef]
2. Parvin, T.; Yadava, R.; Choudhurym, L.H. Recent applications of thiourea-based organocatalysts in asymmetric multicomponent reactions (AMCRs). *Org. Biomol. Chem.* **2020**, *18*, 5513–5532. [CrossRef] [PubMed]
3. Limnios, D.; Kokotos, C.G. Ureas and thioureas as asymmetric organocatalysts. In *Sustainable Catalysis: Without Metals or Other Endangered Elements, Part 2*; North, M., Ed.; The Royal Society of Chemistry: London, UK, 2016; pp. 196–255.
4. Xiang, S.H.; Tan, B. Advances in asymmetric organocatalysis over the last 10 years. *Nat. Commun.* **2020**, *11*, 3786. [CrossRef]
5. Ni, X.; Li, X.; Wang, Z.; Cheng, J.-P. Squaramide equilibrium acidities in DMSO. *Org. Lett.* **2014**, *16*, 1786–1789. [CrossRef] [PubMed]
6. Storer, R.I.; Aciro, C.; Jones, L.H. Squaramides: Physical properties, synthesis and applications. *Chem. Soc. Rev.* **2011**, *40*, 2330–2346. [CrossRef] [PubMed]
7. Alemán, J.; Parra, A.; Jiang, H.; Jørgensen, K.A. Squaramides: Bridging from molecular recognition to bifunctional organocatalysis. *Chem. Eur. J.* **2011**, *17*, 6890–6899. [CrossRef]
8. Li, Z.; Li, X.; Cheng, J.-P. Recent progress in equilibrium acidity studies of organocatalysts. *Synlett* **2019**, *30*, 1940–1949. [CrossRef]
9. Li, X.; Deng, H.; Zhang, B.; Li, J.; Zhang, L.; Luo, S.; Cheng, J.-P. Physical organic study of structure–activity–enantioselectivity relationships in asymmetric bifunctional thiourea catalysis: Hints for the design of new organocatalysts. *Chem. Eur. J.* **2010**, *16*, 450–455. [CrossRef]
10. Jakab, G.; Tancon, C.; Zhang, Z.; Lippert, K.M.; Schreiner, P.R. (Thio)urea organocatalyst equilibrium acidities in DMSO. *Org. Lett.* **2012**, *14*, 1724–1727. [CrossRef] [PubMed]
11. Lu, T.; Wheeler, S.E. Origin of the superior performance of (thio)squaramides over (thio)ureas in organocatalysis. *Chem. Eur. J.* **2013**, *19*, 15141–15147. [CrossRef]
12. Malerich, J.P.; Hagihara, K.; Rawal, V.H. Chiral squaramide derivatives are excellent hydrogen bond donor catalysts. *J. Am. Chem. Soc.* **2008**, *130*, 14416–14417. [CrossRef]
13. Žabka, M.; Šebesta, R. Experimental and theoretical studies in hydrogen-bonding organocatalysis. *Molecules* **2015**, *20*, 15500–15524. [CrossRef]
14. Faisca Phillips, A.M. Organocatalytic asymmetric nitro-Michael reactions. *Curr. Org. Synth.* **2016**, *13*, 687–725. [CrossRef]
15. Alonso, D.A.; Baeza, A.; Chinchilla, R.; Gómez, C.; Guillena, G.; Pastor, I.M.; Ramón, D.J. Recent advances in asymmetric organocatalyzed conjugate additions to nitroalkenes. *Molecules* **2017**, *22*, 895. [CrossRef] [PubMed]
16. Okino, T.; Hoashi, Y.; Takemoto, Y. Enantioselective Michael reaction of malonates to nitroolefins catalyzed by bifunctional organocatalysts. *J. Am. Chem. Soc.* **2003**, *125*, 12672–12673. [CrossRef] [PubMed]
17. Okino, T.; Hoashi, Y.; Furukawa, T.; Xu, X.; Takemoto, Y. Enantio- and diastereoselective Michael reaction of 1,3-dicarbonyl compounds to nitroolefins catalyzed by a bifunctional thiourea. *J. Am. Chem. Soc.* **2005**, *127*, 119–125. [CrossRef]
18. Zhu, R.; Zhang, D.; Wu, J.; Liu, C. Theoretical study of the bifunctional-urea catalyzed Michael reaction of 1,3-dicarbonyl compounds and nitroolefins: Reaction mechanism and enantioselectivity. *Tetrahedron Asymmetry* **2006**, *17*, 1611–1616. [CrossRef]
19. Hamza, A.; Schubert, G.; Soós, T.; Pápai, I. Theoretical studies on the bifunctionality of chiral thiourea-based organocatalysts: competing routes to C−C bond formation. *J. Am. Chem. Soc.* **2006**, *128*, 13151–13160. [CrossRef] [PubMed]
20. Kreienborgm, N.M.; Pollok, C.H.; Merten, C. Towards an observation of active conformations in asymmetric catalysis: Interaction-induced conformational preferences of a chiral thiourea model compound. *Chem. Eur. J.* **2016**, *22*, 12455–12463. [CrossRef] [PubMed]
21. Supady, A.; Hecht, S.; Baldauf, C. About underappreciated yet active conformations of thiourea organocatalysts. *Org. Lett.* **2017**, *19*, 4199–4202. [CrossRef]
22. Luchini, G.; Ascough, D.M.H.; Alegre-Requena, J.V.; Gouverneur, V.; Paton, R.S. Data-mining the diaryl(thio)urea conformational landscape: Understanding the contrasting behavior of ureas and thioureas with quantum chemistry. *Tetrahedron* **2019**, *75*, 697–702. [CrossRef]
23. Neuvonen, A.J.; Noutsias, D.; Topić, F.; Rissanen, K.; Földes, T.; Pápai, I.; Pihko, P.M. Dynamic refolding of ion-pair catalysts in response to different anions. *J. Org. Chem.* **2019**, *84*, 15009–15019. [CrossRef] [PubMed]
24. Zhu, J.-L.; Zhang, Y.; Liu, C.; Zheng, A.-M.; Wang, W. Mechanistic insights on organocatalytic enantioselective decarboxylative protonation by epicinchona-thiourea hybrid derivatives. *J. Org. Chem.* **2012**, *77*, 9813–9825. [CrossRef]
25. Izzo, J.A.; Myshchuk, Y.; Hirschi, J.S.; Vetticatt, M.J. Transition state analysis of an enantioselective Michael addition by a bifunctional thiourea organocatalyst. *Org. Biomol. Chem.* **2019**, *17*, 3934–3939. [CrossRef] [PubMed]
26. Singleton, D.A.; Thomas, A.A. High-precision simultaneous determination of multiple small kinetic isotope effects at natural abundance. *J. Am. Chem. Soc.* **1995**, *117*, 9357–9358. [CrossRef]
27. Becke, A.D. Density-functional thermochemistry. III. The role of exact exchange. *J. Chem. Phys.* **1993**, *98*, 5648–5652. [CrossRef]
28. Grimme, S.; Ehrlich, S.; Goerigk, L.J. Effect of the damping function in dispersion corrected density functional theory. *Comput. Chem.* **2011**, *32*, 1456–1465. [CrossRef]

29. Pliego, J.R., Jr. Theoretical free energy profile and benchmarking of functionals for amino-thiourea organocatalyzed nitro-Michael addition reaction. *Phys. Chem. Chem. Phys.* **2020**, *22*, 11529–11536. [CrossRef] [PubMed]
30. Faisca Phillips, A.M. Applications of carbohydrate-based organocatalysts in enantioselective synthesis. *Eur. J. Org. Chem.* **2014**, 7291–7303. [CrossRef]
31. Azad, C.S.; Khan, I.A.; Narula, A.K. Organocatalyzed asymmetric Michael addition by an efficient bifunctional carbohydrate–thiourea hybrid with mechanistic DFT analysis. *Org. Biomol. Chem.* **2016**, *14*, 11454–11461. [CrossRef] [PubMed]
32. Avila, A.; Chinchilla, R.; Fiser, B.; Gómez-Bengoa, E.; Nájera, C. Enantioselective Michael addition of isobutyraldehyde to nitroalkenes organocatalyzed by chiral primary amine-guanidines. *Tetrahedron Asymmetry* **2014**, *25*, 462–467. [CrossRef]
33. Kucherenko, A.S.; Kostenko, A.A.; Komogortsev, A.N.; Lichitsky, B.V.; Fedotov, M.Y.; Zlotin, S.G. C_2-Symmetric chiral squaramide, recyclable organocatalyst for asymmetric Michael reactions. *J. Org. Chem.* **2019**, *84*, 4304–4311. [CrossRef]
34. Rombola, M.; Sumaria, C.S.; Montgomery, T.D.; Rawal, V.H. Development of chiral, bifunctional thiosquaramides: Enantioselective Michael additions of barbituric acids to nitroalkenes. *J. Am. Chem. Soc.* **2017**, *139*, 5297–5300. [CrossRef] [PubMed]
35. Krautwald, S.; Carreira, E.M. Stereodivergence in asymmetric catalysis. *J. Am. Chem. Soc.* **2017**, *139*, 5627–5639. [CrossRef] [PubMed]
36. Beletskaya, I.P.; Nájera, C.; Yus, M. Stereodivergent catalysis. *Chem. Rev.* **2018**, *118*, 5080–5200. [CrossRef]
37. Ding, P.-G.; Zhou, F.; Wang, X.; Zhao, Q.-H.; Yu, J.-S.; Zhou, J. H-bond donor-directed switching of diastereoselectivity in the Michael addition of azido ketones to nitroolefins. *Chem. Sci.* **2020**, *11*, 3852–3861. [CrossRef]
38. Herrera, R.P.; Sgarzani, V.; Bernardi, L.; Ricci, A. Catalytic enantioselective Friedel–Crafts alkylation of indoles by using a simple thiourea organocatalyst. *Angew. Chem. Int. Ed.* **2005**, *44*, 6576–6579. [CrossRef]
39. Roca-López, D.; Marqués-López, E.; Alcaine, A.; Merino, P.; Herrera, R.P. A Friedel–Crafts alkylation mechanism using an aminoindanol-derived thiourea catalyst. *Org. Biomol. Chem.* **2014**, *12*, 4503–4510. [CrossRef]
40. Pettersen, D.; Herrera, R.P.; Bernardi, L.; Fini, F.; Sgarzani, V.; Fernández, R.; Lassaletta, J.M.; Ricci, A. A broadened scope for the use of hydrazones as neutral nucleophiles in the presence of H-bonding organocatalysts. *Synlett* **2006**, 239–242. [CrossRef]
41. Etter, M.C.; Panunto, T.W. 1,3-Bis(m-nitrophenyl)urea: An exceptionally good complexing agent for proton acceptors. *J. Am. Chem. Soc.* **1988**, *110*, 5896–5897. [CrossRef]
42. Fan, Y.; Kass, S.R. Enantioselective Friedel–Crafts alkylation between nitroalkenes and indoles catalyzed by charge activated thiourea organocatalysts. *J. Org. Chem.* **2017**, *82*, 13288–13296. [CrossRef]
43. Li, B.-J.; Jiang, L.; Liu, M.; Chen, Y.-C.; Ding, L.-S.; Wu, Y. Asymmetric Michael addition of arylthiols to α,β-unsaturated carbonyl compounds catalyzed by bifunctional organocatalysts. *Synlett* **2005**, 603–606. [CrossRef]
44. Vakulya, B.; Varga, S.; Csámpai, A.; Soós, T. Highly enantioselective conjugate addition of nitromethane to chalcones using bifunctional cinchona organocatalysts. *Org. Lett.* **2005**, *7*, 1967–1969. [CrossRef] [PubMed]
45. McCooey, S.H.; Connon, S.J. Urea- and thiourea-substituted cinchona alkaloid derivatives as highly efficient bifunctional organocatalysts for the asymmetric addition of malonate to nitroalkenes: Inversion of configuration at C9 dramatically improves catalyst performance. *Angew. Chem. Int. Ed.* **2005**, *44*, 6367–6370. [CrossRef] [PubMed]
46. Ye, J.; Dixon, D.J.; Hynes, P.S. Enantioselective organocatalytic Michael addition of malonate esters to nitroolefins using bifunctional cinchonine derivatives. *Chem. Commun.* **2005**, 4481–4483. [CrossRef]
47. Grayson, M.N. Mechanism and origins of stereoselectivity in the cinchona thiourea- and squaramide-catalyzed asymmetric Michael addition of nitroalkanes to enones. *J. Org. Chem.* **2017**, *82*, 4396–4401. [CrossRef]
48. Grayson, M.N.; Houk, K.N. Cinchona urea-catalyzed asymmetric sulfa-Michael reactions: The Brønsted acid−hydrogen bonding model. *J. Am. Chem. Soc.* **2016**, *138*, 9041–9044. [CrossRef]
49. Zhang, G.; Zhu, C.; Liu, D.; Pan, J.; Zhang, J.; Hu, D.; Song, B. Solvent-free enantioselective conjugate addition and bioactivities of nitromethane to Chalcone containing pyridine. *Tetrahedron* **2017**, *73*, 129–136. [CrossRef]
50. Duque, M.M.S.; Baslé, O.; Isambert, N.; Gaudel-Siri, A.; Genisson, Y.; Plaquevent, J.-C.; Rodriguez, J.; Constantieux, T. A cooperative participation of the amido group in the organocatalytic construction of all-carbon quaternary stereocenters by Michael addition with β-ketoamides. *Org. Lett.* **2011**, *13*, 3296–3299. [CrossRef] [PubMed]
51. Quintard, A.; Cheshmedzhieva, D.; Duque, M.M.S.; Gaudel-Siri, A.; Naubron, J.-V.; Génisson, Y.; Plaquevent, J.-C.; Bugaut, X.; Rodriguez, J.; Constantieux, T. Origin of the enantioselectivity in organocatalytic Michael additions of β-ketoamides to α,β-unsaturated carbonyls: A combined experimental, spectroscopic and theoretical study. *Chem. Eur. J.* **2015**, *21*, 778–790. [CrossRef]
52. Humbrías-Martín, J.; Pérez-Aguilar, M.C.; Mas-Ballesté, R.; Litta, A.D.; Lattanzi, A.; Sala, G.D.; Fernández-Salas, J.A.; Alemán, J. Enantioselective conjugate azidation of *α,β*-unsaturated ketones under bifunctional organocatalysis by direct activation of $TMSN_3$. *Adv. Synth. Catal.* **2019**, *361*, 4790–4796. [CrossRef]
53. Helder, R.; Arends, R.; Bolt, W.; Hiemstra, H.; Wynberg, H. Alkaloid catalyzed asymmetric synthesis III the addition of mercaptans to 2-cyclohexene-1-one; determination of enantiomeric excess using ^{13}C NMR. *Tetrahedron Lett.* **1977**, *18*, 2181–2182. [CrossRef]
54. Connon, S.J. Asymmetric catalysis with bifunctional cinchona alkaloid-based urea and thiourea organocatalysts. *Chem. Commun.* **2008**, 2499–2510. [CrossRef] [PubMed]
55. Melchiorre, P. Cinchona-based primary amine catalysis in the asymmetric functionalization of carbonyl compounds. *Angew. Chem. Int. Ed.* **2012**, *51*, 9748–9770. [CrossRef]

56. Dai, L.; Wang, S.-X.; Chen, F.-E. A bifunctional cinchona alkaloid-squaramide catalyst for the highly enantioselective conjugate addition of thiols to *trans*-chalcones. *Adv. Synth. Catal.* **2010**, *352*, 2137–2141. [CrossRef]
57. Guo, J.; Wong, M.W. Cinchona alkaloid-squaramide catalyzed sulfa-Michael addition reaction: Mode of bifunctional activation and origin of stereoinduction. *J. Org. Chem.* **2017**, *82*, 4362–4368. [CrossRef]
58. Caner, H.; Biedermann, P.U.; Agranat, I. Conformational spaces of *Cinchona* alkaloids. *Chirality* **2003**, *15*, 637–645. [CrossRef]
59. Dijkstra, G.D.H.; Kellogg, R.M.; Wynberg, H.; Svendsen, J.S.; Marko, I.; Sharpless, K.B. Conformational study of cinchona alkaloids. A combined NMR, molecular mechanics and x-ray approach. *J. Am. Chem. Soc.* **1989**, *111*, 8069–8076. [CrossRef]
60. Grayson, M.N.; Houk, K.N. Cinchona alkaloid-catalyzed asymmetric conjugate additions: The bifunctional brønsted acid–hydrogen bonding model. *J. Am. Chem. Soc.* **2016**, *138*, 1170–1173. [CrossRef]
61. Rana, N.K.; Selvakumar, S.; Singh, V.K. Highly enantioselective organocatalytic sulfa-Michael addition to α,β-unsaturated ketones. *J. Org. Chem.* **2010**, *75*, 2089–2091. [CrossRef]
62. Bahlinger, A.; Fritz, S.P.; Wennemers, H. Stereoselective metal-free synthesis of β-amino thioesters with tertiary and quaternary stereogenic centers. *Angew. Chem. Int. Ed.* **2014**, *53*, 8779–8783. [CrossRef] [PubMed]
63. Lin, Y.; Hirschi, W.J.; Kunadia, A.; Paul, A.; Ghiviriga, I.; Abboud, K.A.; Karugu, R.W.; Vetticatt, M.J.; Hirschi, J.S.; Seidel, D. A selenourea-thiourea Brønsted acid catalyst facilitates asymmetric conjugate additions of amines to α,β-unsaturated esters. *J. Am. Chem. Soc.* **2020**, *142*, 5627–5635. [CrossRef] [PubMed]
64. Martínez, J.I.; Villar, L.; Uria, U.; Carrillo, L.; Reyes, E.; Vicario, J.L. Bifunctional squaramide catalysts with the same absolute chirality for the diastereodivergent access to densely functionalised cyclohexanes through enantioselective domino reactions. Synthesis and mechanistic studies. *Adv. Synth. Catal.* **2014**, *356*, 3627–3648. [CrossRef]
65. Meninno, S.; Quaratesi, I.; Volpe, C.; Mazzanti, A.; Lattanzi, A. Catalytic enantioselective one-pot approach to *cis*- and *trans*-2,3-diaryl substituted 1,5-benzothiazepines. *Org. Biomol. Chem.* **2018**, *16*, 6923–6934. [CrossRef] [PubMed]
66. Chen, C.; Wei, R.; Yi, X.; Gao, L.; Zhang, M.; Liu, H.; Li, Q.; Song, H.; Ban, S.J. Diastereo- and enantioselective synthesis of functionalized cyclopentenes containing a quaternary chiral center via a thiosquaramide-catalyzed cascade Michael−Henry reaction. *Org. Chem.* **2019**, *84*, 15655–15661. [CrossRef]
67. Alishetty, S.; Shih, H.P.; Han, C.C. One-step, effective, and cascade syntheses of highly functionalized cyclopentenes with high diastereoselectivity. *Org. Lett.* **2018**, *20*, 2513–2516. [CrossRef]
68. Held, F.E.; Tsogoeva, S.B. Asymmetric cycloaddition reactions catalyzed by bifunctional thiourea and squaramide organocatalysts: Recent advances. *Catal. Sci. Technol.* **2016**, *6*, 645–667. [CrossRef]
69. Chen, X.; Qi, Z.-H.; Zhang, S.-Y.; Kong, L.-P.; Wang, Y.; Wang, X.-W. Enantioselective construction of functionalized thiopyranoindole annulated heterocycles via a formal thio [3 + 3]-cyclization. *Org. Lett.* **2015**, *17*, 42–45. [CrossRef]
70. Banik, S.M.; Levina, A.; Hyde, A.M.; Jacobsen, E.N. Lewis acid enhancement by hydrogen-bond donors for asymmetric catalysis. *Science* **2017**, *358*, 761–764. [CrossRef] [PubMed]
71. Mathieu, B.; Ghosez, L. Trimethylsilyl bis(trifluoromethanesulfonyl)imide as a tolerant and environmentally benign Lewis acid catalyst of the Diels–Alder reaction. *Tetrahedron* **2002**, *58*, 8219–8226. [CrossRef]
72. James, T.; van Gemmeren, M.; List, B. Development and applications of disulfonimides in enantioselective organocatalysis. *Chem. Rev.* **2015**, *115*, 9388–9409. [CrossRef]
73. Burés, J. A simple graphical method to determine the order in catalyst. *Angew. Chem. Int. Ed.* **2016**, *55*, 2028–2031. [CrossRef]
74. Jarvis, C.L.; Hirschi, J.S.; Vetticatt, M.J.; Seidel, D. Catalytic enantioselective synthesis of lactams through formal [4 + 2] cycloaddition of imines with homophthalic anhydride. *Angew. Chem. Int. Ed.* **2017**, *56*, 2670–2674. [CrossRef] [PubMed]
75. Castagnoli, N. The condensation of succinic anhydride with benzylidinemethylamine. A stereoselective synthesis of *trans*- and *cis*-1-methyl-4-carbosy-5-phenyl-2-pyrrolidinone. *J. Org. Chem.* **1969**, *34*, 3187–3189. [CrossRef]
76. Castagnoli, N., Jr.; Cushman, M. Condensation of succinic anhydrides with Schiff bases. Scope and mechanism. *J. Org. Chem.* **1971**, *36*, 3404–3406. [CrossRef] [PubMed]
77. Esteban, F.; Cieślik, W.; Arpa, E.M.; Guerrero-Corella, A.; Díaz-Tendero, S.; Perles, J.; Fernández-Salas, J.A.; Fraile, A.; Alemán, J. Intramolecular hydrogen bond activation: Thiourea-organocatalyzed enantioselective 1,3-dipolar cycloaddition of salicylaldehyde-derived azomethine ylides with nitroalkenes. *ACS Catal.* **2018**, *8*, 1884–1890. [CrossRef] [PubMed]
78. Liu, Y.; Wu, X.; Li, S.; Xue, L.; Shan, C.; Zhao, Z.; Yan, H. Organocatalytic atroposelective intramolecular [4 + 2] cycloaddition: Synthesis of axially chiral heterobiaryls. *Angew. Chem. Int. Ed.* **2018**, *57*, 6491–6495. [CrossRef]
79. Shan, C.; Zhang, T.; Xiong, Q.; Yan, H.; Bai, R.; Lan, Y. Hydrogen-bond-induced chiral axis construction: Theoretical study of cinchonine–thiourea-catalyzed enantioselective intramolecular cycloaddition. *Chem. Asian J.* **2019**, *14*, 2731–2736. [CrossRef]
80. Manoni, F.; Farid, U.; Trujillo, C.; Connon, S.J. Catalytic asymmetric Tamura cycloadditions involving nitroalkenes. *Org. Biomol. Chem.* **2017**, *15*, 1463–1474. [CrossRef]
81. Cornaggia, C.; Manoni, F.; Torrente, E.; Tallon, S.; Connon, S.J. A catalytic asymmetric reaction involving enolizable anhydrides. *Org. Lett.* **2012**, *14*, 1850–1853. [CrossRef]
82. Trujillo, C.; Rozas, I.; Botte, A.; Connon, S.J. A DFT mechanistic study of the organocatalytic asymmetric reaction of aldehydes and homophthalic anhydride. *Chem. Commun.* **2017**, *53*, 8874–8877. [CrossRef]
83. Vamisetti, G.B.; Chowdhury, R.; Ghosha, S.K. Organocatalytic decarboxylative aldol reaction of β-ketoacids with α-ketophosphonates en route to the enantioselective synthesis of tertiary α-hydroxyphosphonates. *Org. Biomol. Chem.* **2017**, *15*, 3869–3873. [CrossRef]

84. Barros, M.T.; Faísca Phillips, A.M. Organocatalyzed synthesis of tertiary α-hydroxyphosphonates by a highly regioselective modified Pudovik reaction. *Eur. J. Org. Chem.* **2011**, 4028–4036. [CrossRef]
85. Faísca Phillips, A.M.; Barros, M.T.; Pacheco, M.; Dias, R. Synthesis and biological evaluation of α-hydroxyalkylphosphonates as new antimicrobial agents. *Bioorg. Med. Chem. Lett.* **2014**, *24*, 49–53. [CrossRef] [PubMed]
86. Faisca Phillips, A.M.M.M. Synthesis and applications of pharmacologically relevant phosphonates and phosphinates. In *Organic and Medicinal Chemistry*; Banik, B.K., Ed.; Nova Science Publishers: New York, NY, USA, 2018; Volume 2, pp. 249–319.
87. Ni, X.; Li, X.; Cheng, J.-P. Equilibrium acidities of cinchona alkaloid organocatalysts bearing 6′-hydrogen bonding donors in DMSO. *Org. Chem. Front.* **2016**, *3*, 170–176. [CrossRef]
88. Hammar, P.; Marcelli, T.; Hiemstra, H.; Himoa, F. Density functional theory study of the *Cinchona* thiourea- catalyzed Henry reaction: Mechanism and enantioselectivity. *Adv. Synth. Catal.* **2007**, *349*, 2537–2548. [CrossRef]
89. Otevrel, J.; Bobal, P. Diamine-tethered bis(thiourea) organocatalyst for asymmetric Henry reaction. *J. Org. Chem.* **2017**, *82*, 8342–8358. [CrossRef]
90. Alegre-Requena, J.V.; Marqués-López, E.; Herrera, R.P. Optimizing the accuracy and computational cost in theoretical squaramide catalysis: The Henry reaction. *Chem. Eur. J.* **2017**, *23*, 15336–15347. [CrossRef]
91. Ford, D.D.; Lehnherr, D.; Kennedy, C.R.; Jacobsen, E.N. Anion-abstraction catalysis: The cooperative mechanism of α-chloroether activation by dual hydrogen-bond donors. *ACS Catal.* **2016**, *6*, 4616–4620. [CrossRef]
92. Ford, D.D.; Lehnherr, D.; Kennedy, C.R.; Jacobsen, E.N. On- and off-cycle catalyst cooperativity in anion-binding catalysis. *J. Am. Chem. Soc.* **2016**, *138*, 7860–7863. [CrossRef] [PubMed]
93. Kennedy, C.R.; Lehnherr, D.; Rajapaksa, N.S.; Ford, D.D.; Park, Y.; Jacobsen, E.N. Mechanism-guided development of a highly active bis-thiourea catalyst for anion-abstraction catalysis. *J. Am. Chem. Soc.* **2016**, *138*, 13525–13528. [CrossRef] [PubMed]
94. Lehnherr, D.; Ford, D.D.; Bendelsmith, A.J.; Kennedy, C.R.; Jacobsen, E.N. Conformational control of chiral amido-thiourea catalysts enables improved activity and enantioselectivity. *Org. Lett.* **2016**, *18*, 3214–3217. [CrossRef] [PubMed]
95. Mittal, N.; Lippert, K.M.; De, C.K.; Klauber, E.G.; Emge, T.J.; Schreiner, P.R.; Seidel, D.J. A dual-catalysis anion-binding approach to the kinetic resolution of amines: Insights into the mechanism via a combined experimental and computational study. *Am. Chem. Soc.* **2015**, *137*, 5748–5758. [CrossRef]
96. Taylor, J.E.; Bull, S.D.; Williams, J.M.J. Amidines, isothioureas, and guanidines as nucleophilic catalysts. *Chem. Soc. Rev.* **2012**, *41*, 2109–2121. [CrossRef]
97. Seidel, D. The anion-binding approach to catalytic enantioselective acyl transfer. *Synlett* **2014**, *25*, 783–794. [CrossRef]
98. Matador, E.; Iglesias-Sigüenza, J.; Monge, D.; Merino, P.; Fernández, R.; Lassaletta, J.M. Enantio- and diastereoselective nucleophilic addition of *N-tert*-butylhydrazones to isoquinolinium ions through anion-binding catalysis. *Angew. Chem. Int. Ed.* **2021**, *60*, 5096–5101. [CrossRef]
99. Boto, R.A.; Peccati, F.; Laplaza, R.; Quan, C.; Carbone, A.; Piquemal, J.-P.; Maday, Y.; Contreras-García, J.J. NCIPLOT4: Fast, robust, and quantitative analysis of noncovalent interactions. *Chem. Theory Comput.* **2020**, *16*, 4150–4158. [CrossRef]
100. Faisca Phillips, A.M.; Pombeiro, A.J.L. Recent advances in organocatalytic enantioselective transfer hydrogenation. *Org. Biomol. Chem.* **2017**, *15*, 2307–2340. [CrossRef]
101. Massolo, E.; Benaglia, M.; Orlandi, M.; Rossi, S.; Celentano, G. Enantioselective Organocatalytic Reduction of b-Trifluoromethyl Nitroalkenes: An Efficient Strategy for the Synthesis of Chiral β-Trifluoromethyl Amines. *Chem. Eur. J.* **2015**, *21*, 3589–3595. [CrossRef]
102. Dong, Z.; Yan, C.; Gao, Y.; Dong, C.; Qiu, G.; Zhou, H.-B. Tunable bifunctional phosphine–squaramide promoted Morita–Baylis–Hillman reaction of *N*-alkyl isatins with acrylates. *Adv. Synth. Catal.* **2015**, *357*, 2132–2142. [CrossRef]
103. Klausen, R.S.; Kennedy, C.R.; Hyde, A.M.; Jacobsen, E.N. Chiral thioureas promote enantioselective Pictet−Spengler cyclization by stabilizing every intermediate and transition state in the carboxylic acid-catalyzed reaction. *J. Am. Chem. Soc.* **2017**, *139*, 12299–12309. [CrossRef]
104. Klausen, R.S.; Jacobsen, E.N. Weak Brønsted acid−thiourea co-catalysis: Enantioselective, catalytic protio-Pictet−Spengler reactions. *Org. Lett.* **2009**, *11*, 887–890. [CrossRef] [PubMed]
105. Qi, L.; Hou, H.; Ling, F.; Zhong, W. The cinchona alkaloid squaramide catalyzed asymmetric Pictet–Spengler reaction and related theoretical studies. *Org. Biomol. Chem.* **2018**, *16*, 566–574. [CrossRef] [PubMed]
106. Nishiyori, R.; Tsuchihashi, A.; Mochizuki, A.; Kaneko, K.; Yamanaka, M.; Shirakawa, S. Design of chiral bifunctional dialkyl sulfide catalysts for regio-, diastereo-, and enantioselective bromolactonization. *Chem. Eur. J.* **2018**, *24*, 16747–16752. [CrossRef]
107. Werth, J.; Sigman, M.S. Connecting and analyzing enantioselective bifunctional hydrogen bond donor catalysis using data science tools. *J. Am. Chem. Soc.* **2020**, *142*, 16382–16391. [CrossRef] [PubMed]